MAINTAINING GLUCOSE HOMEOSTASIS IN RESPONSE TO AGING AND STRESS: THE ROLE OF PCIF1, BMI1, AND PDX1

Corey Cannon

A DISSERTATION

in

Pharmacology

Presented to the Faculties of the University of Pennsylvania

in

Partial Fulfillment of the Requirements for the

Degree of Doctor of Philosophy

2014

Supervisor of Dissertation:

_____

Doris Stoffers, M.D., Ph.D. Professor of Medicine

Graduate Group Chairperson:

_____

Julie Blendy, Ph.D., Professor of Pharmacology

Dissertation Committee:

Klaus Kaestner, Ph.D., Thomas and Evelyn Suor Butterworth Professor in Genetics

Morris Birnbaum, M.D., Ph.D., Willard and Rhoda Ware Professor of Diabetes and Metabolic Diseases

Margaret Chou, Ph.D., Associate Professor of Pathology and Laboratory Medicine

Alan Diehl, Ph.D., Professor, Department of Cancer Biology

ACKNOWLEDGEMENTS

I would like to acknowledge the many people who made the work presented here possible, the first of which is my advisor, Dr. Doris Stoffers. Doris created an environment that demanded a great deal from me as both a scientist and a person. Her constant challenging of information created a mindset within the lab that forced me, along with everyone else, to approach problems from all angles and to be firm in my convictions without being closed-minded. Over the past six years, I have developed a strong sense of certainty in myself that I can attribute largely to my time in Doris's lab. More than any scientific skill, I thank her for that.

I would also like to thank all past and present Stoffers lab members, especially Dr. Katy Claiborn, for introducing me to the wide world of Pcif1 and answering every single tiny question I had as a new student, Dr. Scott Soleimanpour, for your creative solutions and boundless enthusiasm, Dr. Jeff Raum, for your honest opinions, even when I didn't really want to hear them, Dave Groff, for wrangling more mice than I care to remember and keeping me caught up on all the gossip, Drs. Andrea Rozo, Christine Juliana, and Diana Stanescu, my outlets for girl talk and silliness, and the future Dr. Austin Good, whom I know will go on to do remarkable things.

I greatly appreciate the support and guidance provided by my committee: Drs. Klaus Kaestner, Morrie Birnbaum, Margaret Chou, and Alan Diehl. Throughout the years, they have all helped guide this work past innumerable obstacles. I am also grateful to the entire Birnbaum lab, particularly Drs. Paul Titchenell and Will Quinn, for taking me in as a temporarily orphaned grad student and for being a tremendous source of advice, assistance, and encouragement. I would also like to thank our collaborators as well as the facilities at Penn without whom many of these experiments would not have been

possible. I am also grateful for the support I received from the Pharmacology training grant, as well as from Doris's NIH funding sources.

I would like to thank my friends in the Pharmacology Graduate Group, who were always ready with a celebratory (or consoling) drink and provided a sounding board for problems both personal and scientific. I would especially like to acknowledge Dr. Melissa Love, for always being there with a smile and a hug, Drs. Gabriel Krigsfeld, Michael Brewer, and Edward Chen, for always being there with a friendly insult and a hug, Drs. Ania Payne and Abby Christian, for helping me through the crazy interview process and being incredibly supportive throughout, and the future Dr. Shane Poplawski, for food trucks, scotch, and cynicism that rivals my own. I would also like to acknowledge the wonderful people brought into my life through their association with this crazy PGG program. My time in Philadelphia would not have been the same without some non-scientists to balance us all out.

My family has been a constant source of support, no matter what crazy thing I choose to take on, and for this I am eternally grateful. I could not have made it as far as I have without my mother's enthusiasm and motivation, my father's sage advice and unwavering belief in me, my sister's bottomless encouragement and quirky sense of humor that matches mine so much it's scary, and finally the boisterous cheerleading section comprised of aunts, uncles, grandparents, cousins, and honorary family members.

Lastly, I would like to thank Mike Porter. He taught me to love Philadelphia, appreciate good beer, and grudgingly enjoy sports. I cannot wait to start the next out of what I'm sure will be many adventures. Boston, here we come!

ABSTRACT

MAINTAINING GLUCOSE HOMEOSTASIS IN RESPONSE TO AGING AND STRESS: THE ROLE OF PCIF1, BMI1, AND PDX1

Corey Cannon

Doris Stoffers, M.D., Ph.D.

A sufficient number of functioning beta cells is necessary for maintaining glucose homeostasis. Reduction of beta cell mass or function leads to diabetes. Investigation into the maintenance of both beta cell mass and function is important for the development of therapies to prevent and/or restore functional beta cells. Here, the networks surrounding three proteins in the beta cell, Pcif1, Bmi1, and Pdx1, were studied as they relate to beta cell function and number. The Polycomb protein, Bmi1, has been shown to influence beta cell replication via epigenetic repression of the *Ink4a/Arf* locus, resulting in suppression of p16 protein translation. The adapter protein, Pcif1, facilitates the ubiquitination of Bmi1 and influences beta cell replication, as *Pcif1* heterogyzous mice have increased rates of beta cell proliferation. I hypothesized that Pcif1 regulates beta cell proliferation through a Bmi1-dependent mechanism. Analysis of *Pcif1* heterozygous islets revealed that p16 protein levels were indistinguishable from controls, thus making a p16-dependent mechanism unlikely. Further investigation of Bmi1 targets may reveal another pathway by which Pcif1 and Bmi1 influence beta cell replication. The role of Bmi1 has not been well-described in adult animals. Analysis of *Bmi1* heterozygous animals revealed increased insulin sensitivity, as compared to wildtype. This was found to be due to an enhancement of Akt phosphorylation, with the upstream insulin signaling pathway unaffected. Bmi1 also appears to play a role in the development of insulin resistance, as Bmi1 levels are high in insulin-resistant animals. I also began to explore the possibility that the action of Pcif1 on Bmi1 is responsible for

the role Bmi1 plays in insulin signaling. The transcription factor, Pdx1, regulates numerous processes specific to the beta cell, including multiple pathways regulating translation. Pdx1 levels have been shown to affect the ability of beta cells to respond to ER stress. A global analysis of translational efficiencies using the TRAP methodology indicated that Pdx1 activity may result in repression of translation of some transcripts. Further analysis of these transcripts will help determine how Pdx1 regulates the translatome of the beta cell and, potentially, how Pdx1 influences the beta cell stress response.

TABLE OF CONTENTS

LIST OF FIGURES

CHAPTER 1: INTRODUCTION

1.1 Diabetes

Diabetes is one of the top causes of premature death, affecting nearly 350 million people worldwide [1]. Overt diabetes results when the body's need for insulin, a hormone synthesized and secreted solely from the beta cells of the pancreas and necessary for maintaining glucose homeostasis, exceeds the amount released. The release of insulin is stimulated by elevated blood glucose levels and stimulates glucose uptake by peripheral tissues, as well as inhibiting lipolysis in adipose tissue and liver glucose production. If there is insufficient insulin released, blood glucose levels remain too high, leading to vascular, nerve and renal complications, among others.

Type 2 diabetes is characterized by a relative insulin deficiency and is associated with insulin resistance in the peripheral tissues. Hence, more insulin must be released in order to elicit the same effect [2]. Distinct from Type 1 diabetes, this insulin deficiency is not due to autoimmune destruction of beta cells but rather the failure of beta cells when chronically placed under high demand for insulin.

In the early stages of insulin resistance, the body is able to compensate by releasing more insulin, thereby maintaining normal blood glucose levels. As the condition persists without intervention, insulin-producing beta cells begin to fail and ultimately results in overt diabetes. The point at which beta cell failure and insulin resistance converge, resulting in a diabetic state, varies widely from person to person. In most cases, Type 2 diabetes develops due to a complex combination of environmental factors and multiple

genetic predisposing factors. Single gene mutations are only the cause in rare cases [3], [4].

1.2 Insulin-producing and -responsive tissues

1.2.1 Glucose sensing and insulin release by pancreatic beta cells

Pancreatic islets are clusters of hormone-producing cells of five types: glucagon-producing alpha cells and insulin-producing beta cells, that function antagonistically to maintain glucose homeostasis, somatostatin-producing delta cells, pancreatic polypeptide-producing PP or gamma cells, and ghrelin-producing epsilon cells [5]. When blood glucose levels are low, glucagon action raises glucose levels by stimulating hepatic glucose production. In contrast, when glucose levels are high, insulin action lowers glucose levels by halting hepatic glucose production and stimulating uptake and storage in peripheral tissues.

Sensing of blood glucose levels by the beta cells is a key step in the maintenance of glucose homeostasis. Beta cells express a glucose transporter, GLUT2 (additionally GLUT1 in humans), which brings glucose into the cell. The rate of glycolysis that follows is proportional to the glucose concentration in the blood and results in shifting of the [ATP]/[]ADP] ratio. As Illustrated in **Figure 1.1**, when glucose levels are high, the resulting high [ATP]/[]ADP] ratio causes the ATP-dependent K^+ channels to close and results in a depolarization of the cell membrane and subsequent opening of the voltage-gated Ca^{2+} channel. Calcium influx stimulates the exocytosis of insulin granules, releasing insulin into the bloodstream (reviewed in [6]). Insulin secretion occurs in a biphasic manner. The first phase begins quickly but dissipates after a short time, whereas the second phase is more sustained [7].

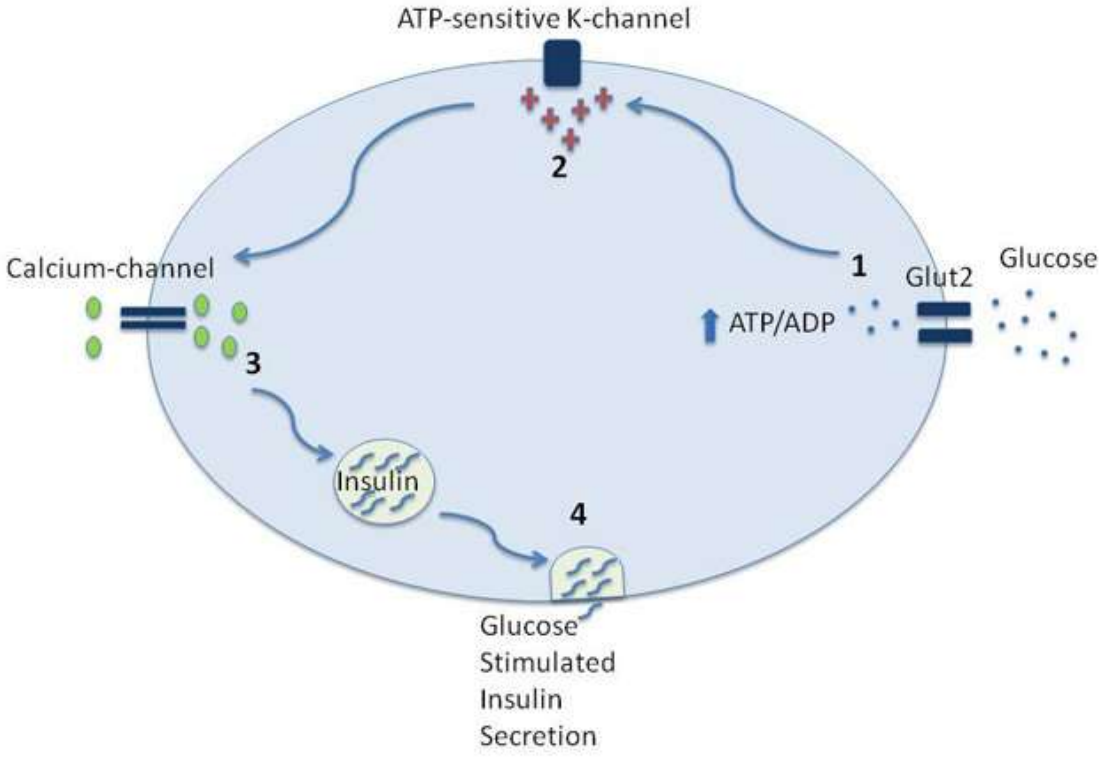

Figure 1.1. Glucose sensing and release in beta cells. (1) GLUT2 transports glucose into the cell, which shifts the ATP/ADP ratio. (2) ATP-dependent K+ channels close. (3) Membrane depolarization opens Ca2+ channels. (4) Calcium stimulates insulin release. (Adapted from [5])

1.2.2 Beta cell proliferation

Beta cell proliferation rates decrease significantly throughout an animal's lifespan [8],[9],[10]. Finegood et al reported a decrease in daily beta cell proliferation rates from 20% at birth to 2% by adulthood [11] while Teta et al demonstrated an even more reduced beta cell proliferation rate in aged adult mice, finding that less than 1% of adult beta cells replicate per day by one year of age [8]. However, modest beta cell injury with low doses of the beta cell toxin streptozotocin was sufficient to induce beta cell proliferation in these aged mice, indicating that the beta cells were not post-mitotic.

Cellular proliferation rates depend on a balance of both stimulatory and repressive signals, illustrated in **Figure 1.2**. In murine beta cells, the cyclin-dependent kinase 4 (Cdk4)- cyclin D2 complex phosphorylates retinoblastoma protein (Rb), inactivating it

and allowing progression into S phase [12],[13]. Further upstream of the Cdk4/D-cyclin complex are products of the *Ink4a/Arf* locus (Inhibitor of Kinase 4/Alternative Reading Frame), including $p16^{ink4a}$ and $p19^{Arf}$. INKs inhibit the kinase activity of CDKs, eliciting cell cycle arrest. It has become clear that INKs also play a role in cell cycle control in the beta cell [14]. Evidence for the role of p16 in cdk4 repression was provided by Rane et al, who created a constitutively active cdk4 by deleting the residues necessary for interaction with p16 [15]. Expression of p16 increases over the lifespan of a murine model of aging and is thought to correlate with cellular senescence [16].

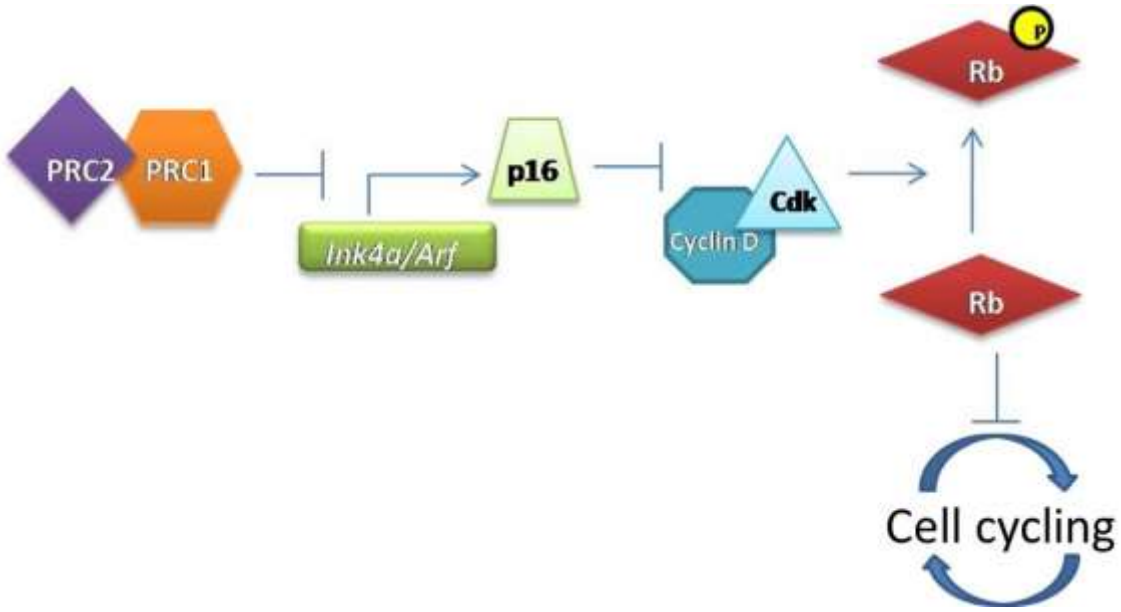

Figure 1.2. Regulation of cellular proliferation

1.2.3 Insulin signaling

On a molecular level, circulating insulin binding to the insulin receptor (IR) initiates a complex cascade of cellular events, illustrated in **Fig. 1.3** [17]. Insulin binding stimulates the autophosphorylation of IR and subsequence recruitment of scaffolding proteins, including the insulin receptor substrate (IRS) proteins 1-6, which are themselves

phosphorylated upon recruitment [18–23]. The most well-characterized targets of the phosphorylated IRS proteins are the p85 regulatory subunit of phosphatidylinositol 3-kinase (PI3K) and the adaptor molecule growth factor receptor-bound protein 2 (Grb2) [24,25].

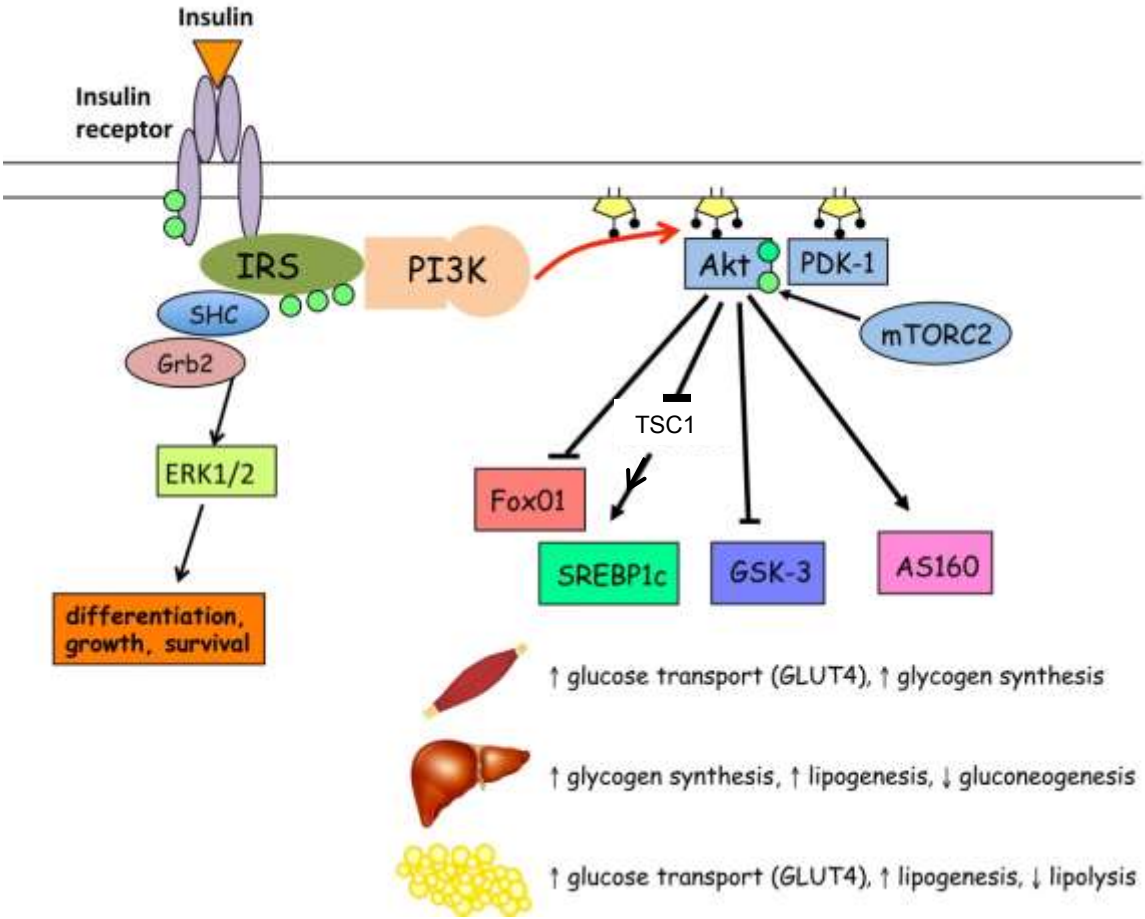

Figure 1.3. Overview of insulin signaling pathway. Insulin binding to receptor initiates insulin signaling cascade. Green circles represent phosphorylation events. Yellow pentagons represent ADP/ATP. (adapted from [5])

Interaction of the IRS proteins with p85 recruits the catalytic subunit, p110, which catalyzes the conversion of phosphatidylinositol-4,5-bisphosphate (PIP_2) to phosphatidylinositol-3,4,5-trisphosphate (PIP_3). PIP3 recruits PH domain-containing proteins, such as 3-phosphoinositide-dependent protein kinases 1 (Pdk1) and Akt (also

known as protein kinase B). Colocalization of Pdk1 and Akt facilitates phosphorylation of Akt, thereby activating it [26]. In turn, Akt phosphorylates glycogen synthase kinase 3 (Gsk3), AKT substrate 160 (AS160), forkhead box O1 (Foxo1), and tuberous sclerosis complex 1 and 2 (Tsc1 and Tsc2) to mediate increased glycogen synthesis, increased glucose uptake, decreased gluconeogenesis, and increased protein synthesis, respectively [27,28].

Co-recruitment of Grb2 and son of sevenless (Sos) to phosphorylated IRS initiates the ERK arm of the insulin signaling cascade. This results in activation of Erk1 and Erk2, whose targets include ribosomal protein S6, involved in protein translation, as well as several transcription factors, leading to the mitogenic effects of insulin. (Insulin signaling reviewed in [25,29])

Shown in **Figure 1.4** is the normal insulin signaling pathway throughout the body. Circulating insulin signals peripheral tissues to take up glucose and signals, given the abundance of available circulating glucose, to repress production of glucose by the liver and lipolysis in fat tissue [30]. Figure 1.3 illustrates multiple factors that can contribute to the diabetic phenotype, targeting both the beta cells themselves as well as the peripheral tissues. Ultimately it is the combination of insulin resistance and beta cell failure that lead to overt diabetes.

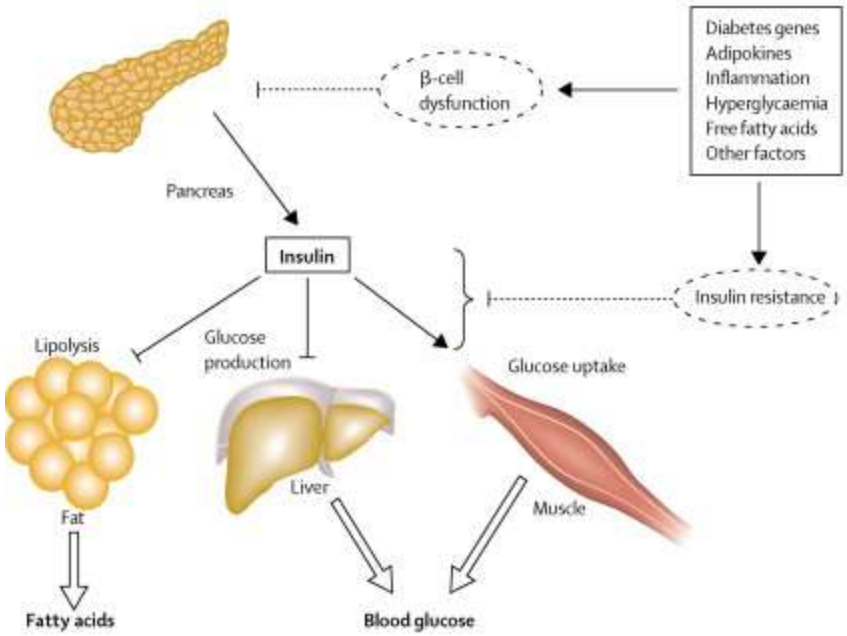

Figure 1.4. Overview of insulin signaling to peripheral tissues and pathophysiological disruptions of normal signaling. (Adapted from [30])

1.2.4 Insulin response in metabolic tissues

One of the primary actions of insulin is to regulate energy storage and production in a tissue specific manner. In the liver, insulin acts to repress glycogenolysis and gluconeogenesis, whereas in adipose tissue it results in halting of lipolysis via activation of a cAMP-dependent protein kinase (PKA) [31].

In addition to halting the production of endogenous energy sources, insulin stimulates the uptake and storage of glucose, in a tissue specific manner, through stimulation and recruitment of the GLUT4 glucose transporter to the cell surface, thereby enabling glucose uptake into the cell. Uptake of glucose by muscle accounts for approximately 75% of glucose disposal, with the remainder taken up by liver and adipose tissue [6]. In

adipose tissue, insulin stimulates activation of enzymes needed for lipid synthesis, and signals the storage of incorporated glucose into lipid.

Insulin receptors are expressed, to varying degrees in all tissues [32]; therefore, in order to dissect the distinct roles of insulin signaling has in individual metabolic tissues, tissue-specific ablation of insulin signaling was induced via Cre/lox-mediated deletion of the insulin receptor in liver, muscle, fat, and beta cells [33–36].

Deletion of IR in the liver (LIRKO mice) highlights the importance of hepatic insulin signaling in glucose homeostasis and insulin sensitivity [33]. These mice display severe fed hyperglycemia and hyperinsulinemia, as well as an abolishment of insulin-induced suppression of hepatic glucose production. Additionally, there is a gene expression pattern consistent with fasted state, despite high circulating glucose levels—high expression of gluconeogenic enzymes and decreased expression of glycolytic enzymes. Circulating levels of free fatty acids and triglycerides are reduced, indicating that the response of adipose tissue to insulin is intact. Additionally, these mice have significant beta cell hyperplasia due to a compensatory response in order to meet demand for high insulin levels. Together, the phenotype of the LIRKO mouse affirms the importance of the liver in whole-body insulin sensitivity. However, given the lack of severe fasting hyperglycemia, dysregulation of insulin signaling in the liver cannot completely explain the development of overt diabetes.

Mice with a targeted deletion of IR in muscle tissue (MIRKO mice) are phenotypically normal, despite almost complete ablation of insulin signaling in muscle on a molecular level, as well as a functional deficiency in insulin-stimulated glucose uptake [34]. The animals display surprisingly normal responsiveness to glucose and insulin boluses but elevated levels of free fatty acids and triglycerides, echoing symptoms of the metabolic

syndrome. Although glucose homeostasis is normal in these animals, in the context of whole-body reduction of IR expression (*IR*$^{+/-}$), deletion of muscle IR results in severe hyperglycemia and insulin resistance. This could imply that insulin resistance in muscle is not the primary defect in the pathogenesis of diabetes but that it can act to exacerbate deficiencies in other tissues. Additionally, functional inactivation of both IR and insulin-like growth factor 1 receptor (*Igf1r*) results in diabetes, suggesting that insulin may be functioning through this alternative pathway in MIRKO animals [37].

Loss of insulin signaling in white and brown adipose tissue via IR deletion (FIRKO mice) results in almost complete ablation of insulin-stimulated glucose uptake and lipolysis inhibition [35]. Fat mass is reduced and leptin levels lose correlation with adiposity. Surprisingly, these mice are protected against age-associated insulin resistance and glucose intolerance as well as hyperphagia-associated obesity. These beneficial phenotypes highlight the complex role of insulin signaling in different tissues.

In additional to the role of insulin signaling on peripheral tissues, insulin also affects the function of the beta cell itself. Loss of the beta cell IR (BIRKO mice) results in a loss of first-phase insulin secretion in response to glucose with no effect on arginine-stimulated insulin release [36]. Not surprisingly, these mice have impaired glucose tolerance with age. Together, the data from these animals demonstrate the importance of insulin signaling for beta cell function that is independent of other metabolic tissues.

1.2.5 Insulin resistance

Insulin resistance is one of the hallmarks preceding development of overt diabetes. It is generally thought that three main, interrelated physiological disruptions contribute to the development of insulin resistance: accumulation of excess lipid, endoplasmic reticulum (ER) stress, and inflammation [38].

Excess adiposity has long been associated with insulin resistance and diabetes. In addition to accumulation of adipose tissue, lipid can also deposit in other metabolic tissues, such as liver and muscle. Further, excess lipid will result in higher than normal levels of circulating lipids. Ectopic accumulation of lipids in muscle has been shown to impair glucose uptake. Lipid accumulation in the liver, hepatic steatosis, typically results specifically in hepatic insulin resistance. Reversal of steatosis improves hepatic insulin sensitivity [38].

As the impairment to insulin responsiveness progresses, glucose levels remain high, thereby stimulating the release of more insulin in order to maintain glucose homeostasis. Given that far less insulin is required to stimulate lipid storage than glucose uptake, this differential response of different arms of the insulin signaling pathway further exacerbates the condition. Therefore, stimulation of lipogenesis is typically preserved much longer and results in continued expansion of adiposity [39].

ER stress is also related to excess adiposity, as an increase in circulating fatty acids can cause ER stress in metabolic tissues. However, the mechanism behind this connection is at this point unclear. ER stress has also been connected to lipid accumulation and energy storage. Activation of the transcription factor X-box binding protein 1 (XBP-1) by ER stress results in upregulation of transcription of target genes involved in lipid synthesis and gluconeogenesis. Thus, activation of ER stress pathways by stimuli such as high glucose results in increased energy storage in tissues. This is especially problematic in tissues such as liver which do not normally store lipid. (Reviewed in [40])

Inflammation results in impaired insulin signaling on a molecular level. The eIF2α kinase protein kinase R (PKR) is activated in response to excess lipid and signals to activate

the inflammatory c-Jun N-terminal kinase (JNK) pathway [41]. Additionally, PKR also inhibits IRS1 activity, thereby directly interfering with insulin signaling.

ER stress and inflammation are connected pathways and activation of one can influence the other, both of which negatively alter insulin sensitivity. For example, activation of the unfolded protein response (UPR) results in production of reactive oxygen species (ROS). Although the UPR has mechanisms in place to negate this, such as upregulation of nuclear factor-like 2 (Nrf2), the cell is often overwhelmed and ROS accumulate. High levels of ROS then elicit inflammatory responses [42]. Additionally, through the IRE1α arm, the UPR activates JNK, which is upstream of many inflammatory genes [43]. Inositol-requiring 1 alpha (IRE1α), activating transcription factor 6 (ATF6), and PKR-like ER kinase (PERK) activation have all been implicated in the activation of the inflammatory nuclear factor kappa-light-chain-enhancer of activated B cells (NF-κB) pathway [44–46].

1.2.6 ER stress and diabetes

ER stress and the UPR

The ER is the site of protein translation and folding in the cell. Newly-translated proteins must fold into their final conformations in order to function properly once exiting the ER. Sometimes, proteins are unable to mature properly and unfolded proteins accumulate in the ER. When this happens, a process known as the unfolded protein response (UPR) is activated. The goal of the UPR is to restore ER homeostasis or, if this is not possible, initiate apoptosis of the cell, thereby removing damaged cells from the organism. The UPR first attempts to resolve ER stress by upregulating production of chaperone proteins to aid in protein folding, expanding the ER membrane, and downregulating protein synthesis until homeostasis can be restored. Together these actions make up the

adaptive response phase of the UPR. It is only after these attempts fail that apoptosis is initiated (reviewed in [47–49]).

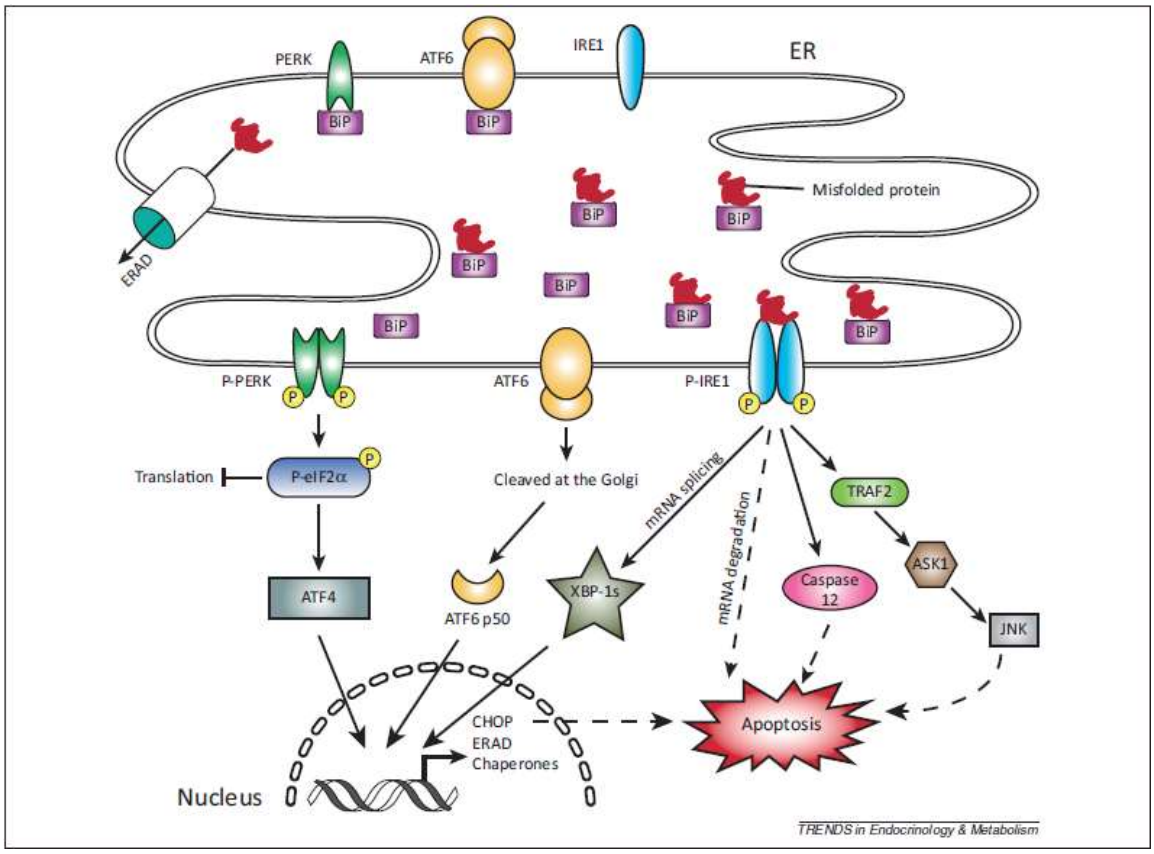

Figure 1.5. Canonical ER stress and UPR pathways. PERK, IRE1α, and ATF6 shown in inactive (top of diagram) and active forms (bottom of diagram). Misfolded proteins (red) are degraded via ERAD and activate UPR pathways. From [46].

There are three transmembrane proteins that serve as sensors of ER stress in the cell: inositol-requiring 1 alpha (IRE1α), activating transcription factor 6 (ATF6), and PKR-like ER kinase (PERK). Normally, these sensors are bound by the chaperone immunoglobulin heavy chain binding protein (BiP). However, BiP preferentially binds misfolded proteins, thereby releasing the ER stress sensors and activating them [47]. More recently, it has been shown that misfolded proteins themselves can bind IRE1α, acting as activating ligands in the absence of BiP [48,50].

Once active, each arm of the UPR acts on independent downstream targets, all with the common goal of restoring ER homeostasis. Activated IRE1α functions as an endoribonuclease, cleaving the *X-box binding protein 1* (*Xbp1*) transcript. Translation of the cleaved *Xbp1* results in translation of spliced XBP1 (XBP1s) protein, a transcription factor targeting UPR-specific genes. Activation of ATF6 results in its translocation and subsequent proteolytic cleavage in the Golgi. Cleaved ATF6 is itself an active transcription factor which targets genes such as chaperones and protein disulfide isomerase (PDI). Activated PERK acts as a protein kinase, phosphorylating the translation initiation factor 2 alpha (eIF2α), Phosphorylation inactivates eIF2α, resulting in an immediate halting of cap-dependent translation initiation. Once translation is downregulated on a global scale, translational machinery can be redirected to upregulate translation of certain transcripts important for restoring ER homeostasis, such as *Atf4*. This translation happens in an eIF2α-independent manner (reviewed in [47,48,51,52]).

Causes of ER stress in the beta cell

Accumulation of misfolded proteins in the ER can occur due to protein demand that overloads the capacity of the ER or due to ER deficiencies that compromise folding efficiency. Beta cells are particularly susceptible to ER stress, given the high protein synthesis load placed on them. Beta cells can manufacture 1 million insulin molecules per minute under high glucose conditions [53]. In the event of inefficient folding or processing, these cells are therefore at a high risk for misfolded protein overwhelming the capacity of the ER. Due to this constantly high need for insulin production, the UPR is often activated in beta cells, at least at a low level, until ER homeostasis is restored. In fact, activation of IRE1α is necessary for the stimulation of proinsulin production in

response to acute glucose exposure [54]. Thus, physiological levels of stimuli, such as glucose, are part of normal beta cell ER function.

However, pathophysiological conditions, such as insulin resistance, can increase the demand for insulin, thereby increasing ER stress in the beta cells [52]. Additionally, chronically high glucose leads to chronic ER stress and inhibition of translation, including translation of proinsulin [54]. Perhaps more important than chronically high glucose levels in causing beta cell ER stress is lipotoxicity, or toxically high levels of circulating fatty acids, a condition common in obesity [55,56]. Experimentally, high fatty acid levels are sufficient to recapitulate ER stress seen in diabetic patients.

Pharmacological ER stress agents, such as thapsigargin and tunicamycin, are often used to generate high levels of ER stress in experimental settings. Typically, the stress generated cannot be resolved by the cells and ultimately leads to apoptosis. This is in contrast to more physiologically relevant settings, where the cells often are able to resolve stress and restore normal protein production [47].

Stress-induced remodeling of translatome

The majority of mammalian translation is dependent on a unique feature of the 5' end of the mRNA, the methylguanate cap. It is this feature that is recognized by translation initiation factors and begins the process of mRNA translation. As noted earlier in this chapter, one of the strategies utilized by the UPR in order to combat ER stress is to globally downregulate protein translation. This repression is typically at the level of translation initiation, targeting cap-dependent factors such as 4E-BPs and eIFs (Reviewed in [51]). However, in order to properly resolve the stress, translation of certain transcripts are upregulated. By activating these factors, the cell can attempt to deal with the stress and if the situation cannot be fixed, an apoptosis cascade can be initiated. In

these situations, translation is carried out in a cap-independent manner. This is thought to occur through an internal ribosome entry site (IRES), which are specialized mRNA elements that allow recruitment of eukaryotic ribosomes to naturally uncapped mRNAs or to capped mRNAs under conditions in which cap-dependent translation is inhibited [57].

Cellular stress can induce a global remodeling of the translatome of a cell. Ventoso et al described the translatome of two cells lines, NIH3T3 and Jurkat, before and after induction of ER stress by thapsigargin. They found that approximately half of the transcripts analyzed had reduced translational efficiency in response to stress, consistent with the model of UPR-mediated downregulation of translation. Interestingly, they also characterized two other groups of transcripts: those that were resistant to downregulation and maintained the same level of translational efficiency and those whose efficiencies were actually increased in response to stress. Not surprisingly, many of the transcripts in these two groups encoded proteins known to be associated with stress response, such as HSPA5 (BiP) and ATF4 [58].

Regulation of translation in the beta cell

One potential regulator of the stress response specifically in beta cells is the pancreatic and duodenal homeobox 1 (Pdx1). Pdx1 is a transcription factor that is indispensable in pancreas development [59–61]. Additionally, Pdx1 is crucial for maintenance of postnatal beta cell identity and function and low Pdx1 expression is associated with the diabetic state [62–64].

Pdx1-deficient mice exhibit evidence of increased ER stress in their beta cells in response to a high fat diet. Additionally, reduction of Pdx1 levels makes cells more susceptible to pharmacologically-induced ER stress and the resulting apoptosis [65].

Pdx1-deficient mouse insulinoma (Min6) cells had reduced levels of a number of genes associated with ER stress response, including *Atf4* and *BiP*. Pdx1 was further found to directly occupy the *Atf4* promoter. In *Pdx1*$^{+/-}$ islets, not only is Atf4 transcript reduced, mirroring the effect in Min6 cells, but the direct target of Atf4, *Eif4ebp1*, is also reduced [65]. The eIF4EBP1 (or 4E-BP1) protein directly inhibits translation by physically sequestering the translation initiation factor, eIF4E. These data suggest that Pdx1 may play a role in regulating rates of cap-dependent translation through regulation of Atf4.

Another target of Pdx1 in the beta cell is microRNA 7 (miR-7). miR-7 was demonstrated to target the mTOR complex and inhibition of miR-7 resulted in increased mTOR activity and upregulation of the downstream target of mTOR, ribosomal protein S6 kinase (p70S6K) [66]. Additionally, miR-7 was shown to target MAPK-interacting Ser/Thr kinase 1/2 (MNK1/2), which regulates translation via eIF4E phosphorylation. Pdx1, via regulation of miR-7, is thereby further implicated in regulation of cellular translation. Given the high level of stress placed on beta cells, as well as the propensity for failure if not kept in check, the specific response of the beta cell to stress will be important in fully understanding the development of diabetes.

1.2.7 Beta cell compensation and failure in Type 2 Diabetes

Beta cell mass is determined by the net result of both cell death and the appearance of new cells, either via proliferation of existing cells or, more controversially, the conversion of non-beta cells into beta cells [67]. As shown by *in vitro* and *in vivo* experiments, glucose is a key stimulus for beta cell proliferation and, under conditions where insulin demand is high, such as insulin resistance and hyperglycemia, beta cell mass will expand to compensate [68–71]. This expansion will increase the amount of insulin the pancreas is able to produce, thereby counterbalancing the increased demand. Individual

beta cells are also able to adjust to increased insulin demand via hypertrophy resulting in an increase in insulin production and secretion per cell [72].

The combination of proliferation and hypertrophy to expand beta cell mass is typically sufficient to respond to physiological increases in demand for insulin, such as growth, pregnancy, and aging. However, beta cells that are unable to expand sufficiently will result in uncontrolled glucose homeostasis, beta cell dysfunction, and, eventually, diabetes [73]. Many factors contribute to whether an individual's beta cells will fail to compensate. Extreme insulin resistance in peripheral tissues that pushes insulin demand far beyond normal will begin to exhaust the capacity of beta cells to compensate [67]. Additionally, genetic factors can determine what the "upper limit" of any one person's beta cell mass will be [73]. Once the demand for insulin surpasses that limit, beta cells are no longer able to maintain glucose homeostasis.

1.3 Ubiquitination

1.3.1 Ubiquitin

Ubiquitin is a small molecule that can be post-translationally conjugated to target proteins in order to modify the action or stability of the protein [74]. The process of adding one or more ubiquitin molecules requires the activity of three enzymes. First, a ubiquitin-activating enzyme, or E1, adenylates and binds the ubiquitin molecule in an ATP-dependent manner, thereby "activating" it. The adenylated ubiquitin molecule is recognized by and transferred to a ubiquitin-conjugating enzyme, or E2, of which there are approximately 30 in mammals. Finally, the E2-ubiquitin complexes with one of over 300 ubiquitin ligases, or E3s, which facilitate the transfer of the ubiquitin onto a lysine residue of the target protein. Ubiquitin molecules typically bind covalently to lysine residues of target proteins, although non-canonical ubiquitination of cysteine, tyrosine,

serine, and threonine sites, as well as the N terminal of target proteins, have been described. There is no known consensus sequence for ubiquitination [75].

Increasing levels of specificity exist as the ubiquitin molecule moves along the process described above. E1 enzymes bind promiscuously to E2s. E2 enzymes interact with a subset of E3s and, finally, each E3 targets an even smaller number of target proteins. This specificity allows for precise targeting of ubiquitin molecules to intended substrate proteins. (Ubiquitination reviewed in [74])

Ubiquitination of identified targets can occur as a monoubiquitination or as a polyubiquitin chain. The ubiquitin molecule contains seven lysine residues. Polyubiquitin chains are formed when the C-terminal glycine residue of a new ubiquitin molecule binds the amine group of one the lysines on the original ubiquitin. This process may be repeated to form long chains of ubiquitin molecules. The presence of seven potential lysines with which to form linkages allows for almost infinite possibilities of heterogeneous ubiquitin chains. These chains can be linear or branched, with more than one ubiquitin linked to the preceding molecule. Additionally, chains of ubiquitin have been identified that contain other non-ubiquitin small molecules, such as the small ubiquitin-like modifier (SUMO) [76]. Single or multiple monoubiquitinations have also been described [77]. Together, these many potential options make ubiquitination one of the most diverse post-translational modifications [77].

1.3.2 Ubiquitination leading to degradation

Polyubiquitin chains can target proteins for degradation by the 26S proteasome [78,79]. The proteasome is a cylindrical protein complex with a protease-lined central pore through which target proteins pass and are degraded. Proteasomal degradation allows for the removal of damaged or unneeded proteins, recycling the amino acids for

incorporation into new proteins. Targeting to the proteasome is the most well-characterized result of ubiquitination and as such, this targeting by polyubiquitin chains homogeneously linked through lysine 48, has historically been thought to be the primary role of ubiquitin.

Polyubiquitin chains formed through linkages at lysine 48 were originally described as identifying target proteins for proteasomal degradation [80,81]. More recently however, other homogenenous chains have been shown to be capable of targeting to the proteasome [82].

1.3.3 Ubiquitin as a non-degradative posttranslational modification

Compared to the classically-described degradative role of polyubiquitination, less is known about the roles of other poly- and monoubiquitin modifications. In some cases, specific E2/E3 combinations result in atypical mono- or polyubiquitinations [82].

Polyubiquitin chains formed through linkages other than lysine 48 have been shown to modify the action of proteins involved in a broad range of cellular functions. The results of these modifications include invocation of the DNA damage response, regulation of cell cycle proteins, trafficking to the membrane, promotion of nuclear translocation, initiation of mitophagy, and activation of cytokine signaling [77,83].

Ubiquitin has also been shown to modify histones, thereby influencing transcription rates of genes at those sites. Ubiquitination of histone H2A has been well described, as well as, more recently, H2B and H3. Generally, ubiquitination of H2A at lysine 119 is thought to be associated with silencing of gene expression, although the exact mechanism is unclear [84].

1.4 Pcif1

1.4.1 Properties of Pcif1

Pdx1 C-terminal interacting factor (Pcif1), also known as speckle-type POZ protein (SPOP), is a substrate-specific adapter that facilitates ubiquitination of target proteins by the Cullin3-based E3 ligases and was initially identified in the serum of a scleroderma patient [85]. The Pcif1 protein contains a meprin and TRAF homology (MATH)/TNF receptor-associated factors (TRAF) domain and a bric-a-brac, tramtrack, and broad complex (BTB)/Pox virus and Zinc finger (POZ) domain and is highly evolutionarily conserved [86]. TRAF-domain containing proteins are generally found to be involved in protein processing and ubiquitination. As in Pcif1, TRAF domains are often found in proteins that also contain BTB domains. TRAF/BTB proteins have been shown to facilitate interaction between E3 ligases and target proteins [87].

Non-mammalian orthologs of SPOP have been shown to exhibit the predicted activity described above. The *C. elegans* ortholog, maternal effect lethal (MEL) -26, facilitates interaction of meiosis inhibitor 1 (MEI-1) with the scaffolding protein Cullin3, resulting in ubiquitination [88,89]. The *Drosophila* ortholog, *Roadkill*, modulates Hedgehog signaling by targeting the Gli-family transcription factor Cubitus interruptus (Ci) for degradation [90]. Additionally, Roadkill promotes TNF-mediated apoptosis via ubiquitination of the JNK phosphatase Puckered (Puc) [91]. The roles for SPOP targeting of Hedgehog and TNF signaling are also conserved in humans [91,92].

1.4.2 Pcif1 in the beta cell

Pcif1 is broadly expressed in many human tissues, including the beta cells [85,86]. Pcif1 was also found to interact with the C terminus of Pdx1, a transcription factor necessary

for maintaining function and identity of the beta cell, thus implicating it in beta cell biology [86]. Further characterization of the role of Pcif1 in the beta cell revealed a direct impact on Pdx1 protein levels via ubiquitination and subsequent proteasomal degradation, as described with other targets [93]. Pcif1 also has a role in the maintenance of beta cell mass via modulation of the rates of both replication and apoptosis, although the mechanism for these processes is not clearly defined at this time.

Pcif1 heterozygosity results in an accumulation of Pdx1 protein [93] and can normalize Pdx1 protein levels in *Pdx1*$^{+/-}$ animals, thereby rescuing many phenotypes associated with decreased Pdx1 protein, including beta cell mass, beta cell survival, and glucose homeostasis.

The role for Pcif1 in cell cycling is complex, as it appears to involve a fine balance between rates of replication and apoptosis that occurs in an age-dependent manner [93]. Pcif1 has been shown to interact with both the death domain-associated protein, Daxx, which has been implicated in both apoptosis and cell cycle regulation [94,95], as well as the polycomb protein Bmi1, which is well known for its role in regulation of p16-dependent cell replication [96] offering a potential mechanistic explanation for the alteration of replication and apoptosis rates in *Pcif1* heterozygous animals.

1.5 Polycomb group proteins

1.5.1 Discovery and classic roles of PcG proteins

Polycomb group (PcG) proteins assemble into multi-subunit complexes and repress target genes. Polycomb Repressive Complex 2 (PRC2) initiates repression and PRC1 maintains repression via histone methyltransferase and ubiquitin E3 ligase activities, respectively [97], [98]. Beyond their histone modifications, the complexes repress

transcription via chromatin compaction, thereby limiting access for transcriptional machinery.

The Polycomb complexes were first characterized in Drosophila but found to be much more complex in mammalian cells, with many subunits having multiple homologues. PRC2 consists of three core elements: the catalytic component enhancer of zeste (EZH), embryonic ectoderm development (EED), and suppressor of zeste (SUZ). PRC2 deposits methylation marks on lysine 27 of histone 3 (H3K27me3), thus initiating repression of the genes in the targeted region [99]. PRC1 consists of 4 components: chromobox-domain protein (CBX), which recognizes the H3K27me3 mark deposited by PRC2, an E3 ligase ring finger protein (RING), a polycomb group RING finger protein (PGCF), and a polyhomeotic-like protein (HPH) [100]. The RING protein catalyzes the deposition of ubiquitin on lysine 119 of histone H2A (H2Ak119ub1) [98,101].

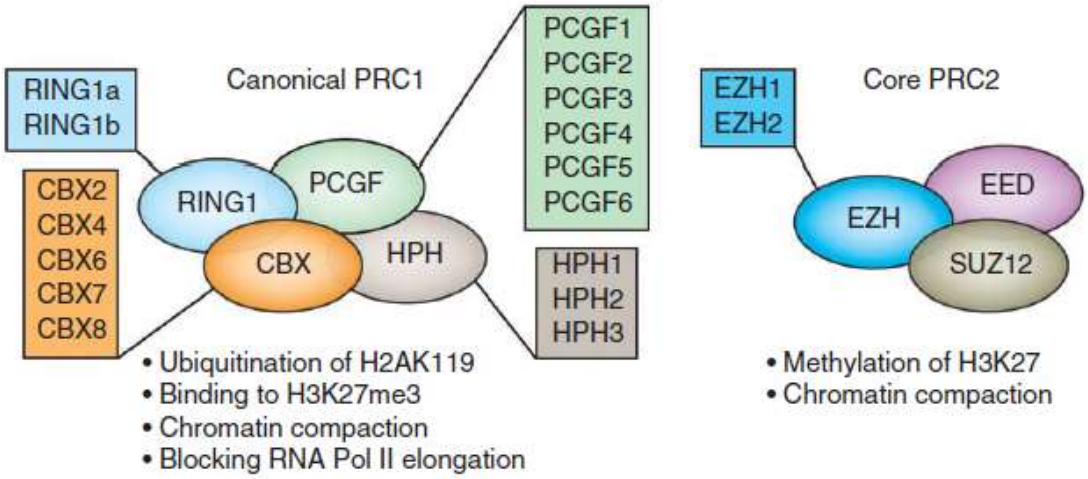

Figure 1.6. Canonical PRC components. (From [102])

PCGF4, also known as Bmi1, is a member of PRC1, which represses the *Ink4a/Arf* locus, and overexpression of Bmi1 allows for rapid proliferation, eventually leading to

immortalization of mouse embryonic fibroblasts in culture [103]. Bmi1 was initially identified as an oncogene that cooperates with *c-myc* in B cell lymphomagenesis and was named as such: B cell-specific Moloney Murine Leukemia Virus integration site 1 [104], 17]. Bmi1 was later found to be involved in cell cycle progression and to be necessary for hematopoetic and neural stem cell renewal, as Bmi1-deficient mice have severe hematopoetic and neurological abnormalities [18, [107] p16 expression is elevated in the islets of *Bmi1*$^{-/-}$ mice and this correlates with a beta cell- specific reduction in proliferation, suggesting a critical role for Bmi1 in beta cell proliferative potential [96].

1.5.2 Non-canonical roles of Bmi1

As described above, numerous reports have been published regarding the necessity of Bmi1 expression in maintaining sufficient cell proliferation in many tissues. More recently, it has also been shown that phenotypes exist outside of the Bmi1-*Ink4a/Arf* axis described in section 1.2.5 of this thesis. For example, Molofsky et al showed that deletion of *Bmi1* resulted in almost a complete loss of neural stem cell renewal capability, in both the central and peripheral nervous systems, as well as an almost 50% reduction in adult body weight. Co-deletion of *Ink4a/Arf* completely rescued the stem cell deficiencies, indicating that this phenotype was caused by dysregulation of the classically described pathway. However, body weight was not even partially rescued by concomitant deletion of *Ink4a/Arf* [108].

Another well-characterized phenotype of *Bmi1* null mouse is its severe hematopoietic deficiency. Mice lacking *Bmi1* have almost a complete ablation of splenocytes and thymocytes. Co-deletion of *Ink4a/Arf* results in a rescue of only about one-third of normal cell numbers for both cell populations [109]. This partial rescue implies that although the

role for Bmi1 in regulating expression at the *Ink4a/Arf* locus is important for hematopoetic cell numbers, it is not the entire story.

Bmi1 appears to play different roles depending on the tissue and cell type that is studied. For example, deletion of *Bmi1* inhibits the ability of hepatic progenitor cells to replicate upon stimulation [110]. However, normal hepatocyte replication rates are unaffected, as measured by both BrDU incorporation as well as Ki67 expression. Thus, even within the same tissue type, Bmi1 differentially impacts distinct cell types.

1.5.4 Regulation of Bmi1 expression

The capacity for renewal of endogenous beta cells decreases over time. Older mice have a limited beta cell expansion capacity compared to young mice in response to stimuli such as high fat diet and streptozotocin treatment [111]. In this study, Bmi1 levels increased in young mice in response to high fat diet, whereas older mice had very low Bmi1 levels. Low Bmi1 and correspondingly elevated p16 levels appeared to correlate with a blunted compensatory beta cell mass expansion in these mice. Pancreatic Bmi1 expression is restricted primarily to the beta cells and declines rapidly with age, concurrent with an increase in *Ink4a/Arf* transcript [96]. This age-dependent decline may be beta cell-specific, as previous studies reported no consistent correlation between *Bmi1* levels and age when comparing many tissue types from young and old mice [16].

Although it is known that Bmi1 levels decline early in life [111], it is currently unclear what happens to Bmi1 levels with age. Due to the severely detrimental phenotypes and resulting shortened lifespan associated with Bmi1 deletion [104,107], the function of Bmi1 has not been well studied past early adulthood.

A yeast two-hybrid screen identified Pcif1 as an interacting protein for Bmi1. Further, immunoprecipitation determined that Pcif1, Cullin3 and Bmi1 formed a complex in 293HEK cells, resulting in ubiquitination of Bmi1 [112]. Hernandez-Munoz et al also reported that ubiquitination did not affect Bmi1 protein stability, but did impact the ability of Bmi1 (as part of the PRC1 complex) to repress target genes [112]. This indicates that ubiquitination most likely alters Bmi1 function in some way.

In 2010, Maertens et al. identified a deubiquitinating enzyme, USP7, that interacts with Bmi1, resulting in removal of ubiquitins from it. Suppression of USP7 via shRNA resulted in an increase in *Ink4a/Arf* transcript and a decrease in Bmi1 protein. This would imply that ubiquitinated Bmi1 protein is less stable and therefore the increase in target transcript is due to decreased Bmi1 levels, not function [113]. This study did not, however, specifically address ubiquitination of Bmi1 by Pcif1. Therefore, the exact role of Pcif1 on Bmi1 stability and/or function remains unclear.

Another modification shown to influence Bmi1 protein is phosphorylation. Nacerddine et al. demonstrated that active Akt can phosphorylate Bmi1 in a number of tumor cell lines and *in vitro*. This phosphorylation enhanced the ability of Bmi1 to facilitate H2A ubiquitination and was found to be necessary for Bmi1's oncogenic activity [114].

Voncken et al. described a correlation between Bmi1 phosphorylation state and its association with chromatin. Phosphorylation and chromatin association were further found to be regulated by cell cycle stage [115]. In a subsequent publication, Voncken et al. demonstrated that Bmi1 is phosphorylated by MAPK-activated protein kinase 3 (3pK) [116]. This phosphorylation caused a dissociation of Bmi1 and other PcG proteins from chromatin, thereby nullifying their ability to repress target genes. Thus, Bmi1 (and PRC2)

activity has been shown to be dynamically regulated by a number of inputs, including activation of both Akt and MAPK pathways.

Chapter 2: Regulation of beta cell proliferation by Pcif1

2.1 Abstract

The ability for beta cells to replicate is crucial for maintaining glucose homeostasis as demands for insulin change with age, obesity, and/or pregnancy. Previously published data indicate that *Pcif1* heterozygosity results in an increase in beta cell replication, whereas *Bmi1* null mice have a severely blunted proliferative capacity. Pcif1 facilitates the ubiquitination of Bmi1, which may lead to its degradation or altered activity. In order to determine whether the ubiquitination of Bmi1 by Pcif1 was responsible for the increase in beta cell replication seen in mice heterozygous for *Pcif1*, glucose homeostasis and Bmi1 activity were assessed in mice heterozygous for *Pcif1* and/or *Bmi1*. A lack of difference in p16 levels in *Pcif1* heterozygous islets indicates that regulation of cell replication via p16 was unlikely. Additionally, *Bmi1* heterozygous animals were more insulin sensitive than controls, making further analysis of beta cell replication in these animals difficult.

2.2 Introduction

Ubiquitination is an important post-translational modification, influencing both protein activity as well as stability. The scaffolding protein Cullin3 (Cul3) has been shown to bind BTB-containing proteins to facilitate the ubiquitination of targets. This complex was first described for the degradation of MEI-1 by Cul3 and MEL-26 in *C. elegans* [117]. This complex has also been shown to form using the mammalian and *Drosophila* orthologs of MEL-26, Pcif1/SPOP and Roadkill, respectively. Pcif and its orthologs have been shown to target a number of critical cellular pathways, including TNF signaling, Hedgehog signaling, Pdx1, and Bmi1 [88,90,94,112,118,119].

A gene trap was inserted into the first intron of the *Pcif1* locus in order to generate mice deficient in *Pcif1* [119]. Homozygous deletion of *Pcif1* is lethal, so the glucose homeostasis of *Pcif1*$^{gt/+}$ mice was studied. In *Pcif1* heterozygous mice, glucose and insulin tolerance are normal. However, closer examination of the pancreas reveals an increase in rates of both replication and apoptosis in beta cells. This results in a no net difference in beta cell mass. However, it does highlight a role for Pcif1 in regulating replication and survival of beta cells. Further, while beta cell survival is impaired in *Pdx1*$^{+/-}$ mice, it is rescued in *Pcif1*$^{gt/+}$;*Pdx1*$^{+/-}$ mice. This is directly due to the fact that Pdx1 is a target of Pcif1. Altering Pcif1 levels were therefore able to shift the balance between replication and apoptosis to rescue beta cell mass and normalize glucose homeostasis [119]. Currently, the mechanism linking Pcif1 to cell cycling is unknown.

Pcif1 facilitates interaction between a Cul3-based E3 ligase complex and target proteins to promote ubiquitination. This has been studied for the beta cell transcription factor, Pdx1, where the overexpression of Pcif1 and Cul3 results in the polyubiquitination and degradation of Pdx1. This is not seen when Cul3 is mutated and unable to interact with Pcif1 [119]. Pcif1 has also been shown to interact with and facilitate ubiquitination of the Polycomb protein Bmi1, a well-characterized epigenetic regulator of p16-dependent cell replication [112].

Bmi1, as a member of PRC1, functions to regulate cellular proliferation rates at least in part through repression of the *Ink4a/Arf* locus. *Bmi1* null mice have a number of abnormalities, including severe ataxia, hematopoetic deficiencies, and skeletal abnormalities [107]. Of particular relevance for this thesis are the phenotypes associated with the beta cell. Beta cell proliferation rates are significantly reduced in *Bmi1* null animals as early as 2 weeks of age, leading to an overall deficiency in beta cell mass [96]. This results in glucose intolerance and blunted glucose-stimulated insulin secretion

(GSIS). Combined, these phenotypes result in a severely shortened lifespan, with almost no animals surviving past 12 weeks of age.

Pcif1 has been shown to ubiquitinate Bmi1 in HEK 293T cells [112]. However, siRNA-mediated suppression of Pcif1 did not affect Bmi1 protein levels, leading Hernandez-Munoz et al. to conclude that Pcif1-mediated ubiquitination was functioning to alter Bmi1 activity, rather than stability. However, without thorough half-life experiments, this conclusion may be premature.

The following studies sought to explain the observation that *Pcif1*$^{gt/+}$ mice have increased rates of beta cell proliferation. We hypothesized that Pcif1 regulates beta cell proliferation through a Bmi1-dependent mechanism, as depicted in **Figure 2.1**. *Pcif1*$^{gt/+}$;*Bmi1*$^{+/-}$ mice were generated in order to test this hypothesis. We predicted that beta cell replication in these animals would be blunted compared to *Pcif1*$^{gt/+}$ mice.

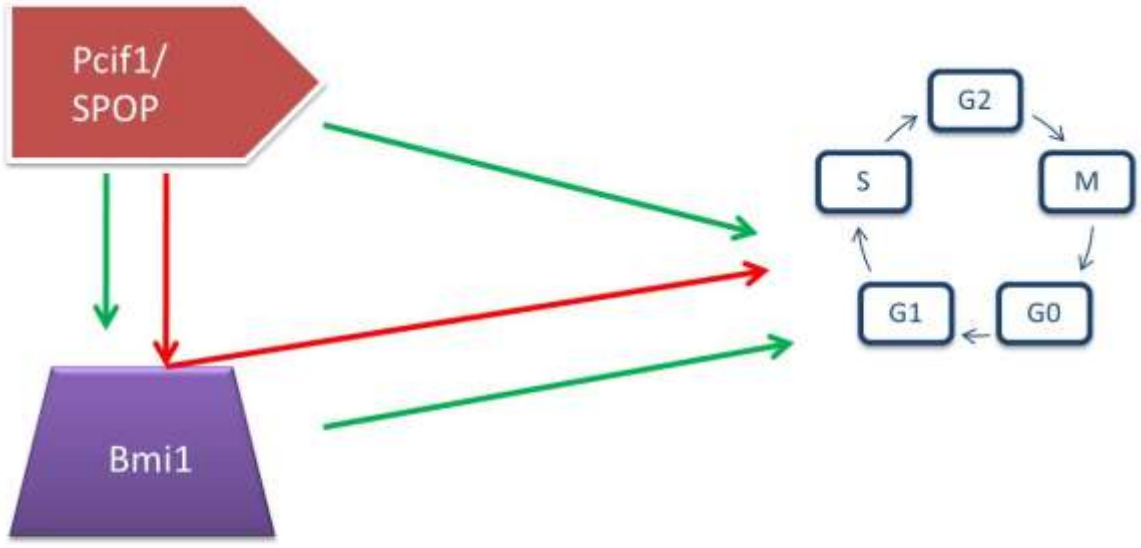

Figure 2.1. Model of known and hypothesized interactions between Bmi1, Pcif1, and cell cycling. Known interactions indicated by green arrows: (1) Pcif1 levels influence cell replication, (2) Pcif1 ubiquitinates Bmi1, possible influencing levels or activity of Bmi1 protein, (3) Bmi1 regulates cell replication via inhibition of the *Ink4a/Arf* locus. Hypothesized pathway connecting Pcif1 to cell replication via Bmi1 indicated by red arrows.

2.3 Materials and Methods

2.3.1 Animals and Physiological Experiments

All animal experiments were performed according to procedures approved by the Institutional Animal Care and Use Committee of the University of Pennsylvania. Animals were placed on high fat diet (60% fat), low fat diet (10% fat) (Research Diets Inc., New Brunswick, NJ) or standard chow at weaning. *Pcif1*$^{gt/+}$ and *Bmi1*$^{+/-}$ mice were previously described [93], [107]. Mice were maintained on a C57BL/6N background. All experiments were performed on males 15-18 weeks of age, except where otherwise noted. For glucose tolerance tests, animals were fasted overnight, given 1 g/kg glucose via IP injection and blood glucose was measured by handheld glucometer at 0, 15, 30, 60, and 120 minutes after injection. For insulin tolerance tests, animals were fasted 6 hours prior to IP injection of 1.0 or 1.5 U/kg insulin (NovolinR, Novo Nordisk, Princeton, NJ) and blood glucose was measured by handheld glucometer at 0, 15, 30, 60, and 120 minutes after injection.

2.3.2 Islet isolation

Islets were isolated from 16 week old males by inflation of the pancreas followed by collagenase digestion, a Ficoll gradient and at least 3 rounds of hand picking. Islets were purity matched for amylase and insulin transcript. Method adapted from [120].

2.3.3 Western blot

Proteins were resolved by sodium dodecyl sulfate polyacrylamide gel electrophoresis (SDS-PAGE) and immunoblotted with the following antisera: rabbit anti-p16 (1:1000,

Santa Cruz), mouse anti-Bmi1 clone F6 (1:1000, Upstate), mouse anti-ran (1:10,000, BD Biosciences)

2.3.4 Measuring beta cell replication

Pancreata were dissected, weighed and fixed overnight in 4% paraformaldehyde. Fixed tissue was embedded into paraffin and sectioned for maximal footprint. Paraffin sections were stained for BrdU (US Biologicals) and insulin (Linco). For BrdU measurements, 1mg/ml BrdU was administered in the drinking water for one week prior to sacrifice. Individual islet images were captured by with iVision software (BioVision Technologies) and the number of $BrDU^{+}$/$Insulin^{+}$ cells was quantified using ImagePro software (Media Cybernetics).

2.3.5 Statistical Analysis

All data are represented as mean +/- SEM. Statistical significance was assessed by two-tailed Student's t test or two-way ANOVA (Prism GraphPad).

2.4 Results

2.4.1 Beta cells of *Pcif1*$^{gt/+}$ mice replicate at a higher rate than controls at 16 weeks of age

The *Pcif1*$^{gt/+}$ mice have been previously shown to have increased beta cell replication as well as increased apoptosis at 16 weeks of age. When BrDU/insulin double-positive cells were counted in animals at 5, 16, and 24 of age, this phenotype was shown to be age-dependent **(Fig 2.2)**. In 5 week old mice, beta cell replication is the highest, as expected for young animals [8]. However, there is no difference in replication rate, as measured by BrDU incorporation, between *Pcif1*$^{+/+}$ and *Pcif1*$^{gt/+}$ beta cells at this age. As previously published, beta cell BrDU incorporation rates are higher in *Pcif1*$^{gt/+}$ animals. When replication rates were assessed in 24 week old beta cells, rates were very low in both

genotypes, as expected [8]. As in young animals, there is no difference between genotypes, indicating that the role of Pcif1 in regulating proliferation is limited to a specific window in early adulthood.

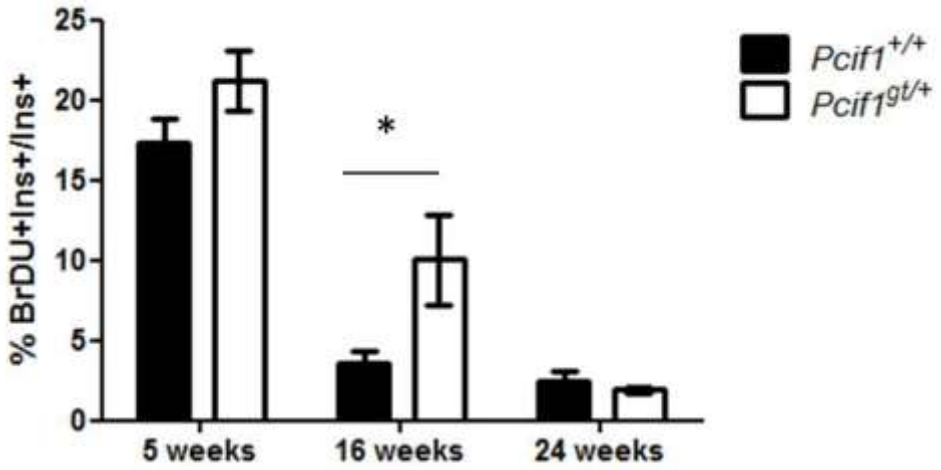

Figure 2.2. *Pcif1* heteozygosity increases beta cell replication in an age-dependent manner. Quantification of BrDU/insulin co-positive cells normalized to total insulin positive cells.
n=4-9 per group *p<0.05

It has been previously published that *Pcif1*$^{gt/+}$ mice have normal glucose and insulin tolerance and normal beta cell mass compared to *Pcif1*$^{+/+}$ mice at 16 weeks [93]. Given the apparent temporal dependence of the Pcif1 phenotype, mice were assessed at ages similar to those in **Figure 2.2**. Additionally, these mice were placed on a high fat diet in order to elicit any additional phenotypes that may have been below the limits of detection on a normal diet. At 4, 8, 12, and 20 weeks of age glucose tolerance was indistinguishable between *Pcif1*$^{+/+}$ and *Pcif1*$^{gt/+}$ mice **(Fig. 2.3)**. At 21 weeks, insulin tolerance was also unchanged in *Pcif1*$^{gt/+}$ mice **(Fig. 2.4)**.

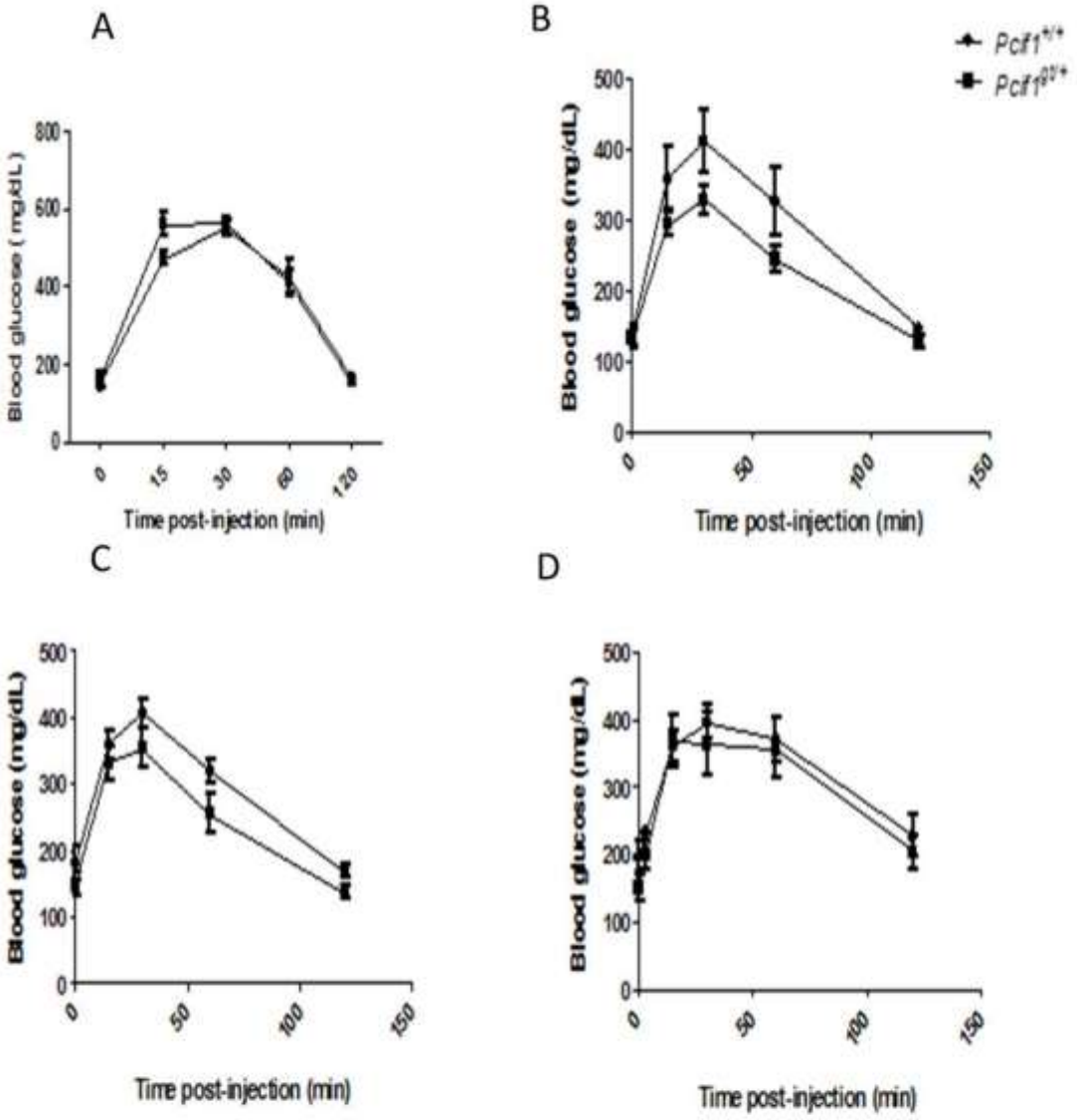

Figure 2.3. *Pcif1* heterozygosity does not influence glucose tolerance at any age. (A) Glucose tolerance test of 4 week old HFD-fed *Pcif1*$^{+/+}$ and *Pcif1*$^{gt/+}$ males after 2 g/kg IP glucose bolus. (B) Glucose tolerance test of 8 week old HFD-fed *Pcif1*$^{+/+}$ and *Pcif1*$^{gt/+}$ males after 2 g/kg IP glucose bolus. (C) Glucose tolerance test of 12 week old HFD-fed *Pcif1*$^{+/+}$ and *Pcif1*$^{gt/+}$ males after 1 g/kg IP glucose bolus. (D) Glucose tolerance test of 17 week old HFD-fed *Pcif1*$^{+/+}$ and *Pcif1*$^{gt/+}$ males after 1 g/kg IP glucose bolus. n=4-7 per group

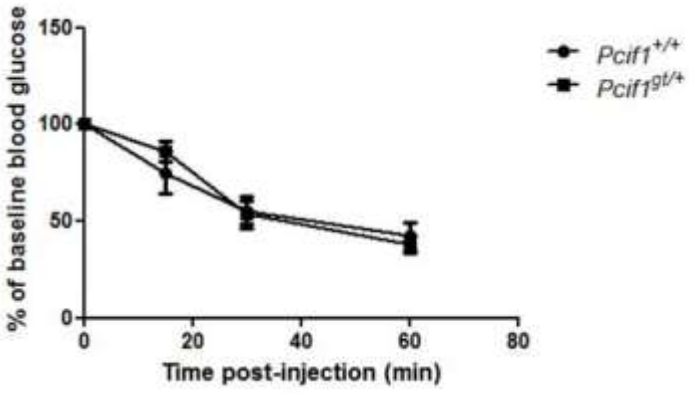

Figure 2.4. *Pcif1* heterozygosity does not influence insulin tolerance. Insulin tolerance test of 17 week old HFD-fed *Pcif1*$^{+/+}$ and *Pcif1*$^{gt/+}$ males after 1.5 U/kg IP insulin bolus. n=4-7 per group

2.4.2 *Bmi1*$^{+/-}$ and *Bmi1*$^{+/-}$; *Pcif1*$^{gt/+}$ mice have normal glucose tolerance

Bmi1 null mice are glucose intolerant at a young age [96]. However, the metabolic phenotype of *Bmi1*$^{+/-}$ mice has not been described. *Bmi1*$^{+/-}$ mice display normal glucose tolerance at 9, 18, and 26 weeks of age, whether on a low or high fat diet **(Fig. 2.5)**, although there was a surprising trend toward improved glucose tolerance at 18 weeks.

Although neither *Pcif1*$^{gt/+}$ nor *Bmi1*$^{+/-}$ mice exhibit an apparent deficiency in glucose homeostasis, we hypothesized that the additional perturbation of *Pcif1* heterozygosity in the context of *Bmi1* heterozygosity (*Pcif1*$^{gt/+}$;*Bmi1*$^{+/-}$) may lead to an alteration of glucose tolerance. Hence, having established the baseline phenotype of the *Pcif1*$^{gt/+}$ and *Bmi1*$^{+/-}$ mice, *Bmi1* heterozygosity was combined with *Pcif1*$^{gt/+}$ animals in order to test this hypothesis. When assessed at 12 weeks of age, no difference in glucose tolerance was seen in *Pcif1*$^{gt/+}$;*Bmi1*$^{+/-}$ animals **(Fig. 2.6)**.

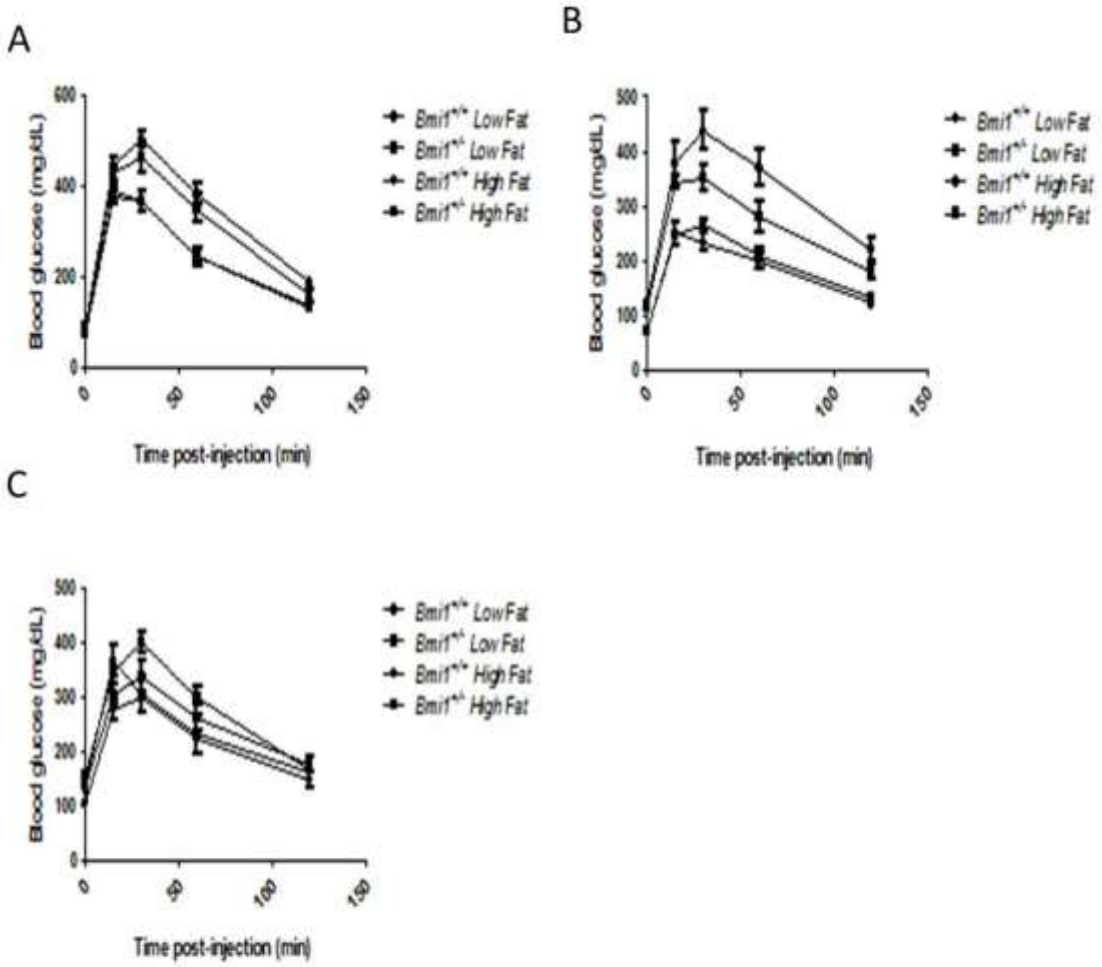

Figure 2.5. *Bmi1* heterozygosity does not affect glucose tolerance. (A) Glucose tolerance test of 9 week old LFD- and HFD-fed *Bmi1*$^{+/+}$ and *Bmi1*$^{+/-}$ males after 2 g/kg IP glucose bolus. (B) Glucose tolerance test of 18 week old LFD- and HFD-fed *Bmi1*$^{+/+}$ and *Bmi1*$^{+/-}$ males after 1 g/kg IP glucose bolus. (C) Glucose tolerance test of 24 week old LFD- and HFD-fed *Bmi1*$^{+/+}$ and *Bmi1*$^{+/-}$ males after 1 g/kg IP glucose bolus.
n=6-8 per group

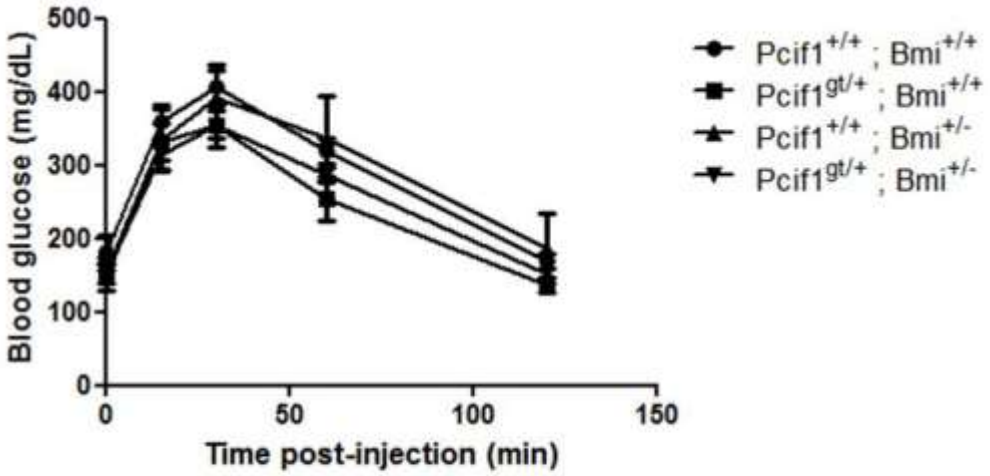

Figure 2.6. Glucose tolerance unaffected by *Bmi1/Pcif1* heterozygosity.
Glucose tolerance test of 12week old males of indicated genotype after 1 g/kg IP glucose bolus.
n=5-8 per group

2.4.3 p16 levels unchanged in *Pcif1*$^{gt/+}$ mice

As described previously [96], Bmi1, as part of PRC1, mediates progression of the cell cycle by inhibiting transcription of p16. If the increase in beta cell replication shown in **Figure 2.2** was due to enhanced Bmi1 activity, we would anticipate a corresponding decrease in p16 protein levels. Islets were harvested from 16 week-old male *Pcif1*$^{+/+}$ and *Pcif1*$^{gt/+}$ mice. Western blot analysis of the protein lysates revealed no difference in p16 protein levels in *Pcif1*$^{gt/+}$ islets, compared to controls **(Fig. 2.7)**. While this would suggest that Bmi1 is not mediating this phenotype through regulation of its traditional cell cycle target, it does not exclude the possibility of other Bmi1 targets contributing to control of replication and/or apoptosis rates in the beta cell. It is interesting to note that there may be an increase in Bmi1 protein in *Pcif1*$^{gt/+}$ islets, suggesting that Pcif1 may in fact regulate Bmi1 levels in islets. However, further experiments would need to be performed in order to confirm this observation.

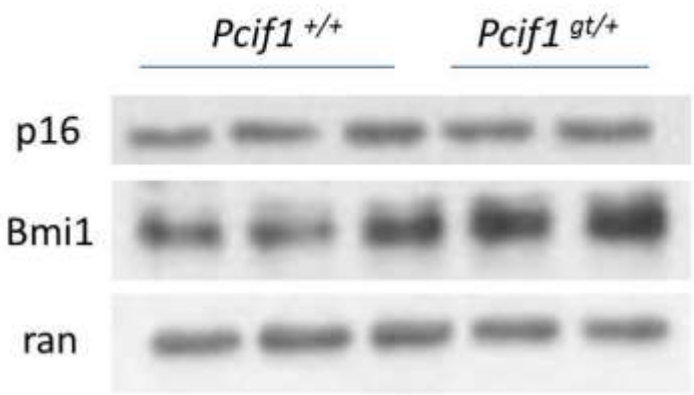

Figure 2.7. p16 unchanged in *Pcif1*$^{gt/+}$ islets. Lysate from freshly isolated, purity-matched islets assessed by western blot. Islets harvested from 16 week old males. Blots showing levels of p16 and Bmi1 protein. Ran immunoreactivity was used as the loading control.

2.4.4 *Bmi1*$^{+/-}$ mice have improved insulin sensitivity

Although no difference in whole body glucose tolerance was detected, there remained a possibility that cell cycling would be perturbed, albeit at too low of a level to impair glucose tolerance test at this age. Before moving forward with histological analysis, we further characterized the physiology of these animals in order to rule out confounding factors. In order to thoroughly phenotype the *Bmi1*$^{+/-}$ mice, insulin tolerance tests were performed in order to assess whole-body insulin sensitivity. 17-week old *Bmi1*$^{+/-}$ mice are more sensitive to an exogenous insulin bolus than *Bmi1*$^{+/+}$ controls **(Fig. 2.8)**. This surprising phenotype complicated any further analysis of beta cell number and replication, as discussed in detail below.

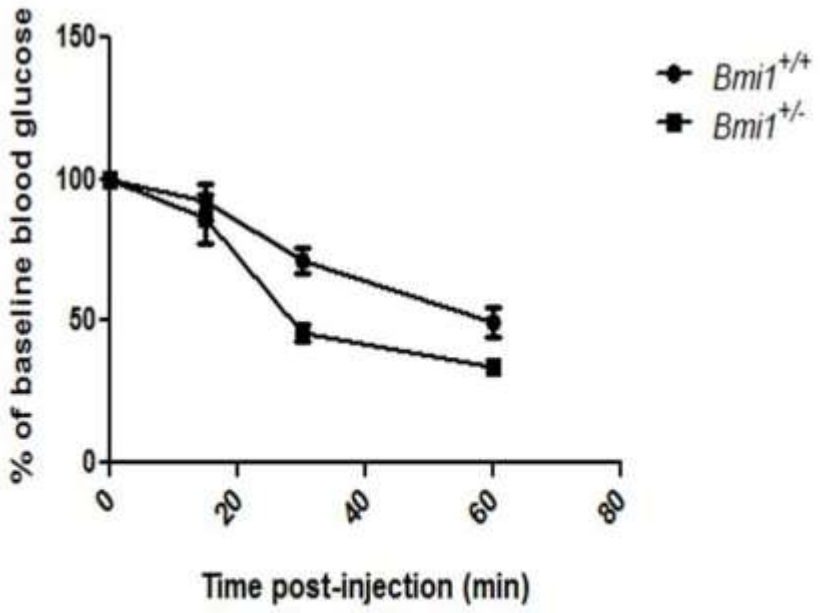

Figure 2.8. *Bmi1* heterozygosity improves insulin tolerance. Insulin tolerance test of 17 week old HFD-fed *Bmi1*$^{+/+}$ and *Bmi1*$^{+/-}$ males after 1.5 U/kg IP insulin bolus.
n=5 per group; P=0.02 by two-way ANOVA

2.5 Discussion

Pcif1$^{gt/+}$ mice have a perturbation in beta cell cycling, with rates of both proliferation and apoptosis higher than in controls [119]. The experiments described in this chapter were performed in an attempt to mechanistically explain this phenomenon. I hypothesized that an alteration in Bmi1 levels or activity may influence cell cycling via the well-described p16 signaling pathway. However, it is unlikely that Bmi1 explains the increase in replication, as p16 protein levels were equivalent in *Pcif1*$^{+/+}$ and *Pcif1*$^{gt/+}$ islets. However, it is possible that the increase in apoptosis seen in *Pcif1*$^{gt/+}$ islets may be the more dominant phenotype or that replication is mediated through another factor.

It was also interesting to see that the western blot data suggested a trend towards increased Bmi1 protein levels in *Pcif1*$^{gt/+}$ islets. Due to the inherent variability of primary tissue, it would be prudent to explore this observation in a larger number of animals before drawing definitive conclusions. However, if this observation were to hold true, it would imply that Bmi1 is, in fact, regulated by Pcif1 in islets. It would also suggest a role for Bmi1 outside of the regulation of the *Ink4a/Arf* locus. This might speak to a type of "prioritizing" of Bmi1 targets that is sensitive to different degrees of Bmi1 protein, rather than just a simple presence or absence that has been studied in the *Bmi1* null model.

It was interesting to note the age dependence of the Pcif1 replication phenotype. There appears to be a narrow window in adulthood wherein Pcif1 levels influence beta cell replication. Further assessment of Pcif1 expression with age would aid in determining whether the age dependence of this phenotype is due to changes in Pcif1 expression or activity.

Interestingly, these studies revealed an unexpected increase in insulin sensitivity associated with *Bmi1* heterozygosity. This observation complicated the overall analysis of beta cell replication. In response to changes in insulin demand, beta cells compensate by adjusting both cell number and function. It is therefore reasonable to expect that *Bmi1*$^{+/-}$ animals would have lower beta cell replication and mass, simply due to the fact that they are more insulin sensitive than the *Bmi1*$^{+/+}$ mice. This would make it extremely difficult to extricate an intrinsic beta cell replication phenotype from one influenced by changes in peripheral insulin sensitivity in our current mouse model.

Both genetic models used in these studies are whole-body heterozygous models. A tissue-specific *Bmi1* deletion could aid in circumventing the complications of beta cell compensation caused by differential whole-body insulin sensitivity. Additionally, deletion

of *Pcif1* and/or *Bmi1* in only the beta cells may allow for complete deletion, rather than heterozygosity, without the fatal phenotypes associated with whole body deletion.

Although these experiments did not result in an explanation for the role of Pcif1 in beta cell replication, they did reveal a surprising protection from high fat diet-induced insulin resistance associated with *Bmi1* heterozygosity. This phenotype will be further described through the studies described in Chapter 3 of this thesis.

CHAPTER 3: THE POLYCOMB PROTEIN, BMI1, REGULATES INSULIN SENSITIVITY

3.1 Abstract

The Polycomb Repressive Complexes (PRC) 1 and 2 function to epigenetically repress target genes. The PRC1 component, Bmi1, plays a crucial role in maintenance of glucose homeostasis and beta cell mass through repression of the *Ink4a/Arf* locus. Due to poor postnatal survival of *Bmi1*$^{-/-}$ mice, no previous studies have explored the role of Bmi1 in regulating glucose homeostasis in the adult animal. Here we report that heterozygous loss of *Bmi1* results in increased insulin sensitivity in adult male C57BL/6N mice, with no impact on body weight or composition. Hyperinsulinemic-euglycemic clamp reveals increased suppression of hepatic glucose production and increased glucose disposal rate, indicating elevated glucose uptake to peripheral tissues, in *Bmi1*$^{+/-}$ mice. Enhancement of insulin signaling, as measured by Akt phosphorylation, in liver and, to a lesser extent, in muscle appear to contribute to this phenotype. Together, these data define a new role for Bmi1 in regulating insulin sensitivity.

3.2 Introduction

Type 2 diabetes is characterized by a relative insulin deficiency and is associated with insulin resistance in the peripheral tissues. At first, pancreatic beta cells are able to compensate by releasing more insulin. As insulin resistance progresses, the beta cells fail, resulting in overt diabetes. Insulin signals to peripheral tissues to take up glucose and to halt hepatic glucose production and lipolysis. An insulin resistance state impairs these responses, causing hyperglycemia, leading to vascular, nerve and renal complications, among others. At this time, many aspects of the molecular progression of insulin resistance remain unclear.

Polycomb group (PcG) proteins assemble into multi-subunit complexes and repress target genes. PRC2 (Polycomb Repressive Complex 2) initiates repression and PRC1 maintains repression via histone methyltransferase and ubiquitin E3 ligase activities, respectively [97],[98]. Bmi1 is a member of PRC1 and is necessary for full activity of the complex. The classically studied targets of the Polycomb complexes are the *Ink4a/Arf* locus and the Hox gene clusters, which PRC1 and PRC2 function to repress. Regulation of the *Ink4a/Arf* locus has been studied particularly extensively due to the impact of this locus on cancer progression and stem cell self-renewal. Overexpression of Bmi1 allows rapid proliferation, eventually leading to immortalization of mouse embryonic fibroblasts in culture [103]. Bmi1 was initially identified as an oncogene that cooperates with *c-myc* in B cell lymphomagenesis and was named as such: B cell-specific Moloney Murine Leukemia Virus integration site 1 [10,7]. Bmi1 was later found to be involved in cell cycle progression and to be necessary for hematopoetic and neural stem cell renewal, as Bmi1-deficient mice have severe hematopoetic and neurological abnormalities [9,11].

The most well-characterized target of Bmi1 is the *Ink4a/Arf* locus, which encodes two key regulators of cell cycling, p16 (Ink4a) and p19 (Arf). While some *Bmi1* null phenotypes can be fully explained by regulation of this locus, others cannot. For instance, the loss of self-renewal capability in *Bmi1*$^{-/-}$ neural stem cells is completely rescued by concomitant deletion of *Ink4a/Arf* [108]. Additionally, the drastic reduction in proliferation after *Bmi1* knockdown is completely rescued by knockdown of *Ink4a* in cultured mouse islets [96]. In contrast, *Bmi1* null mice have a 50% reduction in body weight that is not significantly rescued by the genetic loss of either *Arf* alone or both *Ink4a* and *Arf* [108]. Similarly, the severe hematopoietic deficiency of *Bmi1* null mice is only partially rescued by co-deletion of *Ink4a/Arf* [109]. These observations have contributed to the recognition that Bmi1 (and PRC1) regulates targets beyond *Ink4a/Arf*,

the identity of which are only beginning to be understood. Complicating the identification of Bmi1 targets is the lack of a clear consensus binding sequence that defines the location to which PRC complexes are recruited [121,122].

The severe phenotypes limiting postnatal survival of Bmi1 null mice have precluded exploration of the role of Bmi1 in regulating glucose homeostasis in the adult animal. Here, we study the metabolic role of Bmi1 in adult *Bmi1*$^{+/-}$ mice and, surprisingly, find enhanced insulin sensitivity *in vivo* and enhanced insulin signaling in liver and muscle, thereby defining a novel metabolic role of Bmi1.

3.3 Materials and Methods

3.3.1 Animals and Physiological Experiments

All animal experiments were performed according to procedures approved by the Institutional Animal Care and Use Committee of the University of Pennsylvania. Animals were placed on high fat diet (60% fat), low fat diet (10% fat) (Research Diets Inc., New Brunswick, NJ) or standard chow at weaning. *Bmi1*$^{+/-}$ mice were previously described [107]. Mice were maintained on a C57BL/6N background. All experiments were performed on males 15-18 weeks of age, except where otherwise noted. For glucose tolerance tests, 18 week old males were fasted overnight, given 1 g/kg glucose via IP injection and blood glucose was measured by handheld glucometer at 0, 15, 30, 60, and 120 minutes after injection. For insulin tolerance tests, animals were fasted 6 hours prior to IP injection of 1.0 or 1.5 U/kg insulin (NovolinR, Novo Nordisk, Princeton, NJ) and blood glucose was measured by handheld glucometer at 0, 15, 30, 60, and 120 minutes after injection. For insulin secretion assays, blood was collected at time 0 and 3 minutes after glucose bolus. Insulin concentration was measured by ELISA (Crystal Chem Inc., Downers Grove, IL).

3.3.2 Body Composition Measurements

Body composition was assessed using a 3-in-1 NMR machine by EchoMRI (Houston, TX)

3.3.3 Hyperinsulinemic-Euglycemic Clamp

Hyperinsulinemic-euglycemic clamp was performed according to previously published procedures [123–125]. Briefly, [3–3H] glucose was used to measure baseline glucose kinetics. The hyperinsulinemic clamp utilized a continuous infusion of 2.5 mU kg^{-1} min^{-1} insulin (Humulin; Eli Lilly, Indianapolis, IN) and a variable intravenous infusion of 20% glucose (w/v) to maintain blood glucose levels at 120–140 mg/dL. 2-deoxy-D-[1-14C] glucose was used to estimate glucose uptake.

3.3.4 Western Blot Analysis

Livers, gastrocnemius muscles, and isolated hepatocytes were sonicated in lysis buffer (50 mM Tris-Cl, pH 7.8, 2% SDS, 10% glycerol, 10 mM $Na_4P_2O_7$, 100 mM NaF, 6 M urea, 10 mM EDTA). Proteins were resolved by SDS-PAGE and immunoblotted with the following antisera: rabbit anti-Akt (1:1000, Cell Signaling), rabbit anti-phospho-Akt (1:1000, Cell Signaling), mouse anti-Ran (1:10,000, BD Biosciences).

3.3.5 Hepatocyte Isolation

Hepatocytes were isolated from 15 week old male mice following a 5 hour fast using Liver Perfusion Media (Invitrogen, Carlsbad, CA) and Kreb's Ringer Bicarbonate Buffer (Sigma, St. Louis, MO) supplemented with Collagenase and DNase (Worthington Biochemical Corporation, Lakewood, NJ) with a modified two-step perfusion protocol [126]. Hepatocytes were seeded at a density of 2.5 x 10^5 cells per well in collagen-I-coated 12-well plates M199 media plus 10% FBS plus penicillin/streptomycin. Cells were

allowed to attach ~2 hours prior to 2 hour serum starvation. Cells were then treated with the indicated concentrations of insulin for 20 minutes.

3.3.6 RNA sequencing

RNA sequencing libraries were generated using the Tru-Seq RNA Sample Prep Kit (Illumina). RNA sequencing was performed on an Illumina hiSeq2000 by the Next Generation Sequencing Core at the University of Pennsylvania.

3.3.7 Statistical Analysis

All data are represented as mean +/- SEM. Statistical significance was assessed by two-tailed Student's t test or two-way ANOVA (Prism GraphPad).

3.4 Results

3.4.1 *Bmi1*$^{+/-}$ mice are partially protected from HFD-induced insulin resistance.

In order to exacerbate what we predicted might be a mild defect in beta cell replication, *Bmi1*$^{+/-}$ males and *Bmi1*$^{+/+}$ littermates were placed on a high fat diet at weaning and followed through 18 weeks of age. *Bmi1* heterozygosity resulted in an approximate 60% reduction in Bmi1 protein **(Fig. 3.1a)**. High fat diet induced an equivalent degree of weight gain in both genotypes. Surprisingly, glucose tolerance was not worse in *Bmi1*$^{+/-}$ mice; rather, there was a trend toward improved glucose tolerance (**Fig. 3.1b**; P=0.12 by two-way ANOVA for HFD-fed Bmi***1***$^{+/+}$ vs. HFD-fed *Bmi1*$^{+/-}$). Insulin tolerance testing (ITT) revealed that *Bmi1* heterozygosity confers partial protection from high fat diet-induced insulin resistance (**Fig. 3.1c**; P=0.0095 by two-way ANOVA for HFD-fed *Bmi1*$^{+/+}$ vs. HFD-fed *Bmi1*$^{+/-}$). *Bmi1* null animals have multiple phenotypes resulting from severe deficiencies in cell replication, including stunted growth [107]. In contrast, body weight and composition were indistinguishable between *Bmi1*$^{+/+}$ and *Bmi1*$^{+/-}$ littermates **(Fig.**

3.1d-e). These observations indicate that the role of Bmi1 in whole-body insulin sensitivity is independent of body weight or adiposity.

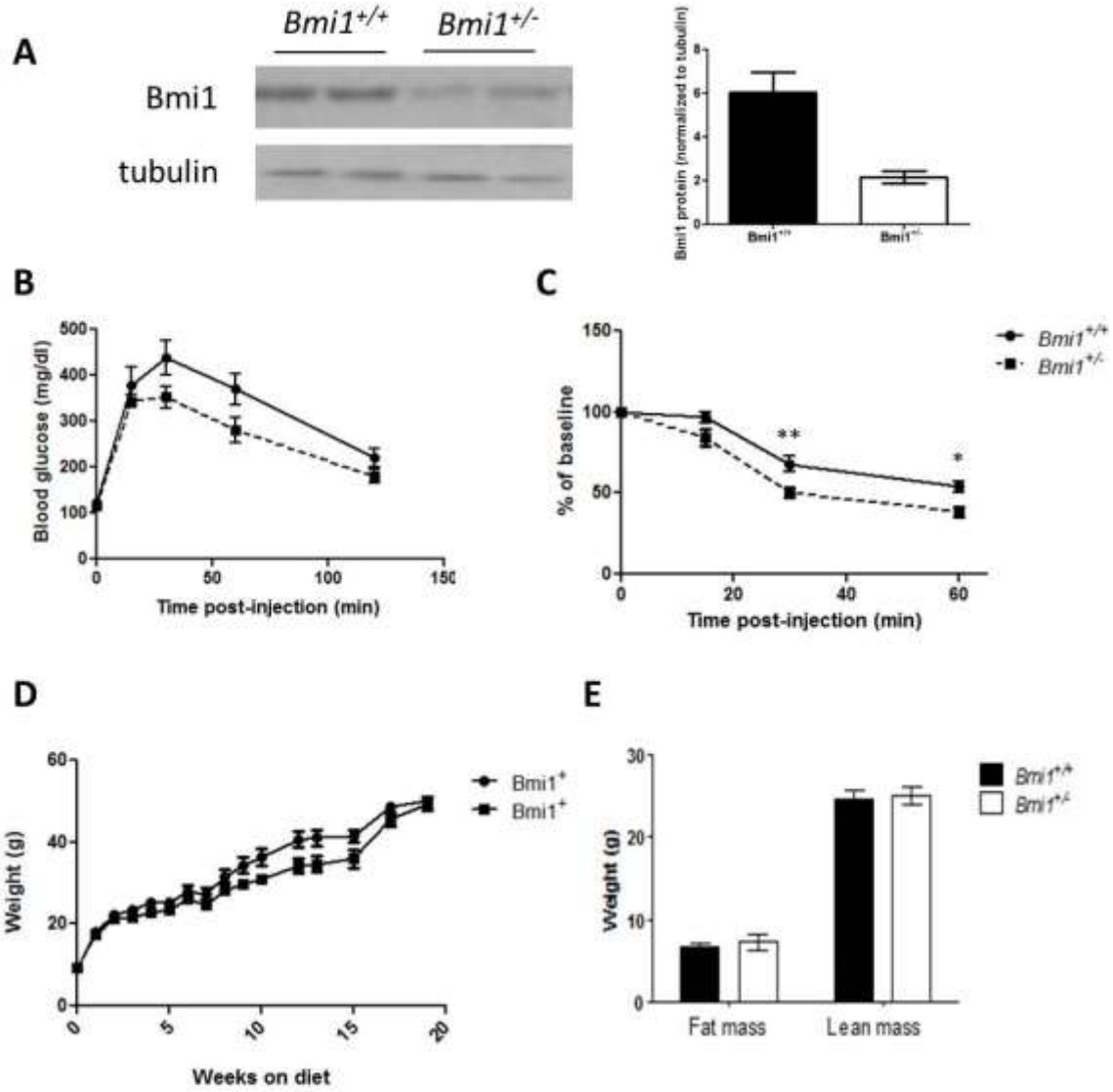

Figure 3.1. *Bmi1*$^{+/-}$ mice are partially protected from high fat diet-induced insulin resistance.
(A) Western blots of lysates from *Bmi1*$^{+/+}$ and *Bmi1*$^{+/-}$ male liver lysates showing levels of Bmi1 protein. (B-C) Glucose and insulin tolerance tests of 16-18 week old HFD-fed *Bmi1*$^{+/+}$ and *Bmi1*$^{+/-}$ males (B) 1 g/kg IP glucose bolus, P=0.1211 by two-way ANOVA and (C) 1.5 U/kg IP insulin, P=0.0095 by two-way ANOVA. (D) Similar weight gain in *Bmi1*$^{+/+}$ and *Bmi1*$^{+/-}$. (E) Lean and fat mass unaffected by Bmi1 heterozygosity, as measured by NMR. n=7-8 mice per genotype for all assessments. .*p < 0.05 **p < 0.01 vs *Bmi1*$^{+/+}$

3.4.2 *Bmi1* null mice may be hypersensitive to insulin

Impaired glucose tolerance at an early age due to reduced insulin secretion has been observed in *Bmi1* null animals [96]. This phenotype was recapitulated in our hands, with marked hyperglycemia evident at 10 weeks of age **(Fig. 3.2a)**. We also observed a trend toward hyper-responsiveness to insulin on insulin tolerance testing **(Fig. 3.2b)**. Due to grossly impaired survival of *Bmi1* null mice beyond weaning, this observation could not be extended. However, combined with our observations of adult $Bmi1^{+/-}$ animals, these data suggest a gene-dosage dependent role of Bmi1 in whole animal insulin sensitivity.

3.4.3 $Bmi1^{+/-}$ mice require less circulating insulin to maintain glucose homeostasis

Similar to HFD-fed $Bmi1^{+/-}$ mice, $Bmi1^{+/-}$ mice fed a low fat diet (LFD) had normal glucose tolerance **(Fig. 3.3a)**. Although insulin tolerance was not different between LFD-fed $Bmi1^{+/-}$ mice and wild type littermates, we observed lower insulin secretion in response to a glucose bolus in $Bmi1^{+/-}$ animals **(Fig. 3.3b)**. In contrast to $Bmi1^{-/-}$ mice, in which decreased insulin secretion due to reduced beta cell mass is associated with marked impairment of glucose homeostasis, the reduction of insulin in the face of normal glucose tolerance in LFD-fed $Bmi1^{+/-}$ mice suggests an appropriate adaptive response to enhanced insulin sensitivity.

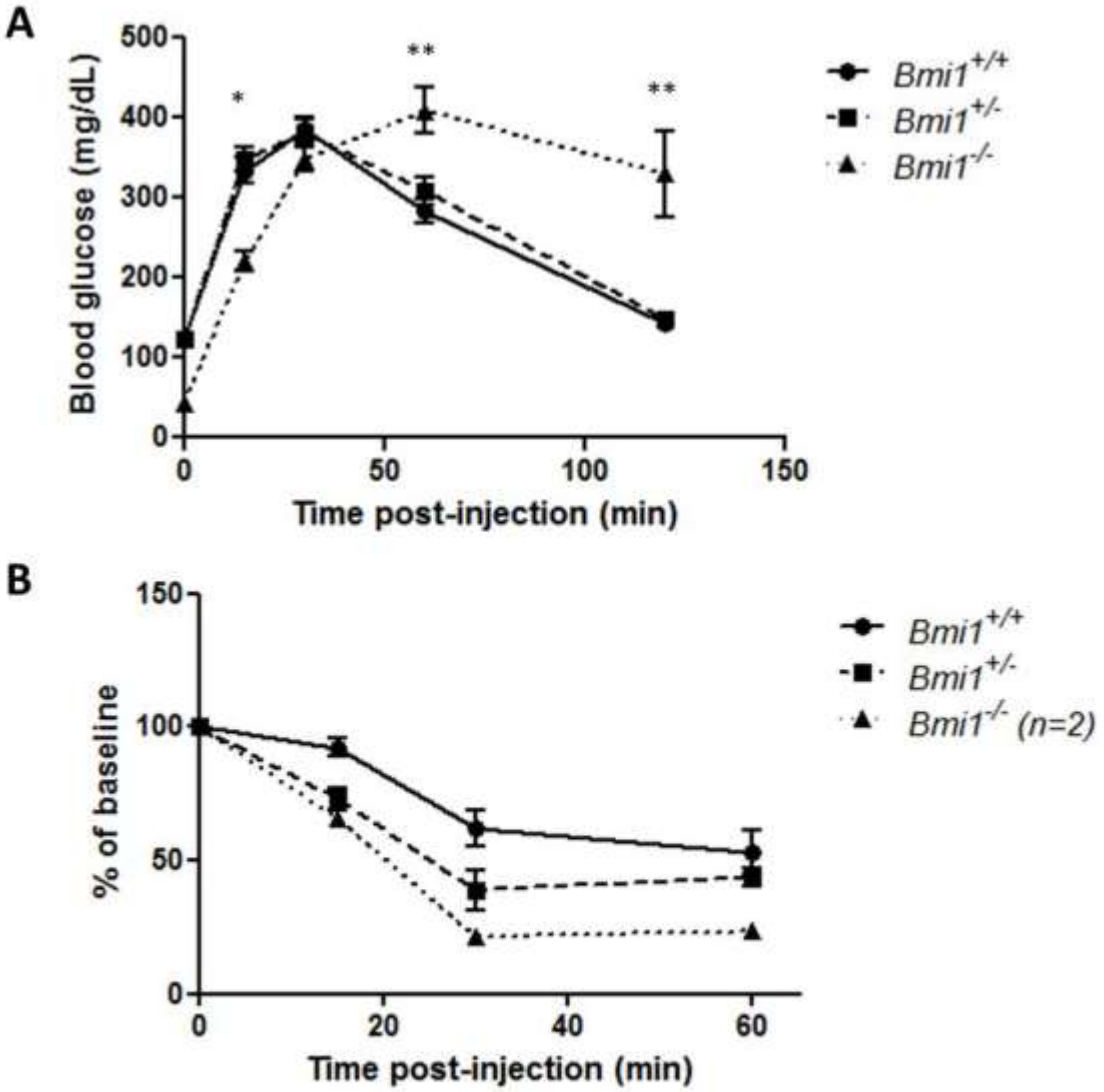

Figure 3.2. *Bmi1* null mice exhibit glucose intolerance and insulin hypersensitivity.

Glucose and insulin tolerance tests of 9-10 week old *Bmi1*$^{+/+}$, *Bmi1*$^{+/-}$, and *Bmi1*$^{-/-}$ males (A) 2 g/kg IP glucose bolus (P=0.4314 by two-way ANOVA) and (B) 0.75 U/kg IP insulin. *$p < 0.01$ **$p < 0.001$ *Bmi1*$^{-/-}$ vs *Bmi1*$^{+/+}$; n=11-15 for *Bmi1*$^{+/+}$and *Bmi1*$^{+/-}$, n=2-3 for *Bmi1*$^{-/-}$

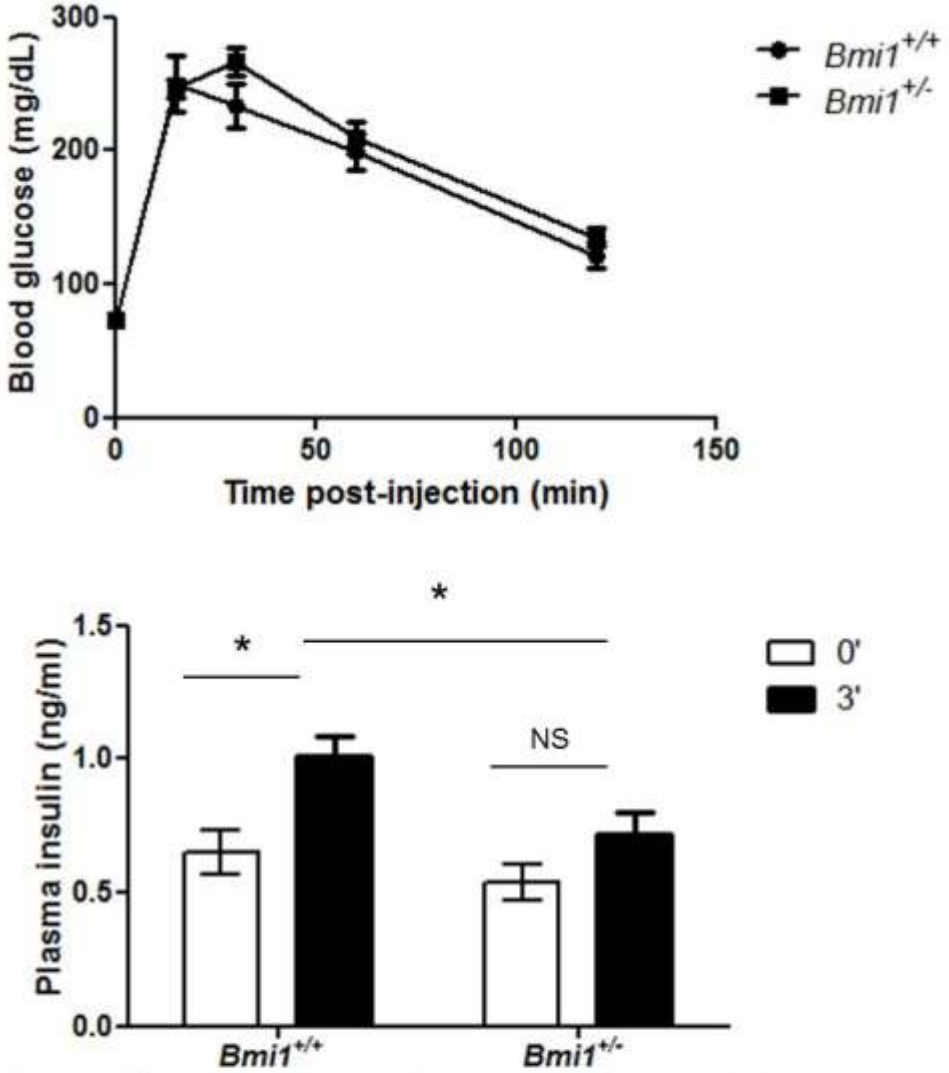

Figure 3.3. *Bmi1*$^{+/-}$ mice require less circulating insulin to maintain glucose homeostasis

(A) Glucose tolerance test of 18 week old LFD-fed *Bmi1*$^{+/+}$ and *Bmi1*$^{+/-}$ males after 1 g/kg IP glucose bolus. n=8 per genotype (B) Plasma insulin at 0 and 3 minutes after 2 g/kg IP glucose bolus. *$p<0.05$; n=13-15 per genotype

3.4.4 Hyperinsulinemic-euglycemic clamp reveals increased insulin sensitivity in low fat diet-fed *Bmi1*$^{+/-}$ mice

We hypothesized that a more sensitive measure might reveal an insulin sensitivity phenotype in *Bmi1*$^{+/-}$ animals. Therefore, we assessed insulin sensitivity in LFD-fed mice using a hyperinsulinemic-euglycemic clamp. There was no difference in basal blood glucose levels or hepatic glucose production (HGP; **Fig. 3.4a-b**); however, *Bmi1*$^{+/-}$ mice required a glucose infusion rate (GIR) more than twice that of *Bmi1*$^{+/+}$ mice to maintain the target blood glucose level of 120-140 mg/dl, echoing our previous observations of improved whole-body insulin sensitivity **(Fig 3.4c)**. The suppression of HGP by insulin during the clamp was greatly increased in *Bmi1*$^{+/-}$ mice (**Fig. 3.4d**; 77% suppression vs 40% in controls; $p=6.5 \times 10^{-5}$), suggesting that *Bmi1* heterozygosity results in greater responsiveness of the liver to insulin stimulation. During the clamp, the glucose disposal rate (Rd) was 67% higher in *Bmi1*$^{+/-}$ mice (**Fig. 3.4e**; p=0.0011), indicating a difference in responsiveness of peripheral tissues to insulin as well. Glucose uptake to muscle was elevated 57% (**Fig. 3.4f**; p=0.06), while there was no difference in glucose uptake to adipose tissue **(Fig. 3.4g)**. Together, these results suggest a role for Bmi1 in modulation of insulin signaling in liver and muscle. Given the robust phenotype observed in liver, we first examined insulin signaling in that tissue.

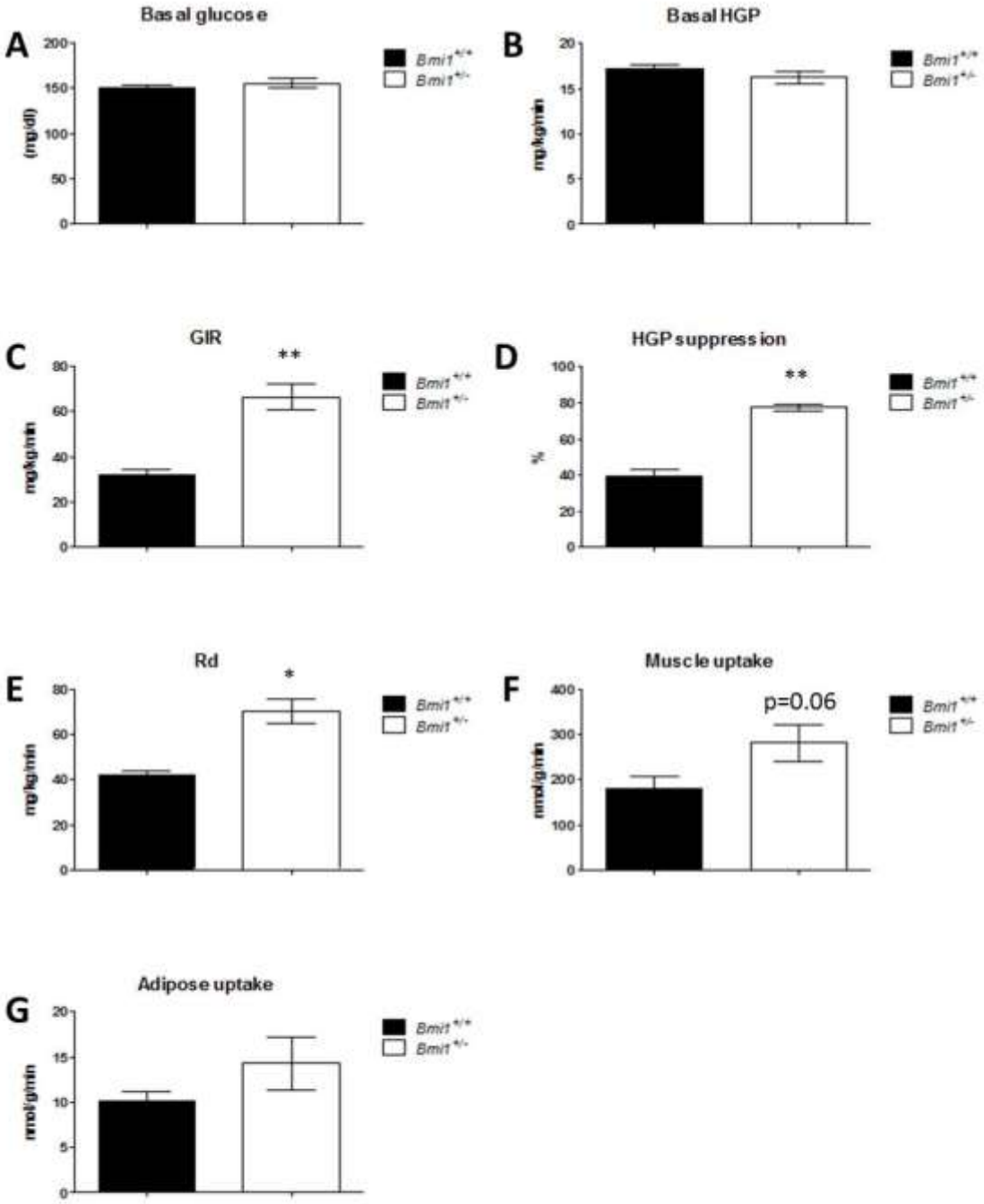

Figure 3.4. Hyperinsulinemic-euglycemic clamp reveals increased insulin sensitivity in low fat diet-fed *Bmi1*$^{+/-}$ mice.

Hyperinsulinemic-euglycemic clamp performed on 30 week-old males on LFD. Target glucose 120-140 mg/dL. n=5 mice per genotype. (A) Basal blood glucose levels, (B) basal hepatic glucose production, and (C) glucose infusion rate during clamp. Radioactive tracers were administered and quantitated to calculate (D) hepatic glucose suppression, (E) glucose disposal rate, and glucose uptake to muscle (F) and adipose tissue (G). *$p<0.005$ compared to *Bmi1*$^{+/+}$; **$p<0.001$ compared to *Bmi1*$^{+/+}$

3.4.5 Hepatic insulin signaling is enhanced by *Bmi1* heterozygosity

After a 5 hour fast to minimize stimulation by endogenous insulin, *Bmi1*$^{+/+}$ and *Bmi1*$^{+/-}$ mice were injected with saline or insulin 20 minute prior to sacrifice. Western blot analysis of liver lysates revealed no effect of either genotype or insulin treatment on total Akt levels (**Fig. 3.5a**); however, Akt phosphorylation levels in heterozygous mice were lower at baseline as compared to controls, suggesting reduced basal insulin signaling in *Bmi1*$^{+/-}$ livers. This supports the observation from whole animal physiology that less insulin is needed to maintain normal glucose homeostasis in the *Bmi1* heterozygous animals (**Fig. 3.3**). Upon insulin stimulation, Akt phosphorylation was higher in *Bmi1*$^{+/-}$ liver lysates, compared to controls, indicating enhanced signal transduction in response to insulin (**Fig. 3.5a-b**; 2.2-fold change in *Bmi1*$^{+/+}$ vs 8.9-fold in *Bmi1*$^{+/-}$).

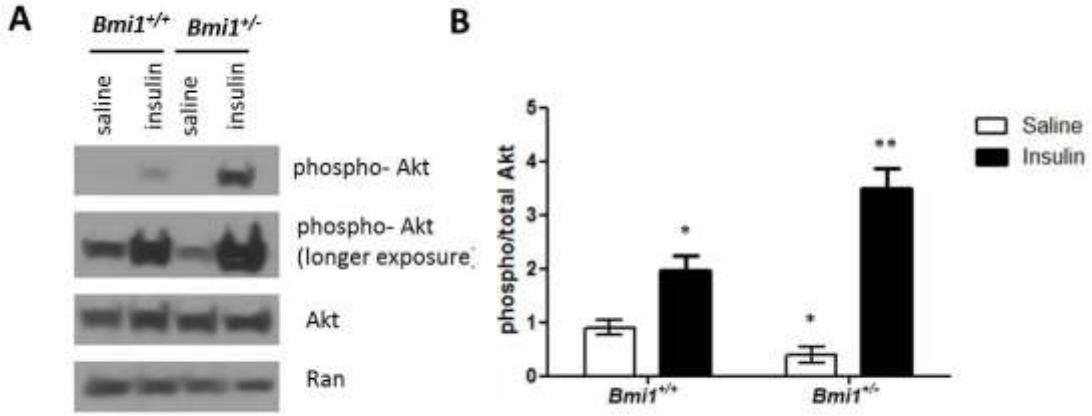

Figure 3.5. Hepatic insulin signaling is enhanced by *Bmi1* heterozygosity.
15 week old males fasted 5 hours and then injected IP with saline or 1.125 U/kg insulin. Livers harvested 20 minutes later and lysates assessed by Western blot. (A) Representative Western blots showing levels of phospho-Akt and total Akt. Ran immunoreactivity was used as the loading control. (B) Quantification of phospho- and total Akt levels. The ratio of phospho-Akt/total Akt is shown. n= 4-5 per genotype and treatment. *$p < 0.05$ vs *Bmi1*$^{+/+}$ saline ; **$p < 0.05$ vs *Bmi1*$^{+/+}$ insulin

To determine whether these findings reflect an alteration of insulin sensitivity within hepatocytes, we performed studies in cultured primary hepatocytes isolated from *Bmi1*$^{+/+}$ and *Bmi1*$^{+/-}$ mice. Here we compared total and phosphorylated Akt levels in response to a range of insulin doses. Hepatocytes isolated from *Bmi1*$^{+/-}$ animals had detectable levels of Akt phosphorylation at lower doses of insulin as compared to *Bmi1*$^{+/+}$ hepatocytes (**Fig. 3.6a-b**). Additionally, the maximal level of Akt phosphorylation was higher in mutant hepatocytes. Together, these experiments suggest a hepatocyte-autonomous role for Bmi1 in modulating sensitivity of insulin signaling, specifically Akt phosphorylation.

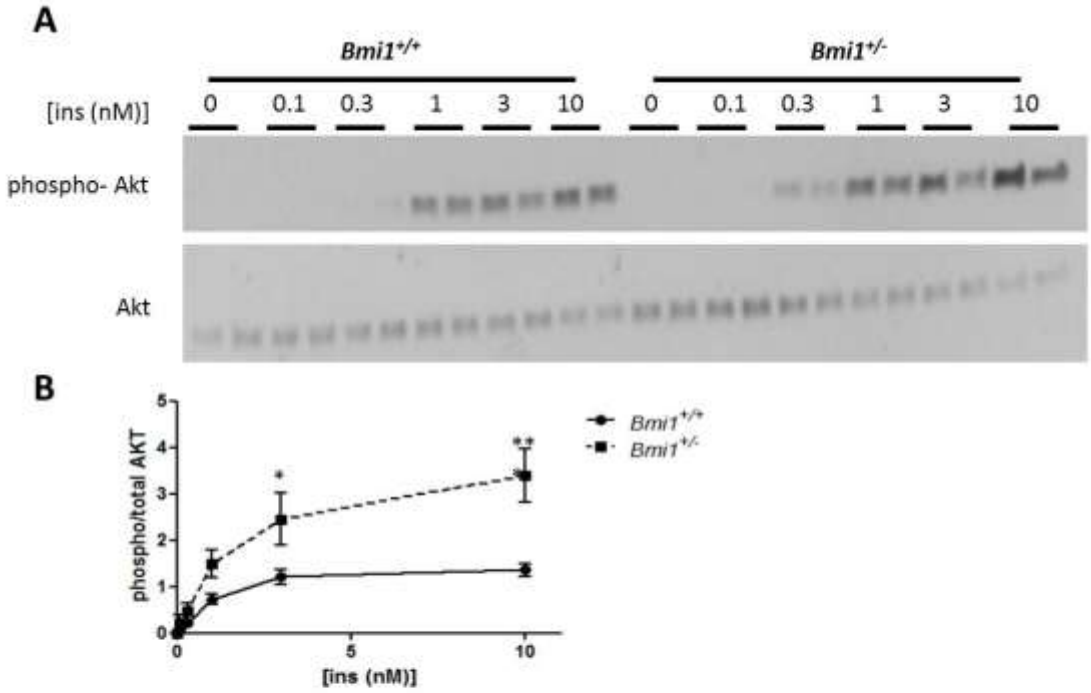

Figure 3.6. Hepatic insulin signaling is enhanced by *Bmi1* heterozygosity.
Cultured hepatocytes isolated from 15 week old males treated with indicated dose of insulin for 20 minutes prior to harvest. Lysates assessed by western blot. (A) Representative Western blots showing levels of phospho-Akt and total Akt. (B) Quantification phospho- and total Akt levels. The ratio of phospho- Akt /total Akt is shown. Results shown obtained from n=5 independent hepatocyte isolations per genotype. P<0.001 by two-way ANOVA. *p < 0.05 vs WT; **p<0.001 vs WT

3.4.6 Activity of early insulin signaling pathway not altered in *Bmi1*$^{+/-}$ mice

In order to further investigate the effect of *Bmi1* heterozygosity on insulin signaling, critical signaling events upstream of and parallel to Akt phosphorylation were assessed by immunoblot **(Fig. 3.7a)**. The first step in the insulin signaling pathway, insulin receptor phosphorylation, showed a comparable response to insulin in both groups, although there was a slight increase in basal levels of IR phosphorylation in *Bmi1*$^{+/-}$ animals **(Fig. 3.7b)**. Similarly, there was no statistically significant difference in IRS1 phosphorylation between genotypes when stimulated by insulin, although a trend toward reduced IRS1 phosphorylation was observed at baseline in the *Bmi1*$^{+/-}$ animals (p=0.07) **(Fig. 3.7c)**. As an important pathway parallel to Akt signaling, ERK1/2 phosphorylation was also measured. The response to insulin was variable at this time point and no significant difference was observed between genotypes **(Fig. 3.7d)**.

Given the well-described role of Bmi1 in repressing transcription of target genes, we sought to determine whether the expression of the insulin signaling proteins upstream of Akt was altered in *Bmi1*$^{+/-}$ livers. There were no differences in the levels of the receptors (*IR, Igf1r),* adaptor proteins *(Irs1, Irs2, p85*) or proteins that regulate activity of the core pathway components (*Pten, Ptb1b, Pdk1, Sos1, Pp2a, Phlpp1, Phlpp2*), suggesting that Bmi1 does not regulate expression of these genes.

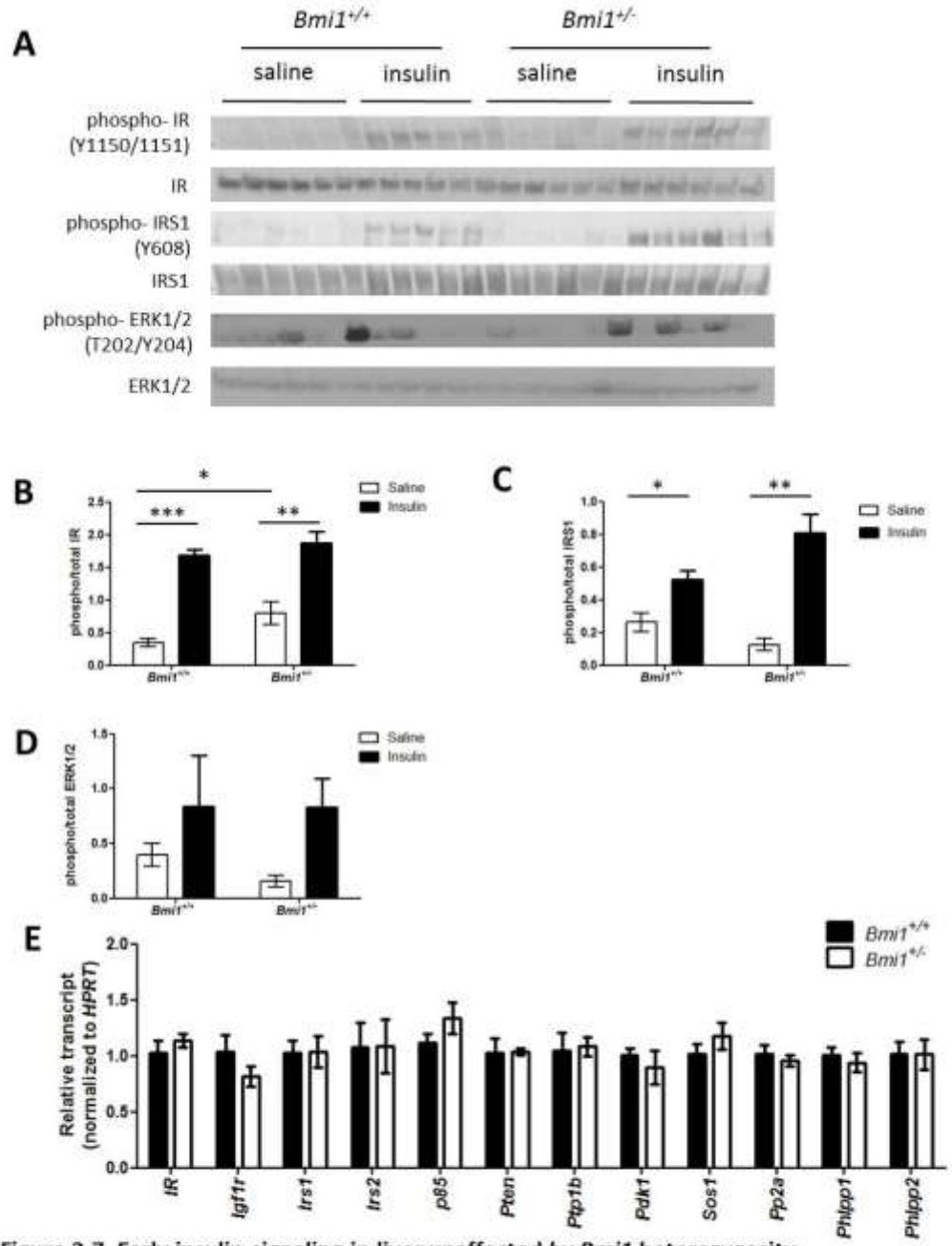

Figure 3.7. Early insulin signaling in liver unaffected *by Bmi1* heterozygosity.
(A-D) 15 week old males fasted for 5 hours and then injected with saline or 5U insulin into the IVC. Livers were harvested 2 minutes later and lysates assessed by western blot. (A) Western blots showing levels of phosphorylated and total IR, IRS1, and ERK1/2. (B) Quantification of phospho- and total IR levels. The ratio of phospho- IR /total IR is shown. (C) Quantification of phospho- and total IRS1 levels. The ratio of phospho- IRS1 /total IRS1 is shown. (D) Quantification of phospho- and total ERK1/2 levels.The ratio of phospho- ERK1/2 /total ERK1/2 is shown. (E) RNA isolated from 15 week old male livers and assessed by qRT-PCR. n=5-6 per genotype and treatment. *$p < 0.05$; **$p<0.01$; ***$p<0.0001$

3.4.7 Insulin signaling is enhanced in muscle of *Bmi1*$^{+/-}$ mice.

Given the robust enhancement of Akt signaling in liver **(Fig. 3.5)**, we hypothesized that a similar enhancement may be responsible for the trend toward increased glucose uptake seen in the muscle of *Bmi1*$^{+/-}$ animals during the clamp **(Fig. 3.4)**. Lysates of muscle tissue taken from the same animals as above were analyzed by western blot. As expected, Bmi1 protein was reduced in *Bmi1*$^{+/-}$ muscle **(Fig. 3.8a)**. Similar to liver, Akt phosphorylation increased higher above baseline in response to insulin stimulation in *Bmi1*$^{+/-}$ muscle, as compared to *Bmi1*$^{+/+}$, due to lower phospho-Akt levels at baseline (**Fig. 3.8b;** 1.6-fold change in *Bmi1*$^{+/+}$ vs 3.6-fold in *Bmi1*$^{+/-}$).

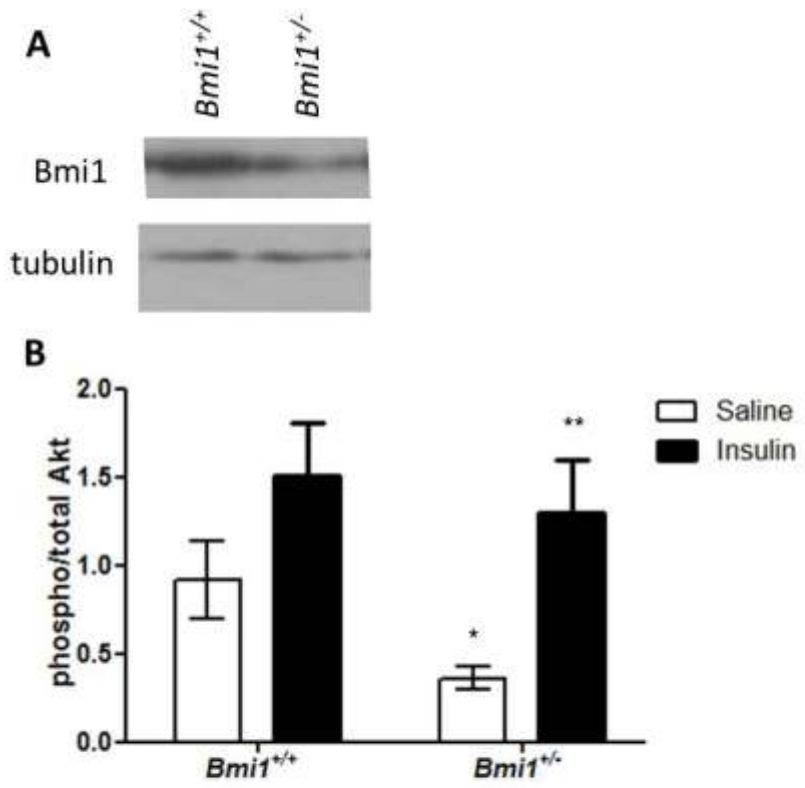

Figure 3.8. Insulin signaling in muscle is enhanced by Bmi1 heterozygosity. (A) Representative western blots of lysates from *Bmi1*$^{+/+}$ and *Bmi1*$^{+/-}$ male muscle lysates showing levels of Bmi1 protein. (B) 15 week old males fasted 5 hours and then injected IP with saline or 1.125 U/kg insulin. Gastrocnemius muscle harvested 20 minutes later and lysates assessed by Western blot. Quantification of the ratio of phospho-Akt/total Akt is shown. n= 5-6 per genotype and treatment. *$p < 0.05$ vs *Bmi1*$^{+/+}$ saline; **$p < 0.05$ vs *Bmi1*$^{+/+}$ insulin

3.4.8 RNA-sequencing suggests potential mechanisms for Bmi1-mediated insulin sensitivity

In order to quantitatively compare gene expression in livers from *Bmi1*$^{+/+}$ and *Bmi1*$^{+/-}$ mice, we performed RNA sequencing, which revealed 23 differentially-regulated genes with an FDR <10% **(Fig. 3.9)**. Of these, 8 were upregulated in *Bmi1* heterozygous livers and 15 were downregulated. Two noteworthy genes from this list were members of the core circadian clock machinery, *Bmal1* (*Arntl*) and *Npas2*. By expanding the stringency of our list of differentially-regulated genes to include those with p-values below 0.01, we identified two additional circadian genes affected by *Bmi1* heterozygosity: *Nr1d1* and *Nr1d2*, also known and *Rev-erbα* and *Rev-erbβ*, respectively.

Together, these 4 clock genes were particularly interesting, as they contribute to the maintenance of circadian rhythmicity of clock target genes. Circadian expression of target genes has been shown to be critical in maintaining normal metabolic function (reviewed in 9). We confirmed a significant ~25% reduction in *Bmal1* transcript and a trend towards reduction in *Nr1d2* transcript in *Bmi1*$^{+/-}$ liver at 5 PM (**Fig 3.10**). This time point corresponds with high expression of *Nr1d2* and repressed expression of *Bmal1*. There was no difference in transcript 12 hours earlier at 5AM, when the overall expression patterns were reversed.

Gene	Fold Change	FDR
Ypel2	0.56	0.02
Cish	3.30	0.02
Rdh9	2.09	0.02
Cyp2a4	8.89	0.03
Npas2	0.10	0.04
Tubb2a	0.45	0.04
Slc15a2	0.22	0.05
Pitx3	0.36	0.06
Slc34a2	0.24	0.06
Lpl	0.47	0.06
Bmi1	1.53	0.06
Thbs1	0.37	0.06
1700001L05Rik	1.82	0.06
Gm14420	1.63	0.08
Chka	0.39	0.08
Btbd19	2.75	0.08
Rnf125	0.52	0.09
Gm14403	1.57	0.09
Arntl	0.33	0.09
Dtx4	0.51	0.09
Bcl6	0.53	0.09

Figure 3.9. Differential expression of genes in Bmi1 heterozygous liver. List of transcripts identified in RNA-seq comparing *Bmi1*$^{+/+}$ and *Bmi1*$^{+/-}$ livers. n=5 per genotype

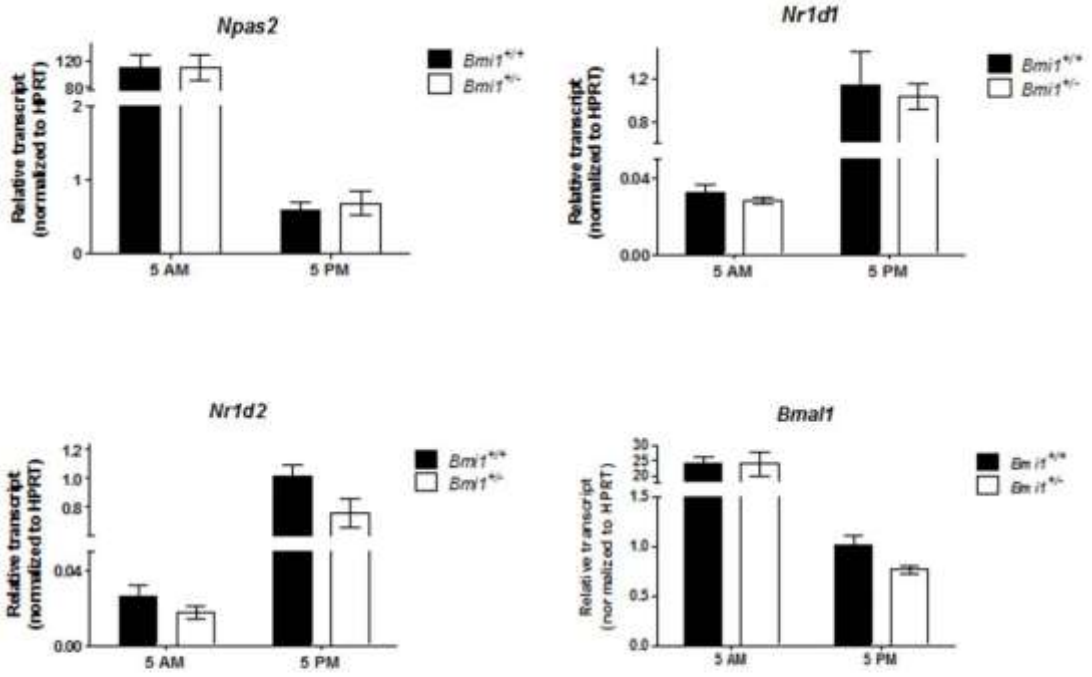

Figure 3.10. Expression of clock genes in *Bmi1*$^{+/+}$ and *Bmi1*$^{+/-}$ liver. qPCR comparing expression of clock genes identified in RNA-seq. n=5-6 per genotype and time

Another group of genes identified as differentially expressed in *Bmi1* heterozygous livers were those associated with JAK/STAT signaling, specifically *Cish*, *Myc*, and *Ccnd1*. These targets were first assessed by qPCR **(Fig. 3.11a)**. *Cish* expression was found to be significantly increased in *Bmi1*$^{+/-}$ livers, whereas *Myc* and *Ccnd1* expression was not significantly different between genotypes. In order to further assess the activity of this pathway, STAT5 phosphorylation was measured by western blot analysis after saline or insulin injection. Insulin induced a statistically significant increase in STAT5 phosphorylation in *Bmi1*$^{+/+}$ livers, whereas the stimulated levels of phospho-STAT5 were significantly reduced in *Bmi1*$^{+/-}$ livers **(Fig. 3.11b)**.

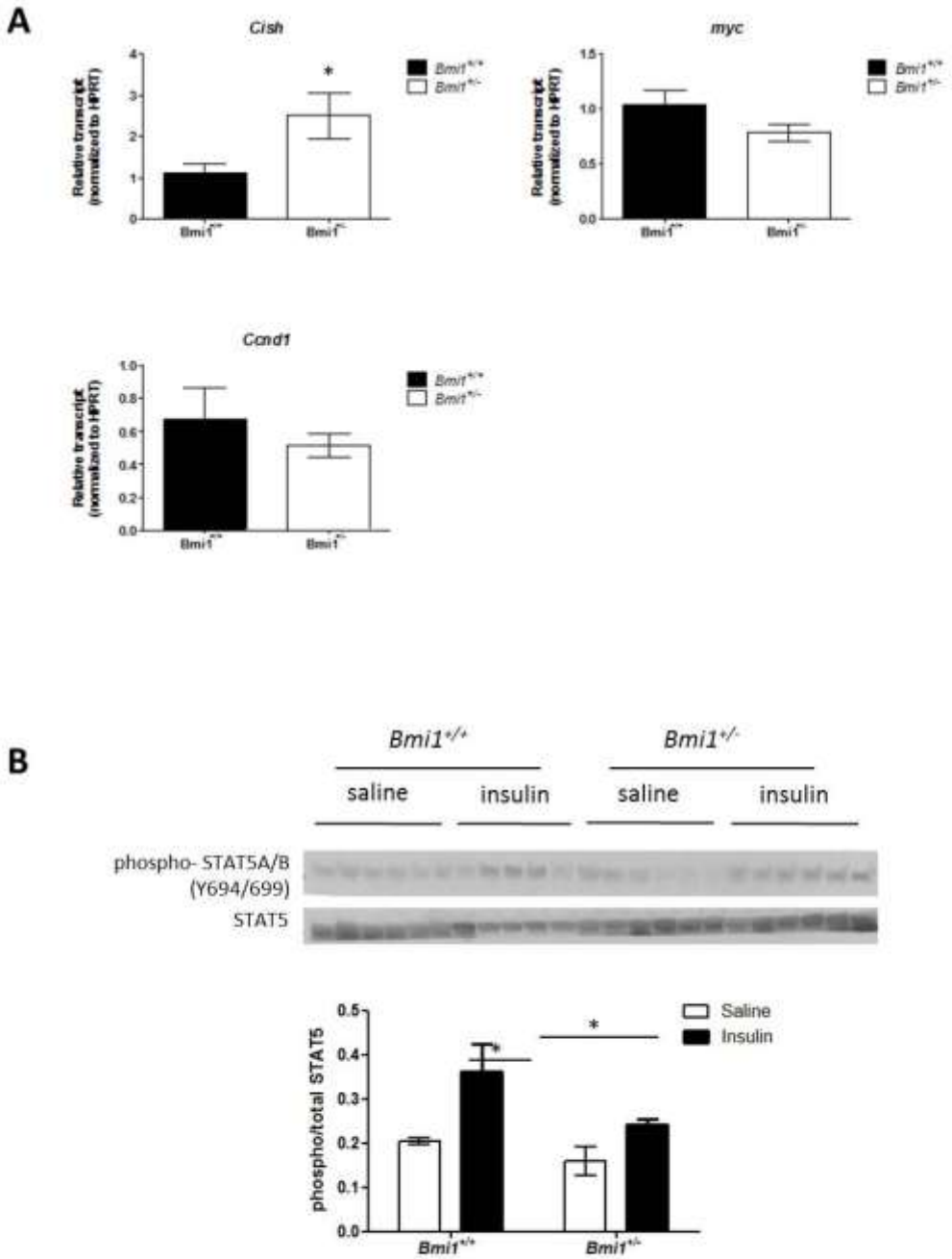

Figure 3.11. Expression of JAK/STAT genes in *Bmi1*$^{+/+}$ and *Bmi1*$^{+/-}$ liver. (A) qPCR comparing expression of JAK/STAT-related genes identified in RNA-seq. (B) 15 week old males fasted for 5 hours and then injected with saline or 5U insulin into the IVC. Livers were harvested 2 minutes later and lysates assessed by western blot. Western blots and quantification showing levels of phosphorylated and total STAT5. n=5-6 per genotype *$p < 0.05$

3.5 Discussion

We identify a novel role for the Polycomb protein, Bmi1, in regulating insulin sensitivity. Alterations in insulin signaling in both liver and muscle tissue appear to contribute to a striking improvement in whole-body insulin sensitivity. Homozygous loss of *Bmi1* has been associated with severe glucose intolerance and diabetes due to stunted beta cell replication [96]. It was therefore surprising to discover the favorable metabolic phenotype of *Bmi1*$^{+/-}$ mice. Not only was there no impairment of glucose homeostasis, there was a trend toward protection from HFD-induced glucose intolerance and a clear sensitization of insulin responsiveness in these animals. Our data therefore indicate a role for Bmi1 in extra-islet tissues in regulating glucose homeostasis.

We find a striking effect of Bmi1 gene dosage on Akt activity. A comprehensive analysis of early insulin signaling events revealed no difference in activation of IR, IRS1, or ERK1/2, nor alterations in the transcript levels of known regulators of Akt, including IRS1, Akt phosphatases, and the PI3K regulatory subunit p85. Thus, the mechanism by which Bmi1 influences Akt activity warrants further investigation.

We also noted a decrease in plasma insulin levels in *Bmi1*$^{+/-}$ animals following a glucose bolus. While we interpret this to indicate an adaptive response to reduced insulin requirement by more sensitive *Bmi1*$^{+/-}$ tissues, at this time we cannot rule out the possibility that the livers of these animals are clearing glucose more rapidly from the blood. Given the supporting molecular data showing enhancement of insulin signaling, we believe this to be an unlikely explanation.

The observations that *Bmi1* null animals have no discernible difference in hepatocyte proliferation compared to wildtype [110] and that p16 expression is not detectable in

hepatocytes (data not shown) suggest a non-classical, proliferation-independent role of Bmi1 in the liver. Although recent studies have begun to explore the potential for Bmi1 action independent of its regulation of the *Ink4a/Arf* locus, Bmi1 targets identified in neural stem cells [128] were not dysregulated in *Bmi1*$^{+/-}$ liver (data not shown), suggesting that Bmi1 targets may be tissue-specific. Further, the lack of a clear consensus sequence for mammalian PRC1 binding [121,122], complicates efforts to predict Bmi1 targets in the liver. A direct determination of Bmi1 targets in liver by chromatin immunoprecipitation and high throughput sequencing will be required to identify the direct Bmi1 targets involved in insulin action in the liver. Further, it is likely that derepression of multiple genes contributes to this phenotype.

Our current model is limited by the global and heterozygous nature of the genetic deletion, which complicates interpretation of how specific tissues are contributing to the overall improvement in insulin sensitivity. It is likely that tissues in addition to liver contribute to the insulin sensitivity phenotype. The marked increase in glucose disposal rate indicates that glucose uptake in the peripheral tissues is a key contributor to this phenotype, which we speculate is due, at least in part, to Bmi1 regulation of insulin signaling in muscle. Additionally, it is still unclear whether the role of Bmi1 in insulin sensitivity is gene dosage dependent, since the severely shortened lifespan of the *Bmi1* null mice precludes the type of analysis we present here. Future work in a tissue-specific model, when one becomes available, will circumvent these limitations. Complete ablation of Bmi1 in liver may further protect animals from age- and/or high fat diet-induced insulin resistance, compared to the heterozygous deletion described here.

Given the myriad of negative phenotypes associated with *Bmi1* deletion, it was unanticipated to see such a strikingly positive effect of *Bmi1* heterozygosity. Our observations not only highlight the role of Bmi1 in regulating insulin sensitivity but also

broaden the scope of phenotypes that Bmi1 and PRC1 play a role in beyond their classical regulation of cell cycling.

CHAPTER 4: BMI1 PROTEIN LEVELS ARE DYNAMIC

4.1 Abstract

Phenotypes associated with Bmi1, such as regulation of beta cell proliferation, as described previously, and the development of insulin resistance, as described in the previous chapter, seem to occur only at specific ages. Regulation of Bmi1 function and/or levels with age therefore appears to be critical in regulating the downstream effects of Bmi1. Previous work indicates that Bmi1 can be regulated at a transcriptional level as well as post-translationally modified. Analysis of Bmi1 protein levels revealed that Bmi1 increases with both age and insulin resistance, whereas acute insulin treatment reduces Bmi1 protein independent of transcript. Pcif1 ubiquitinates Bmi1 in 293T cells and this may provide one explanation for the post-translational regulation of Bmi1 levels in response to insulin.

4.2 Introduction

Bmi1 protein and transcript levels have been shown to decrease dramatically early in life in pancreatic islets [111]. Additionally, in islets, Bmi1 protein levels remain low in mice throughout late adulthood. However, the observed age-dependence of the phenotypes described in Chapter 3 raised the question of the role of Bmi1 with age in the liver. One particularly relevant phenotype associated with aging is insulin resistance. Here we will focus on 4 models of insulin resistance: aging, deletion of the leptin gene ($Lep^{ob/ob}$), deletion of insulin receptor in the liver (LIRKO), and deletion of Akt1/2 in the liver (DLKO). Although induced by different mechanisms, all of these animals exhibit some degree of hyperglycemia and insulin intolerance [33,129].

Although Bmi1 levels are known to change with age, little is known about the mechanism behind this. Bmi1 has been shown to be regulated at a transcriptional level by the transcription factors E2F-1 and c-Myc [130,131]. Other known regulators of Bmi1 have been shown to act in a post-translational manner and therefore cannot explain the transcriptional changes seen early in life [114,116,132]. However, post-translational regulation of Bmi1 may provide an explanation for the appearance of the phenotypes described in Chapter 3 later in life.

Bmi1 has been shown to be both ubiquitinated and phosphorylated, both of which have been implicated in destabilizing the protein [114,116,132]. As noted earlier, Pcif1 has been shown to ubiquitinate Bmi1 [112]. Additionally, knockdown of deubiquitinating enzymes that act on Bmi1 results in accumulation of ubiquitinated Bmi1 and reduction of Bmi1 protein levels [113].

Phosphorylation of Bmi1 has been shown to negatively influence the activity of Bmi1, primarily by inhibiting association with chromatin [115]. Two kinases in particular have been shown to phosphorylate Bmi1: MAPKAP kinase 3 (3pK) and Akt [114,116,133]. It is noteworthy when considering the metabolic impact of differential Bmi1 levels to note that both of these kinases can be activated by insulin [25,134,135].

In the studies described below, we find that Bmi1 protein levels appear to be influenced by insulin levels. Additionally, we find that Pcif1 facilitates the ubiquitination of Bmi1 and that this results in decreased Bmi1 protein.

4.3 Materials and Methods

4.3.1 Animals and physiological experiments

All animal experiments were performed according to procedures approved by the Institutional Animal Care and Use Committee of the University of Pennsylvania. Animals were placed on high fat diet (60% fat), low fat diet (10% fat) (Research Diets Inc., New Brunswick, NJ) or standard chow at weaning. *Bmi1*$^{+/-}$ mice were previously described [107]. Mice were maintained on a C57BL/6N background.

Lep$^{ob/ob}$ and wildtype mice were obtained from Jackson Laboratories. Liver samples from LIRKO mice were a gift from Morris Birnbaum (2 month old animals) and Rohit Kulkarni (6 month old animals).

4.3.2 Tissue culture

HEK293T cells were maintained in DMEM with 25 mM glucose (Invitrogen) supplemented with 10% FBS, and 1% penicillin/streptomycin. Cells were transfected with Lipofectamine 2000 according to manufacturer's instructions using indicated plasmids.

4.3.3 Western blot analysis

HEK 293T cells, livers, and isolated hepatocytes were sonicated in lysis buffer (50 mM Tris-Cl, pH 7.8, 2% SDS, 10% glycerol, 10 mM $Na_4P_2O_7$, 100 mM NaF, 6 M urea, 10 mM EDTA). Proteins were resolved by SDS-PAGE and immunoblotted with the following antisera: mouse anti-Bmi1 clone F6 (Millipore, 1:1000), mouse anti-FLAG (Sigma, 1:1000), mouse anti-Ran (1:10,000, BD Biosciences), anti-HA-Peroxidase (Roche, 1:1000).

4.3.4 Ubiquitination assay

Ubiquitination assay was performed as described previously [93]. Briefly, HEK293T cells were transfected with Lipofectamine 2000 according to manufacturer's instructions using constructs for HA-Bmi1 and myc-ubiquitin with and without FLAG-Pcif1 and FLAG-Cul3. Cells were harvested after 48 hours and lysed in RIPA buffer, followed by immunoprecipitation for myc as well as an IgG control. Immunoprecipitated proteins were analyzed by western blot analysis. Input lysate was also analyzed to compare overall protein levels and verify loading controls.

4.3.5 RNA isolation and quantitative RT-PCR

Total RNA was isolated from snap-frozen liver using Trizol (Invitrogen, Carlsbad, CA), according to the manufacturer's instructions. Ribosome-associated RNA was isolated using the RNeasy mini kit (Qiagen). DNA was digested using the TURBO DNA-free kit (Life Technologies). RNA concentrations were measured on a Nanodrop ND-1000 spectrophotometer (Thermo-Scientific, Wilmington, DE). RNA integrity was assessed using an Agilent 2100 Bioanalyzer (Agilent Technologies, Santa Clara, CA). To synthesize cDNA, RNA was reverse-transcribed with SuperScript III (Invitrogen) according to manufacturer's instructions. Quantitative real time PCR was performed on a Bio-Rad CFX384 384-well thermal cycler.

4.3.6 Statistical Analysis

All data are represented as mean +/- SEM. Statistical significance was assessed by two-tailed Student's t test or two-way ANOVA (Prism GraphPad).

4.4 Results

4.4.1 Bmi1 protein levels change with age

The decline in Bmi1 transcript and protein early in life has been well-described in the beta cells [111]. However, to date, no studies have explored Bmi1 levels with age in liver. Liver was harvested from mice 2 weeks, 8 weeks, 16 weeks, and 24 weeks of age. From 2 weeks to 8 weeks, there was a strong decline in Bmi1 protein and transcript, correlating with observations in other tissues **(Fig. 4.1)**. Surprisingly, in older animals there was a dramatic increase in protein levels with no change in transcript. Given the well-established decline in insulin sensitivity with age, we hypothesized that Bmi1 protein may be correlated to serum insulin levels.

4.4.2 Effect of liver-specific insulin resistance on Bmi1 levels

To determine whether Bmi1 levels correlate inversely with insulin sensitivity in another model, we examine Bmi1 levels in the LIRKO (liver insulin receptor knockout) model of insulin resistance. LIRKO mice display reduced body weight, severe fed hyperglycemia and hyperinsulinemia, as well as an abolishment of insulin-induced suppression of

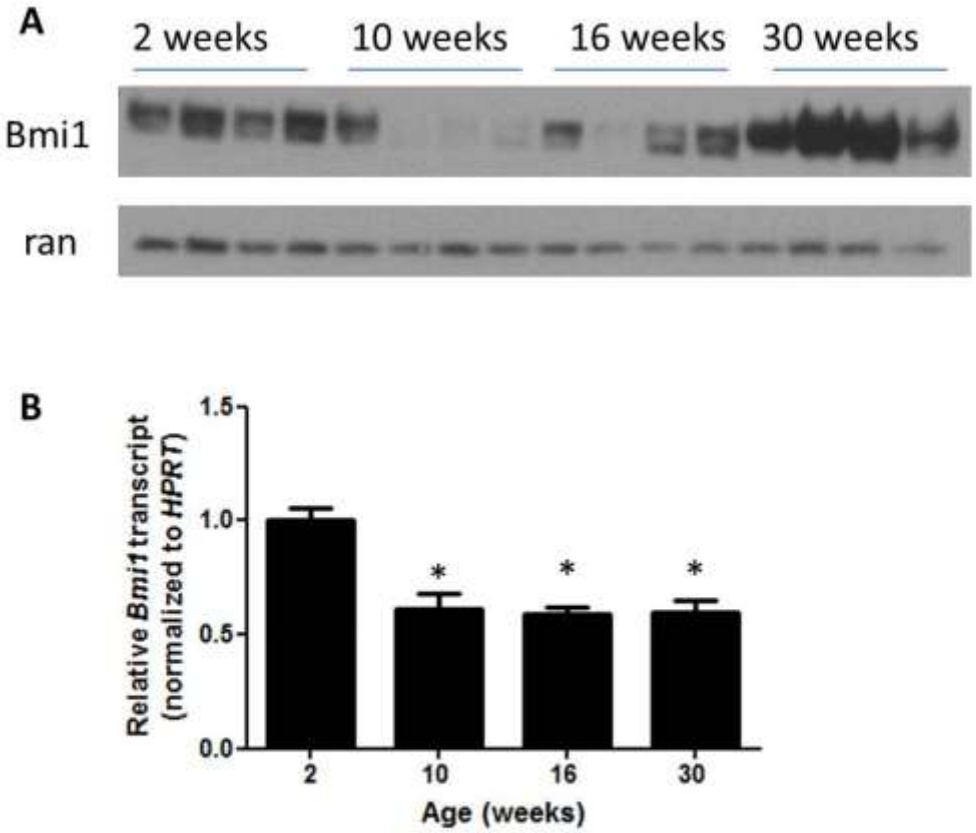

Figure 4.1. Bmi1 levels change dramatically with age. Livers harvested from mice of indicated ages. (A) Western blot of lysates from snap-frozen livers showing levels of Bmi1 protein with age. (B) *Bmi1* transcript levels normalized to *HPRT* transcript.
n=4 mice per age; *p<0.05 vs 2 weeks

hepatic glucose production [136]. In liver from 2 month old animals, there was no difference in Bmi1 levels between LIRKO and control in either the fasted or fed state **(Fig. 4.2a)**. Notably, Bmi1 protein levels were increased in the livers of 6 month old LIRKO mice, compared to control littermates **(Fig. 4.2b)**. Consistent with insulin resistance, these LIRKO animals displayed the expected phenotypes of hyperglycemia, hyperinsulinemia, and reduced body weight **(Fig. 4.2c-e)**. Thus, Bmi1 protein levels are inversely correlated with insulin sensitivity in two well established models of insulin resistance.

Deletion of Akt 1 and 2 in liver (DLKO mice) results in severe hyperglycemia, disrupted insulin signaling, and insulin resistance [129]. Additionally, serum insulin levels are increased approximately 5 times above control levels. Analysis of lysates from livers lacking Akt1/2 from 8-week old animals revealed a decrease in Bmi1 protein compared to controls **(Fig. 4.3)**.

4.4.3 Effect of leptin deletion on Bmi1 levels

As a final model of insulin resistance, Bmi1 levels in the livers of 16 week old *Lep*$^{ob/ob}$ (ob/ob) males were measured by western blot analysis. These animals are severely obese, hyperinsulinemic, glucose intolerant, and insulin resistant due to deletion of the leptin gene [137]. When compared to controls, Bmi1 protein levels were dramatically lower in ob/ob livers **(Fig 4.4)**.

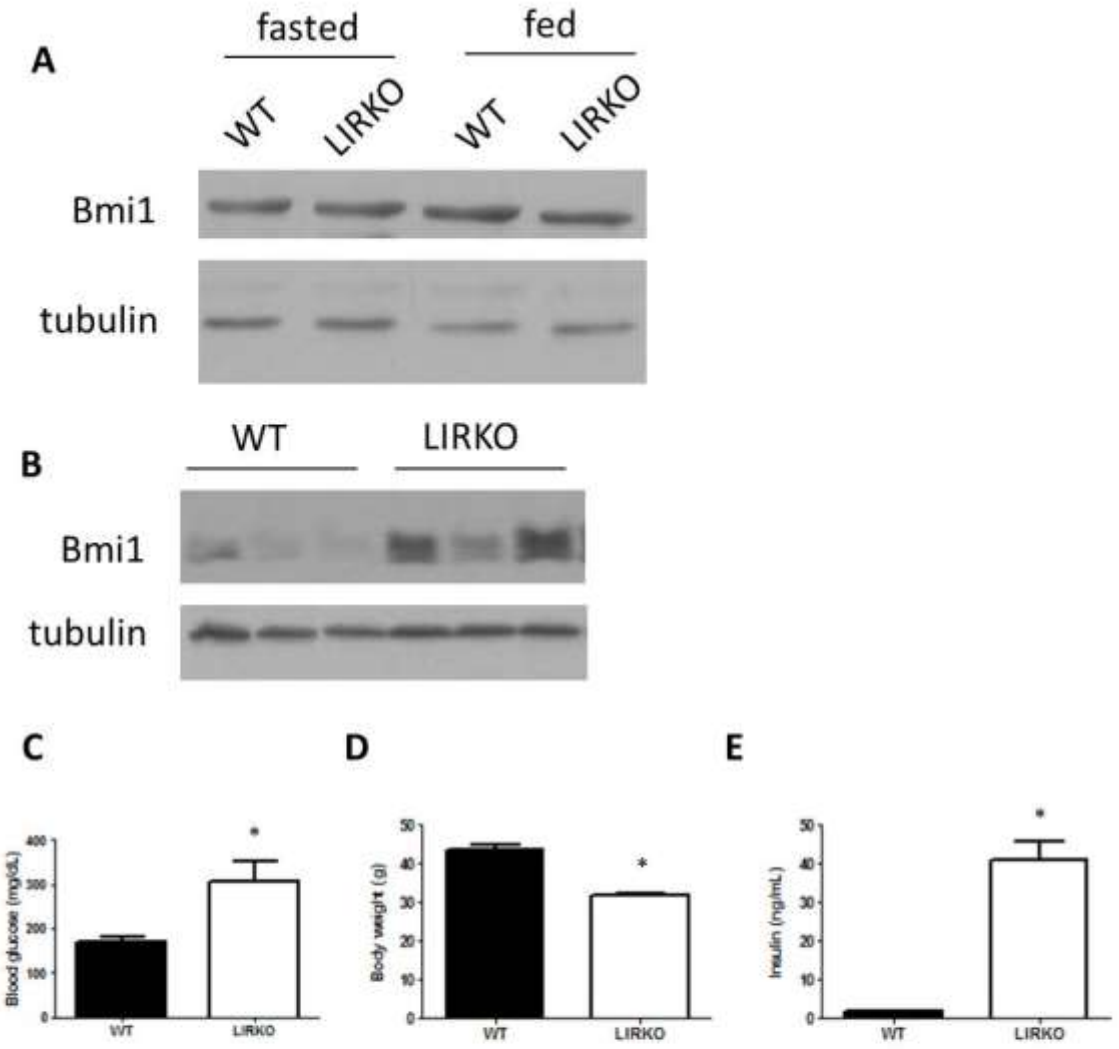

Figure 4.2. Prolonged liver insulin resistance results in increased Bmi1 protein. Livers harvested from LIR WT and LIR KO mice of indicated ages. (A) 2 months old LIRKO or control mice fasted overnight. Fed animals re-fed 2 hours. Western blot of lysates from snap-frozen livers probed for Bmi1 protein. (B) Western blot of lysates from snap-frozen livers from 6 month old animals probed for Bmi1 protein. (C-E) Physiological analysis of (C) blood glucose levels, (D) body weight, and (E) serum insulin levels from 6 month old LIRKO and control animals.

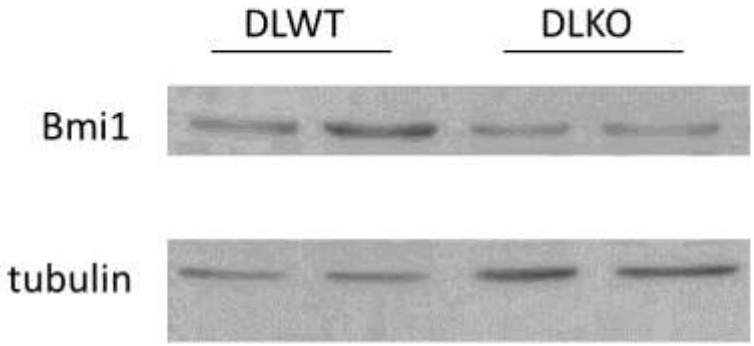

Figure 4.3. Bmi1 protein decreased in DLKO livers at 2 months of age. Livers harvested from 2 month old DLWT and DLKO mice. Western blot of lysates from snap-frozen livers probed for Bmi1 and tubulin.

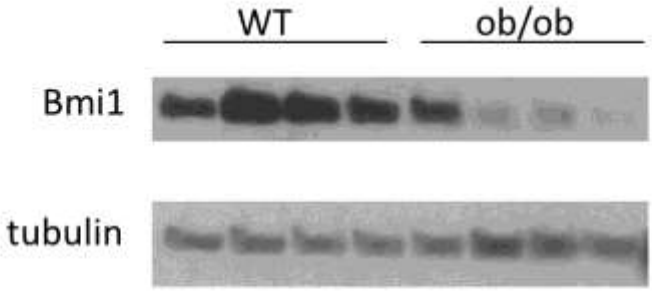

Figure 4.4. Bmi1 protein is reduced in ob/ob livers. Livers harvested from 16 week old ob/ob mice. Western blot of lysates from snap-frozen livers probed for Bmi1 protein. Tubulin was used as a loading control.

4.4.4 Acute insulin stimulation leads to decrease in Bmi1 protein in liver

Given the potential correlation between insulin levels and Bmi1 protein, we next assessed the effect of acute insulin stimulation on Bmi1. After a 5 hour fast to minimize stimulation by endogenous insulin, wildtype mice were injected with saline or insulin 20 minute prior to sacrifice. Western blot analysis revealed a 54% reduction in Bmi1 protein **(Fig. 4.5)**. Based on observations that Bmi1 is regulated at both the transcriptional and post-transcriptional levels ([111,114,116] and **Fig 4.1**), *Bmi1* transcript was also

measured. Transcript levels were unchanged in the livers from insulin-treated animals as compared to saline-treated controls, indicating that the insulin-mediated reduction in Bmi1 protein occurred post-transcriptionally. Given the acute nature of the treatment, it is unlikely that the differences in protein levels were due to changes in translation rates, although not impossible. The more likely explanation involves post-translational regulation of Bmi1 levels.

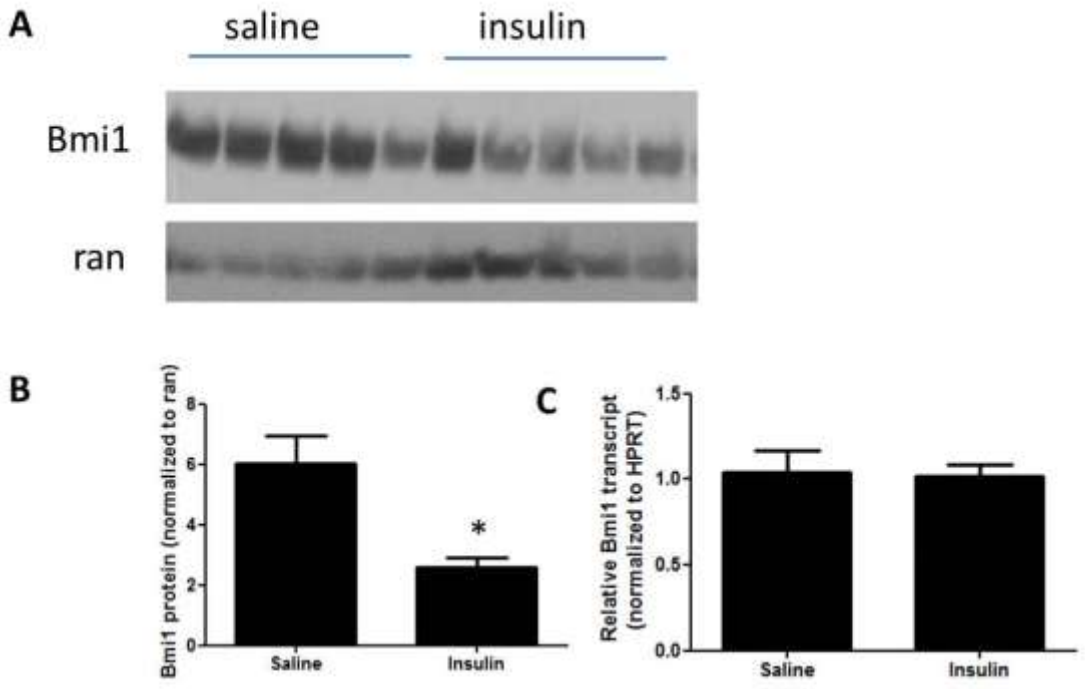

Figure 4.5. Acute insulin lowers Bmi1 protein in liver. Livers harvested from 16-week old wildtype mice injected with saline or insulin (1.5 U/kg) and harvested 20 minutes later. (A) Western blot of lysates from snap-frozen livers probed for Bmi1 protein. (B) Quantification of Bmi1 western blots. *p<0.05 (C)) *Bmi1* transcript levels normalized to *HPRT* transcript. n=6 per condition

4.4.5 Pcif1 ubiquitinates Bmi1 in HEK293T cells and results in lower protein levels

In order to further characterize the post-transcriptional modifications of Bmi1, a cell-based ubiquitination assay was used. Bmi1 and ubiquitin were overexpressed in HEK293T cells with and without Pcif1 and Cul3. Lysates were then immunoprecipitated

for ubiquitin and immunoblotted for Bmi1 **(Fig. 4.6a)**. Laddering of ubiquitinated Bmi1 was present at low levels in lysates with Bmi1 alone, Bmi1 plus Pcif1, and Bmi1 plus Cul3. Levels of ubiquitinated Bmi1 were dramatically increased in the presence of both Pcif1 and Cul3. Additionally, substituting a mutated Cul3, without the ability to bind Pcif1, reduced the laddering. Low levels of ubiquitination when Pcif1 and Cul3 are not overexpressed are likely due to endogenous Pcif1 and Cul3 in HEK293T cells. Expression of indicated plasmids was as expected **(Fig. 4.6b)**. Overexpression of Bmi1 with or without Pcif1 and Cul3 in HEK293T cells revealed that Pcif1 overexpression lowered Bmi1 protein levels **(Fig. 4.7)**.

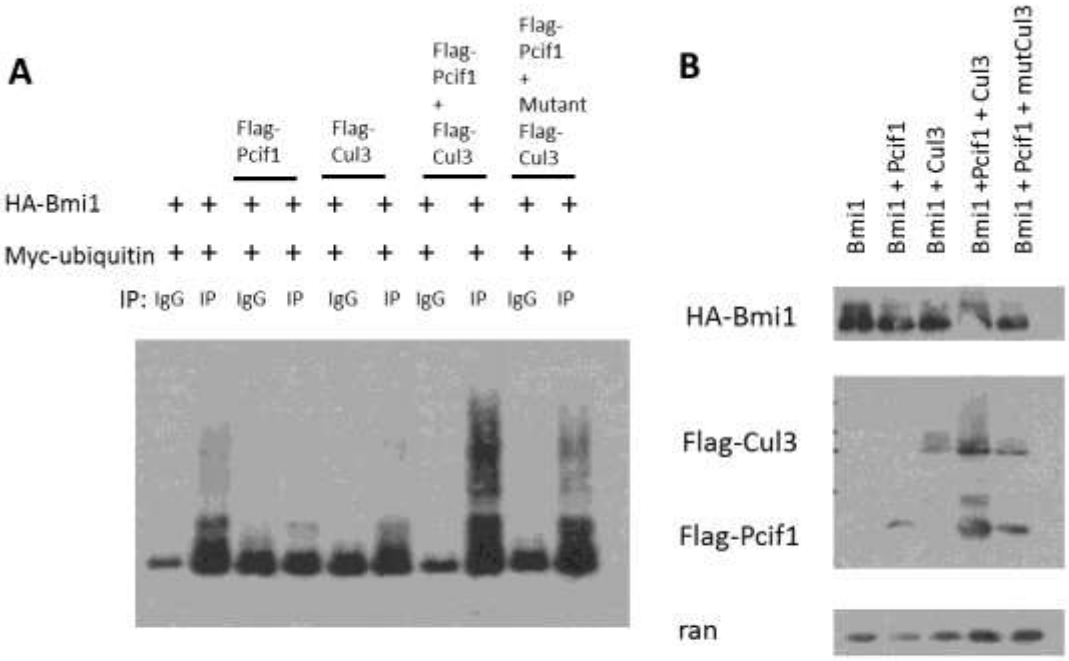

Figure 4.6. Bmi1 ubiquitination is enhanced by Pcif1 overexpression. HEK293T cells transfected with the indicated constructs and harvested 48 hours later. (A) Immunoprecipitation for myc or IgG control, followed by immunoblot for HA. (B) Immunoblots showing expression of indicated constructs.

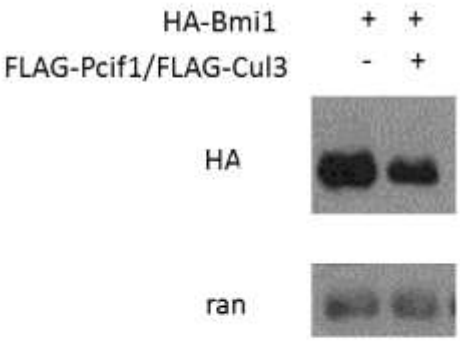

Figure 4.7. Pcif1/Cul3 overexpression results in lowered Bmi1 protein. HEK293T cells transfected with the indicated constructs and harvested 48 hours later. Immunoblot showing expression of HA. Ran was used as a loading control.

4.5 Discussion

An age related decline in Bmi1 expression has been observed in mutiple tissues and is associated with a decline in replication [111]. An initial reduction of Bmi1 protein levels occurs between 2 and 8 weeks in liver as well; however, Bmi1 levels subsequently increase dramatically with progressive age, surpassing the levels seen in juvenile livers by 30 weeks. The mechanisms underlying these temporally dynamic changes in Bmi1 levels warrant further investigation.

Here we describe two seemingly incongruous phenotypes. One, where elevated insulin appears to result in an increase in Bmi1 protein and another, where hyperinsulinemia results in less Bmi1 protein.

Bmi1 protein increases with age, independent of transcriptional changes. Hepatic insulin resistance and hyperinsulinemia caused by *IR* deletion also results in increased Bmi1 protein in an age-dependent manner. Surprisingly, obesity and insulin resistance caused by deletion of leptin results in decreased Bmi1 protein at 4 months of age. Acute administration of insulin results in decreased Bmi1 protein with no change in transcript. Additionally, hyperinsulinemia early in life, via *Akt1/2* deletion, results in decreased Bmi1 protein. Although these mice are insulin resistant, they are quite young, compared to the 6 month old LIRKO animals.

The data from all of the described mouse models lead us to hypothesize that, acutely and early in life, insulin stimulates pathways that reduce Bmi1 protein. We show that high levels of Bmi1 are indicative of insulin resistance but the explanation for this is less clear. Further, it is unclear what the primary phenotype is in this situation. The first possibility is that insulin resistance causes Bmi1 protein to accumulate because the pathways upstream of Bmi1 cannot respond appropriately to insulin. This would place

Bmi1 as more of a passive hallmark of insulin resistance. Another possibility is that Bmi1 itself is involved in inhibition of insulin signaling under basal conditions and is reduced in response to insulin in order to allow signaling to progress. Therefore high Bmi1 levels are actually contributing to insulin resistance. Given the observations from Chapter 3 that reducing Bmi1 levels results in improved insulin sensitivity, we believe this to be the more likely explanation.

The mechanism by which insulin influences Bmi1 is unclear at this point. Here, we explored one possibility—that Bmi1 is ubiquitinated by Pcif1 in response to insulin. Further work would need to be done to characterize the result of this ubiquitination, although the data in Figure 4.7 are suggestive that ubiquitination by Pcif1 may lead to proteasomal degradation, as that is a well-described pathway for other Pcif1 targets [88,90,94,112,118,119]. Additionally, it would be interesting to characterize the phosphorylation of Bmi1 in response to insulin, especially given that two insulin-stimulated kinases, Akt and MAPKAP kinase 3 (3pK), have been shown to phosphorylate Bmi1 [114,116,132].

CHAPTER 5: MAPPING THE BETA CELL TRANSLATOME

5.1 Abstract

ER stress results in a complex cellular response in order to attempt to restore ER homeostasis. One strategy is to reduce the translational load placed on the cell until stress can be resolved. Beta cells are placed under a particularly high level of stress, given the high demand for insulin production placed on them. Characterizing the stress response in beta cells may help to identify ways to maintain beta cell mass by helping to resolve ER stress prior to failure and apoptosis. Here we apply the immunoprecipitation-based translating ribosome affinity purification (TRAP) methodology in order to study translation in beta cells on a global scale. A pilot screen in Min6 cells using thapsigargin to induce ER stress validated that transcripts with the predicted ability to escape ER stress showed an increase in translational efficiency. Translational efficiencies were then assessed on a global scale in the context of Pdx1 knockdown. Analysis of this dataset indicated that Pdx1 may be repressing translation under normal conditions, as the efficiencies of a subset of genes was increased with Pdx1 knockdown, with the translational efficiency of only one transcript being significantly reduced.

5.2 Introduction

ER stress has been implicated in the development of diabetes, specifically beta cell dysfunction and death [49,138]. Mutation of the eukaryotic translation initiation factor 2-alpha kinase (EIF2AK3) gene in humans results in a form of monogenic diabetes known as Wolcott-Rallison syndrome [139]. EIF2AK3 is the human ortholog of PERK, one of the key mediators of the ER stress response in rodents. Additionally, a mutation in Wolfram syndrome gene 1 (Wfs1) results in disruption of an ER calcium channel, causing ER stress and diabetes [140].

In addition to the severe monogenic forms of diabetes, ER stress has been associated with Type 2 diabetes as well. Markers of ER stress are upregulated in islets of Type 2 diabetic patients [56]. Additionally, treatment of Min6 cells with palmitate to simulate the high levels of free fatty acids seen in diabetic patients led to an induction of the ER stress program and eventual apoptosis [56]. Chronic exposure to high glucose levels, characteristic of a diabetic state, results in activation of the UPR in rat islets [141], thus also implicating the ER in glucotoxicity. In addition to glucose and fatty acids, cytokines have also been shown to activate the UPR in beta cells [142], thus implicating ER stress in the beta cell dysfunction and death associated with Type 1 diabetes as well.

Sarcoplasmic/endoplasmic reticulum Ca^{2+}-ATPase 2b (SERCA2b) is a calcium transporter important for maintaining ER homeostasis whose expression is reduced under diabetic conditions [143,144]. Thapsigargin is a SERCA inhibitor that results in depleted ER Ca^{2+} and inhibited autophagy, resulting in ER stress [145]. Many SERCA inhibitors exist but thapsigargin is by far the most popular and therefore the most well-described in literature. Ca^{2+} concentrations are disproportionally high in the ER, compared to the rest of the cell [146]. These high levels are attained through the actions of the SERCA pumps. Inhibition of these pumps depletes calcium in the ER, resulting in ER stress [147]. Treatment with thapsigargin results in severely decreased protein synthesis and dissolution of polysomes [148] as well as upregulation of ER stress-associated genes [149].

As discussed in Chapter 1, one result of ER stress is a general downregulation of protein translation, with the exception of a subset of genes whose upregulation aids in resolution of ER stress. Multiple methods exist to characterize those genes. The goal of all of these methods is to isolate ribosome-associated transcripts, with the assumption that transcripts bound by ribosomes are those that are actively being translated. The

traditional approach is to use a sucrose density gradient to isolate polysomes, along with the associated mRNA [51,150]. While effective, this method requires a large amount of starting material, thus making it difficult to apply to small amounts of material, such as primary tissue. Additionally, unless a pure cell population is used as input, it is not possible to distinguish the translatome of a specific cell type. This makes analysis of heterogeneous tissues complicated [151].

Newer published methods utilize immunoprecipitation of ribosomal proteins to isolate ribosomes, as well as associated transcripts. The RiboTag method uses an HA-tagged ribosome protein, Rpl22, while the TRAP method uses an EGFP-tagged ribosome protein L10a [152–154]. The epitope-tagged ribosomal proteins can be overexpressed in cell lines or targeted to specific cell types *in vivo* via appropriate Cre drivers, eliminating the difficulty in analyzing the translatome of specific cell types. Further, these immunoprecipitation-based methods require less starting material than traditional methods, making analysis of small cell populations more viable.

Based on the association of ER stress with diabetes, characterization of the translational response to beta cell stressors may aid in more completely characterizing the role of ER stress in beta cell dysfunction and death, as well as the mechanisms by which beta cells respond to stress. Analysis of the beta cell translatome under conditions of ER stress will reveal common characteristics of transcripts important for ER stress response and possibly identify novel components of the beta cell stress response.

5.3 Materials and Methods

5.3.1 Tissue culture

293T cells were maintained in DMEM with 25 mM glucose (Invitrogen) supplemented with 10% FBS and 1% penicillin/streptomycin. Cells were transfected with Lipofectamine 2000 according to manufacturer's instructions using indicated plasmids.

Min6 cells were maintained in DMEM with 25 mM glucose (Invitrogen) supplemented with 10% FBS, 1% penicillin/streptomycin, and 0.001% betamercaptoethanol.

For thapsigargin treatment, 1 uM thapsigargin (Sigma) or vehicle (DMSO, Sigma) was added to the medium 6 hours before harvest.

For knockdown experiments, cells were nucleofected by AMAXA with an siRNA pool against either *Pdx1* or a non-targeting control (ON-TARGETplus SMARTpool, Dharmacon). 1 nmol siRNA was used per nucleofection. After 96 hours, cells were harvested for RNA expression analysis or TRAP immunoprecipitation.

5.3.2 Creation of stable cell lines

The EGFP-L10a plasmid has been described previously [153,154]. EGFP-L10a or EGFP alone was cloned into the retroviral pBABE-puro vector. BOSC retroviral producing cells were transfected and the media used 48 hours later to transduce Min6 cells for 6 hours. Cells were selected using puromycin for 5 days. Overexpression of EGFP-L10a was confirmed by qPCR and western blot.

5.3.3 Measuring protein translation

Amino acid-deficient DMEM was supplemented with 10% dialyzed FBS and 4mM L-glutamine. Min6 cells were seeded into 6-well tissue culture dishes. To each well, 2 mL AA-deficient media plus 165 uCi EasyTag Express protein labeling mix (Perkin Elmer) was added for labeling at 37C. Cells were then lysed and protein extracted using TCA precipitation. Incorporation of protein labeling mix was measured by scintillation counting. Counts were normalized to DNA content as measured by Nanodrop ND-100 spectrophotometer (Thermo-Scientific, Wilmington, DE).

5.3.4 Immunoprecipitation of ribosomes

The translating ribosome affinity purification (TRAP) method was used as previously described, with minor modifications [153,154]. Briefly, 293T or Min6 cells overexpressing EGFP-L10a or EGFP alone were harvested and immunoprecipitated overnight at 4C with anti-GFP (clones 19C8 and 19F7, Sloan Kettering). After immunoprecipitation, bound material was either isolated for western blotting or qPCR analysis. RNA was isolated using the RNeasy Mini Kit (Qiagen). Input protein and RNA was isolated from material collected prior to immunoprecipitation.

5.3.5 Western blotting

Proteins were resolved by SDS-PAGE and immunoblotted with the following antisera: goat anti-GFP (Abcam, 1:1000), mouse anti-RPL10a (Abnova, 1:1000), rabbit anti-RPL7 (Novus Biologicals, 1:1000), rabbit anti-S6 (Cell Signaling, 1:1000), mouse anti-tubulin (Sigma, 1:10,000).

5.3.6 RNA isolation and quantitative RT-PCR

Total RNA was isolated using Trizol (Invitrogen, Carlsbad, CA), according to the manufacturer's instructions. Ribosome-associated RNA was isolated using the RNeasy mini kit (Qiagen). DNA was digested using the TURBO DNA-free kit (Life Technologies). RNA concentrations were measured on a Nanodrop ND-1000 spectrophotometer (Thermo-Scientific, Wilmington, DE). RNA integrity was assessed using an Agilent 2100 Bioanalyzer (Agilent Technologies, Santa Clara, CA). To synthesize cDNA, RNA was reverse-transcribed with the High-Capacity Reverse Transcription kit (ABI). Quantitative real time PCR was performed on a Bio-Rad CFX384 384-well thermal cycler.

5.3.7 RNA sequencing

RNA sequencing libraries were generated using the Tru-Seq RNA Sample Prep Kit (Illumina). RNA sequencing was performed on an Illumina hiSeq2000 by the Next Generation Sequencing Core (NGSC) at the University of Pennsylvania.

5.3.8 Calculations and statistical analysis

Translational efficiency rates were calculated using the ratio of the reads for the ribosome-associated transcripts over the reads for the total input transcript. RNA-seq analysis was performed as previously described [155] by the NGSC at the University of Pennsylvania. All other data are represented as mean +/- SEM. Statistical significance was assessed by two-tailed Student's t test or two-way ANOVA, as appropriate (Prism GraphPad).

5.4 Results

5.4.1 Adapting TRAP methodology for use in beta cells

In order to study the role of translational regulation in the beta cell, a mouse insulinoma cell line, Min6, was used for initial experiments. A previously-described construct encoding an EGFP-tagged ribosomal protein, L10a, was used in order to facilitate immunoprecipitation [153]. This construct was stably overexpressed via retrovirus in Min6 cells to create the Min6-L10a cell line. As a control during immunoprecipitations, EGFP alone was expressed in separate cells to create the Min6-EGFP cell line.

To validate the TRAP methodology in our Min6 system, EGFP was immunoprecipitated from both cells lines. As shown in **Figure 5.1**, EGFP was efficiently depleted from both cell lines by immunoprecipitation. EGFP and EGFP-L10a are readily detectable in the immunoprecipitated material. Both endogenous and EGFP-tagged L10a are depleted in the Min6-L10a lysates, indicating that polysomes containing ribosomes both with and without EGFP-tagged L10a expressed are successfully being isolated using the TRAP methodology. We further validated this system by confirming co-immunoprecipitation of ribosomal proteins L7 and S6 specifically from the Min6-L10a cells. These experiments confirm that polysomes containing proteins from both ribosomal subunits can be isolated by immunoprecipitation of EGFP-tagged L10a in Min6 cells.

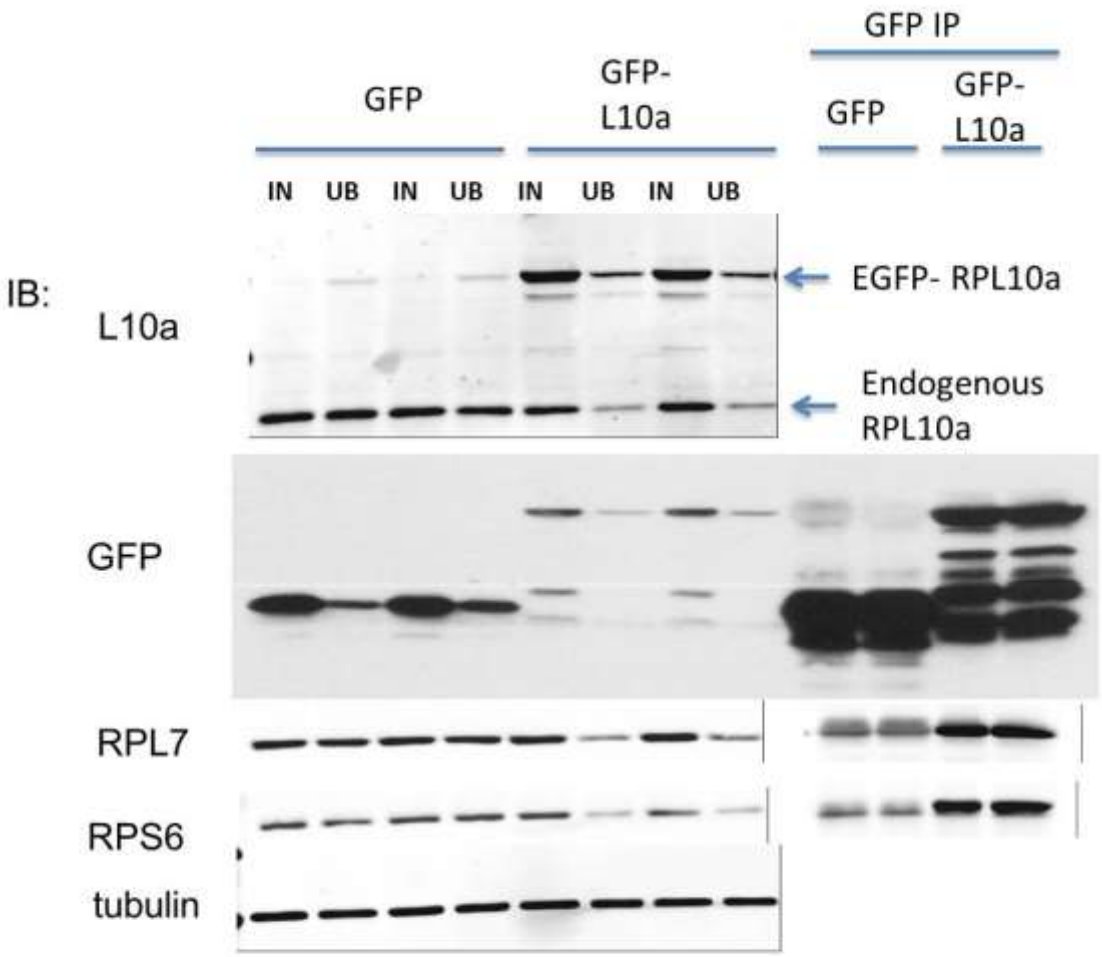

Figure 5.1. TRAP method isolates intact polysomes. Western blot of total lysates from Min6-EGFP and Min6-L10a cells before and after GFP immunoprecipitation (left 8 lanes), as well as bound, immunoprecipitated protein (right 4 lanes). Representative blots showing levels of L10a, GFP, RPL7, RPS6, and tubulin loading control.

IN: input lysate; UB: unbound post-IP lysate

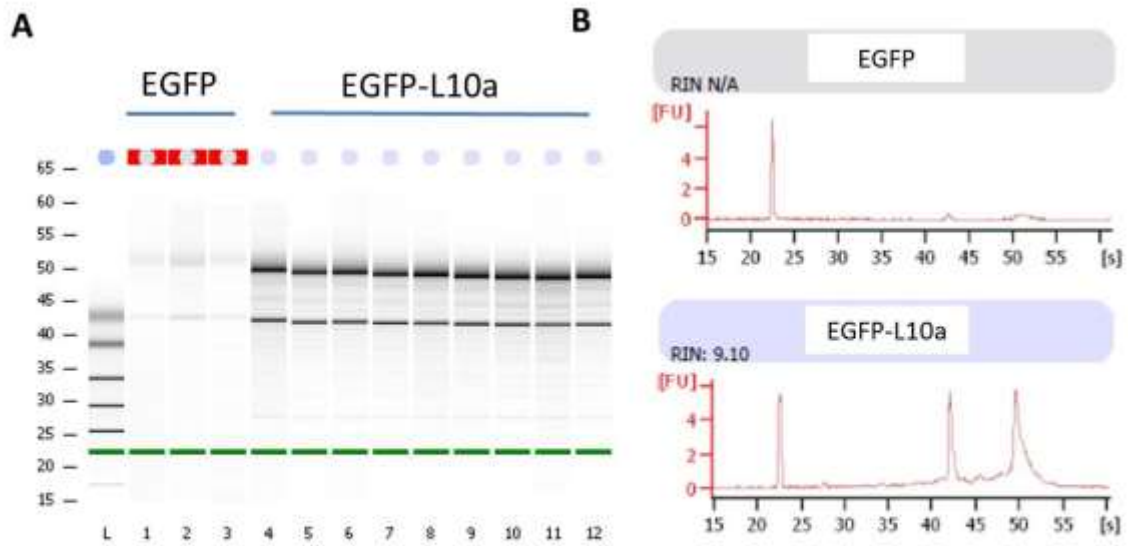

Figure 5.2. TRAP isolates high-quality ribosomal RNA from Min6 cells. (A) Bioanalyzer gel of RNA isolated from 3 or 9 IPs of Min6-EGFP or Min6-L10a, respectively. (B) Representative Bioanalyzer traces from Min6-EGFP and Min6-L10a lysates after immunoprecipitation. RIN: RNA integrity number

5.4.2 Pilot screen of transcripts escaping global downregulation due to ER stress

In order to further validate this system, we assessed the quantity and quality of transcript recovered from EGFP-L10a immunoprecipitation. The isolated RNA was found to be high-quality and suitable for use in downstream applications **(Fig. 5.2)**. Again, these results were specific to the Min6-L10a cell line, as no transcript was detected in the Min6-EGFP cells.

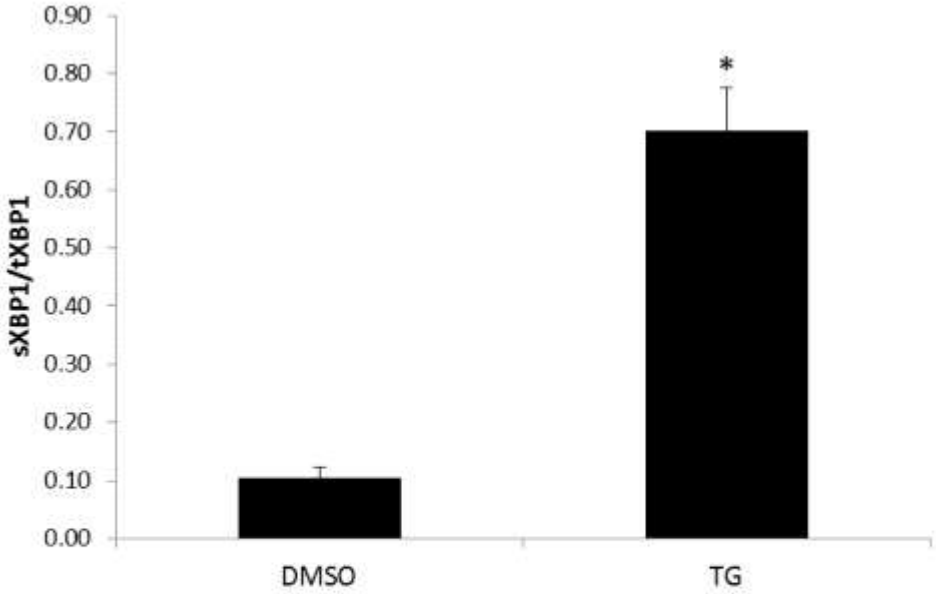

Figure 5.3. Thapsigargin induces ER stress in Min6 cells. Min6 cells harvested after 6 hr TG treatment. RNA isolated and subjected to qPCR analysis. Ratio of spliced to total XBP1 is shown. n=6; *p<0.00005

In Min6 cells thapsigargin induces significant ER stress after 6 hours, as measured by spliced XBP1 **(Fig. 5.3)**. This treatment also reduces overall levels of translation, as assessed by S^{35}-labeled cysteine and methionine incorporation **(Fig. 5.4)**. We recognizing that thapsigargin is not a physiologically relevant stressor but chose to utilize it to induce large changes in translation and then estimate translational efficiencies in selected pilot genes.

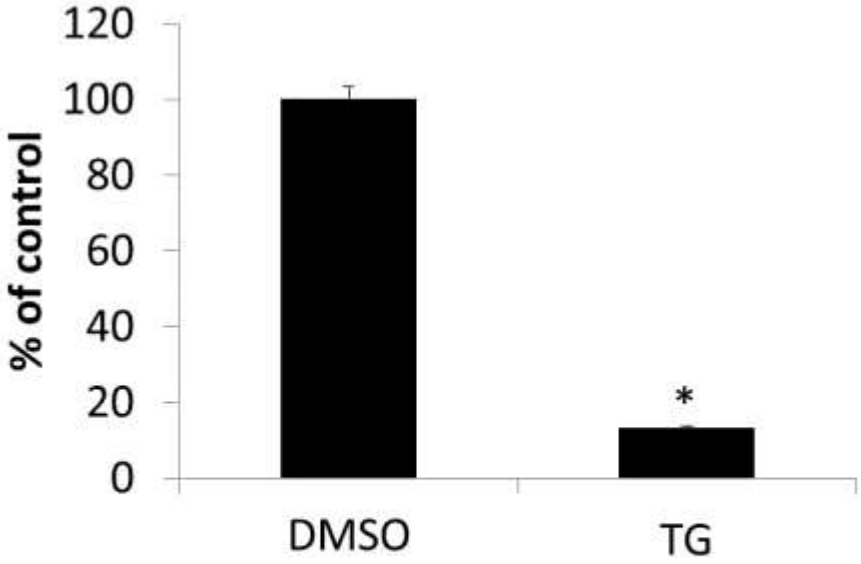

Figure 5.4. ER stress drastically reduces overall levels of translation in Min6 cells. Min6 cells treated 6 hours with thapsigargin (TG) or DMSO vehicle control. Protein synthesis measured by S35-methionine and-cysteine incorporation after 30 minute pulse. n=3; *p<0.0005

A small group of genes was chosen for a pilot screen to validate our methodology in this system. Genes were chosen based on indications in the literature predicting an ability to escape the global downregulation of translation in response to stress. Indications included the presence of an identified IRES, interaction with RNA stabilizing proteins, and others, detailed in **Figure 5.5**. Additionally, we identified several genes in the literature whose translation rates were shown to be specifically sensitive to stress.

Transcript	Predicted response	Reason for selection	Reference
Insulin	escape	Under certain conditions, insulin appears to be translated in a cap-independent manner	Fred RG. Biochem Biophys Res Comm. 2011
PC1/3, PC2, ICA512	escape	mRNA stabilized by glucose due to PTB binding	Knoch K. Nature. 2004
Nkx6.1	escape	IRES in 5′ UTR	Watada H. JBC 2000
Srebp1a	escape	IRES activity induced during ER stress in hepatocytes; dependent on ITAF, hnRNPA1	Damiano F. Biochem J. 2013
Beta actin	sensitive	Translation attenuated after TG treatment	Wong WL. Biochem J. 1993 and others
Cofilin, SOD1	sensitive	Reduced translation efficiency after TG treatment	Ventoso I. PLOS One 2012
CPE	sensitive	Not stabilized by glucose or PTB binding	Knoch K. Nature. 2004

Figure 5.5. Panel of genes selected for pilot screen or translational response to ER stress. Genes selected based on published work. [76,85–89]

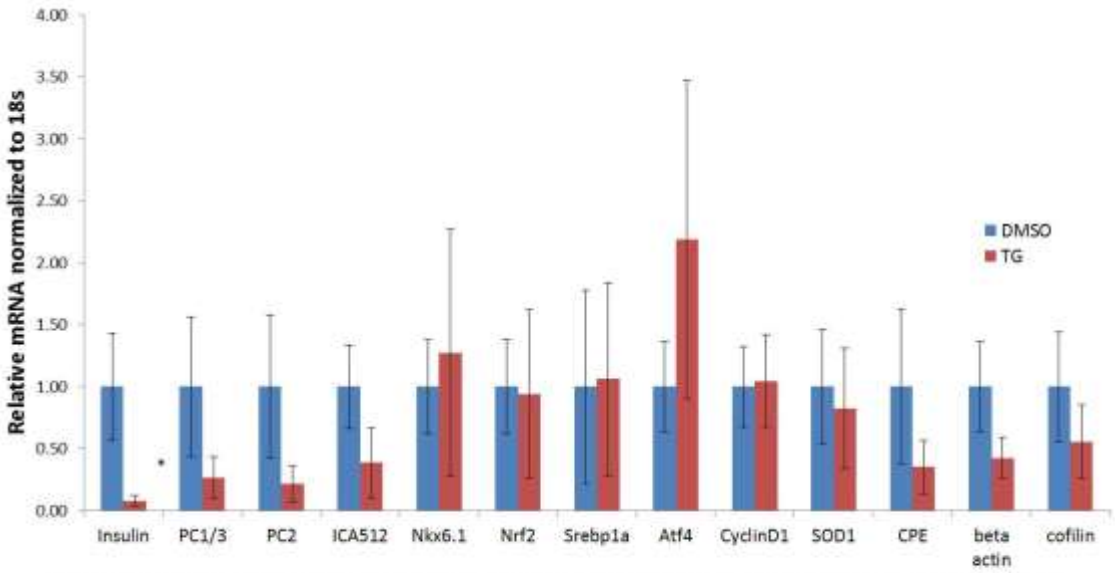

Figure 5.6. Impact of thapsigargin on steady state transcript levels. Min6 cells harvested after 6 hr thapsigargin (TG) of DMSO vehicle control treatment and total transcript levels measured and normalized to 18s transcript. n=6; * $p<0.05$

Following a 6 hour treatment with thapsigargin or DMSO, ribosome-associated RNA was isolated from Min6-L10a cells, as well as Min6-EGFP cells as a control specificity of the immunoprecipitation. This treatment led to a decrease on total transcript levels of some genes **(Fig. 5.6)**. Additionally, the majority of the transcripts predicted to be able to escape global downregulation showed an increase in translational efficiency when treated with thapsigargin **(Fig. 5.7)**. The genes selected as controls showed no difference in translational efficiencies upon treatment with thapsigargin.

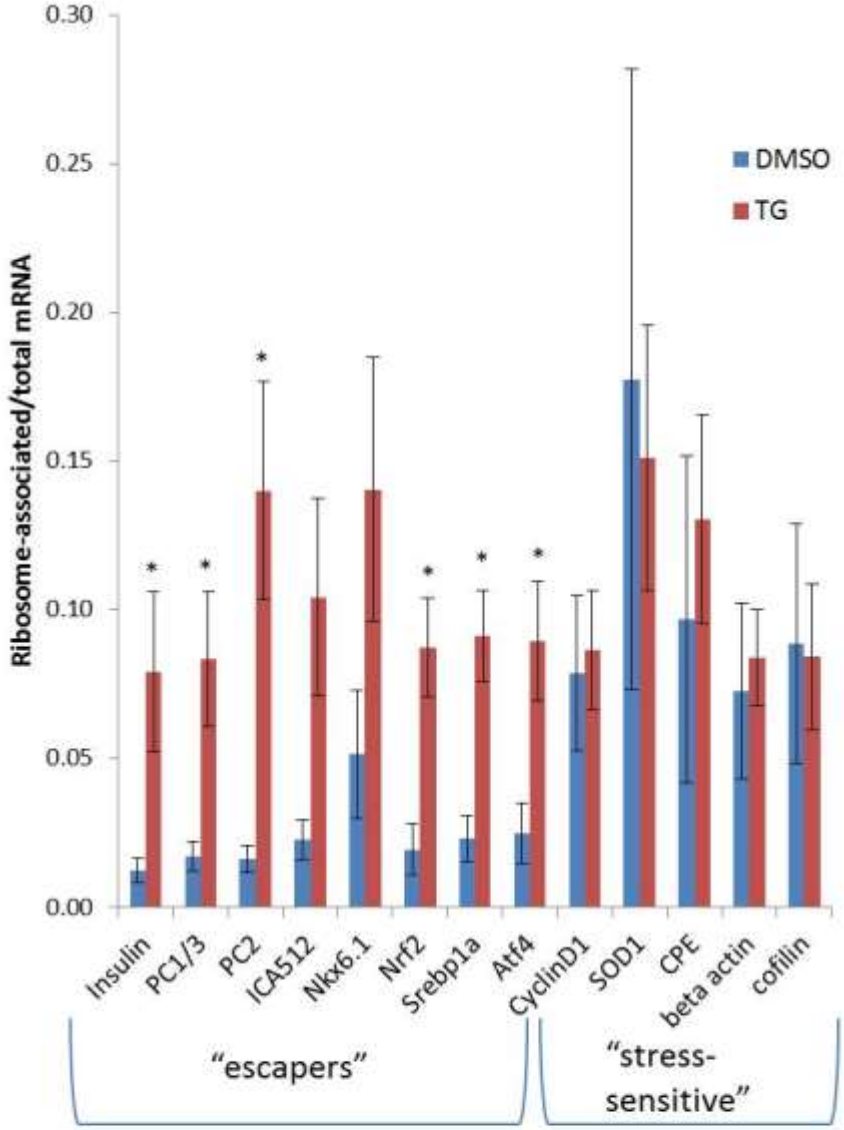

Figure 5.7. Thapsigargin treatment increases translation efficiency in a subset of transcripts. Min6 cells harvested after 6 hr thapsigargin (TG) of DMSO vehicle control treatment and total transcript levels measured and normalized to 18s transcript.

n=6; * $p<0.05$

5.4.3 High-throughput sequencing of translational efficiency following Pdx1 knockdown

Given the previously described role for Pdx1 in regulating many genes involved in protein translation [65], we sought to explore the effect of Pdx1 knockdown on translational efficiencies on a global scale. Pdx1 knockdown by siRNA was optimized in Min6-L10a cells **(Fig 5.8)**. Pdx1 knockdown was observed at 48 hours and maintained through 96 hours. Additionally, perturbation of key Pdx1 targets was seen, indicating that knockdown was affecting pathways downstream of Pdx1. At 72 hours, the direct target of Pdx1, Atf4, was reduced 39% in response to Pdx1 knockdown **(Fig 5.8b)**. Atf4 is directly upstream of 4E-BP1, a key regulator of the rate at which translation initiation occurs. After 96 hours of Pdx1 knockdown, 4E-BP1 was reduced 54% **(Fig 5.8c)**, thus confirming that the perturbation of Pdx1 resulted in changes in secondary targets as well as direct targets.

Translational efficiency was then measured on a global scale. Both total RNA and ribosome-associated RNA were used to calculate ratios of translational efficiency in Min6-L10a cells with and without Pdx1 knockdown. Using a moderately lenient cutoff of a 20% false discovery rate, over 200 genes were identified whose efficiencies were altered by Pdx1 knockdown **(Fig 5.9)**. Interestingly, the translational efficiencies of all but one of the identified transcripts were increased with Pdx1 knockdown, implying that Pdx1 has a negative impact on translational efficiency for a subset of genes.

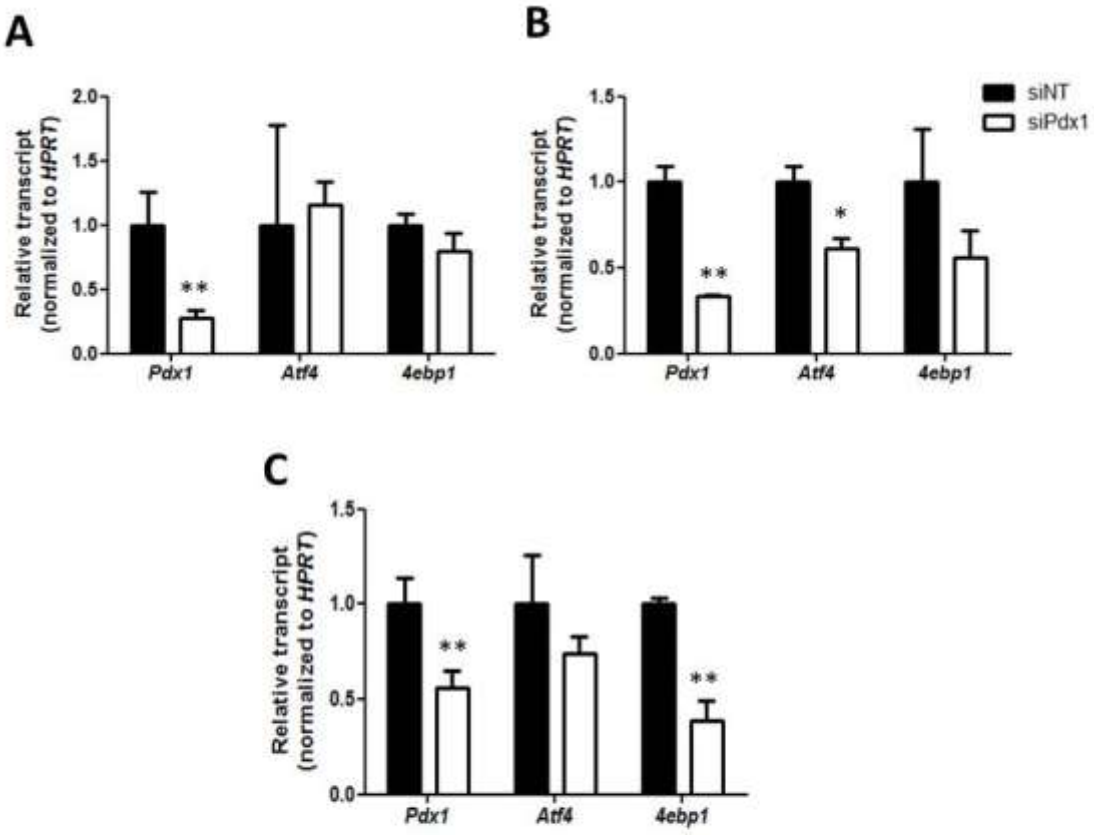

Figure 5.8. Pdx1 knockdown reduces expression of translational regulators. Quantitative RT-PCR showing expression of indicated genes after (A) 48, (B) 72, or (C) 96 hours treatment with siRNA against Pdx1 (siPdx1) or a non-targeting control (siNT) in Min6 cells. n=3; *p<0.05 **p<0.01 vs siNT

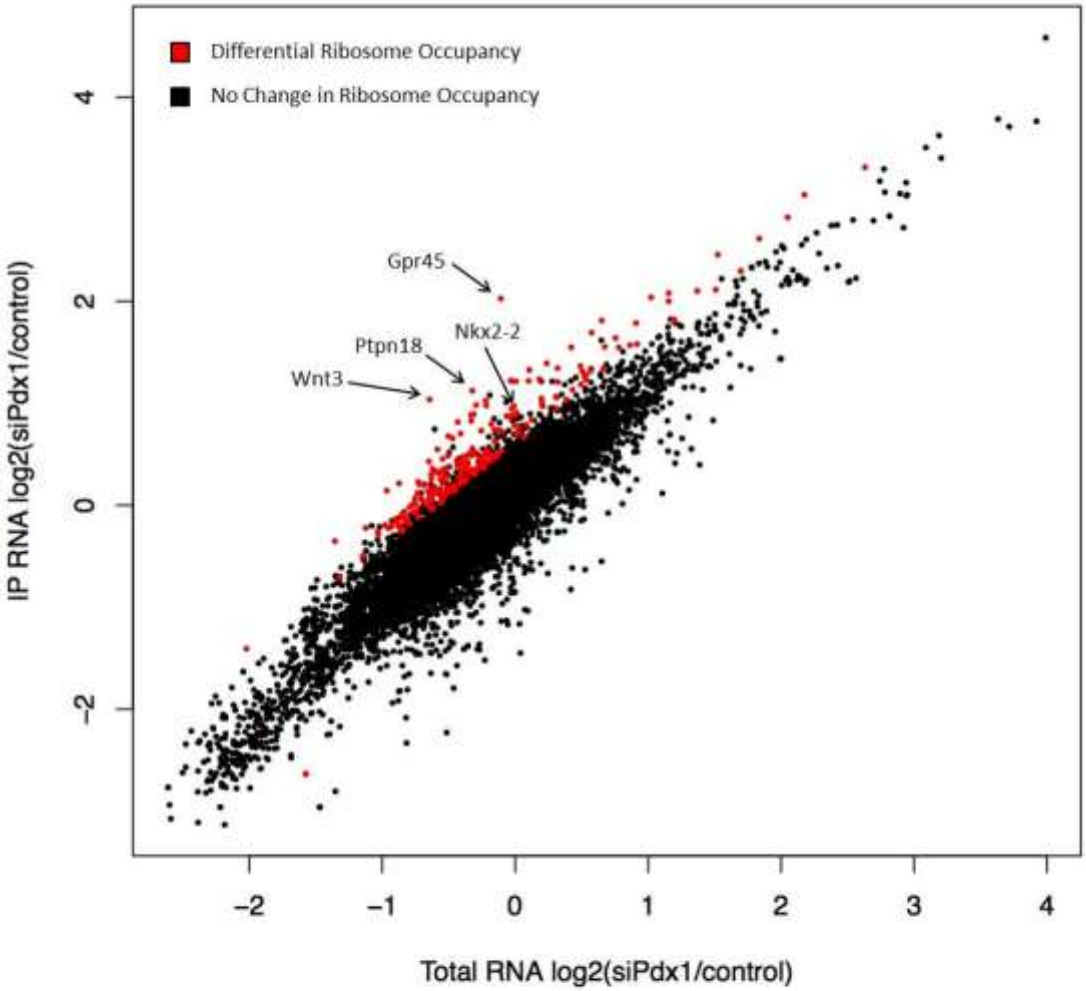

Figure 5.9. Pdx1 knockdown increases translational efficiency of a subset of genes. RNA sequencing of Min6-L10a cells nucleofected with siPdx1 or non-targeting control. Red dots indicate genes differentially regulated with an FDR cutoff of 20%.

5.5 Discussion

A pilot screen in Min6 cells revealed that transcripts with a predicted ability to escape global down-regulation of translation have higher translation efficiencies after thapsigargin treatment. One fundamental question that arose from the pilot screen was why “sensitive” genes did not show decreased translational efficiency upon thapsigargin treatment. A number of possibilities exist and would need to be addressed prior to moving forward with a large-scale analysis of how this particular stressor influences the

translatome. One possibility is that the methods used for normalization were not optimal for this experiment. Both ribosome-associated and total RNA were normalized to the amount of ribosomal 18s transcript. The ratio of those normalized values then resulted in cancelation of the normalization. Because we were not attempting to directly compare actual amounts of transcript, rather we were interested in percentage efficiency, this seemed to be an acceptable method. However, given the large variation in the expression of the genes analyzed, it is possible that small error or variability in the measurement of the total expression of lowly expressed genes was amplified by the fact that this number was the denominator in our equation. One solution to this might be to increase the number of replicates or the number of sequencing reads, especially to reduce variability on lowly expressed genes. This would also likely aid in decreasing the large variability and allow for more statistically significant results to be seen above the noise.

Another potential reason why genes whose efficiencies should be lower in response to stress did not behave as predicted could have to do with the length of thapsigargin treatment in these experiments. Preliminary experiments showed that 6 hours of thapsigargin treatment induced ER stress, as measured by XBP1 splicing, and reduced new protein synthesis **(Fig 5.3 and 5.4)**. In retrospect, it may have been helpful to also assess how total transcript levels change with this treatment. An argument could be made that the ideal time point would be one where stress is still in an early stage, with protein synthesis globally blunted but before transcript levels have been largely affected. Further optimization would be needed to find the optimal timing and treatment, as well as whether this approach would aid in characterizing the translatome more accurately.

Based on global analysis of the beta cell translatome in Min6 cells after siRNA-mediated knockdown of Pdx1, it appears that Pdx1 is a negative regulator of translation for a

subset of transcripts. Given the role of Pdx1 as a transcription factor, it is likely that Pdx1 mediates its effect on translation via transcriptional control of genes responsible for translational control. Some of these genes have been previously identified [65] but a more complete characterization of the overlap between Pdx1-occupied genes and differentially translated genes downstream of Pdx1-occupied genes would likely identify new Pdx1-regulated mediators of the beta cell translatome.

Pdx1 deficiency has also been shown to make cells more susceptible to ER stress [65]. This might imply that the genes identified in **Figure 5.9** contribute to the beta cell UPR program. In future work, it would be particularly interesting to combine Pdx1 deficiency with ER stress and characterize the translatome. Genes whose translational efficiencies were increased in response to stress as well as Pdx1 deficiency may be part of the beta cell-specific stress response program.

CHAPTER 6: FUTURE DIRECTIONS AND DISCUSSION

6.1 Thesis summary

The inability of beta cells to maintain adequate function and mass is central to the development of all forms of diabetes. A more complete understanding of the molecular mechanisms behind both functional failure as well as expansion will be important in developing new approaches to maintain functional beta cell mass. This thesis describes three approaches toward this goal: 1) studying the role of Bmi1 in the replication of beta cells and the potential role of Pcif1 in regulating this expansion, 2) exploring the role of Bmi1 in modulating demand for insulin, thus influencing the required functionality of the beta cells, and 3) characterizing how beta cells respond to stress in order to maintain or restore function. Transcriptional regulators are key to all of these processes; specific to this work are the transcription factor, Pdx1, and the epigenetic modifier, Bmi1, both of which interact with the substrate adapter, Pcif1, which mediates ubiquitination of both Pdx1 and Bmi1. The network surrounding these three proteins as well as the functional outcomes of their action was described in the preceding chapters.

It was first determined that regulation of p16 by Bmi1 cannot explain the elevated beta cell replication rates seen in *Pcif1*$^{gt/+}$ animals. Further work would need to be completed in order to explore whether other Bmi1 targets are differentially expressed in *Pcif1*$^{gt/+}$ beta cells. Unexpectedly, the data from the analysis of *Bmi1* heterozygous animals led to the observation that *Bmi1*$^{+/-}$ mice are protected from age-induced insulin resistance. Further assessment of this phenotype revealed that insulin signaling, specifically Akt phosphorylation, is enhanced in the liver and muscle of *Bmi1*$^{+/-}$ mice. Bmi1 appears to be regulated by insulin, at least in liver tissue. Acute insulin stimulation reduces Bmi1 protein levels, whereas chronically high insulin levels associated with insulin resistance increases Bmi1. Preliminary work in 293T cells confirmed previous publications

indicating that Bmi1 is ubiquitinated by a Pcif1/Cul3-based E3 ligase [112]. This appears to result in lowered Bmi1 levels and lays the groundwork for one possible explanation of the insulin-mediated reduction in Bmi1.

It is likely that analysis of the beta cell translatome will help to develop a more complete picture of how the beta cell responds to different stimuli at a translational level. The immunoprecipitation-based TRAP method was optimized in the Min6 beta cell line. In a pilot screen, in response to ER stress, the translational efficiencies of transcripts with a predicted ability to resist ER stress-induced downregulation of global translation were increased. The effect of *Pdx1* knockdown on the translatome was also assessed. It appears that Pdx1 is inhibitory to the translational efficiency of a subset of transcripts in Min6 cells, as the efficiencies of about 200 genes were increased in response to *Pdx1* knockdown.

6.2 Future Directions

6.2.1 Assess *Pcif1* expression with age

It was interesting to note the time-dependence of the increase in beta cell proliferation seen in *Pcif1* heterozygous mice. It would be very informative to assess Pcif1 expression at both the transcript and protein levels at different ages. Pcif1 has been shown to be regulated at the transcript level by miR-145 [156] as well as hypoxia-inducible factor (HIF) [118]. However, little else is known about Pcif1 regulation, especially with age. Thorough analysis is further complicated by lack of a reliable antibody against Pcif1 protein. As a surrogate, the ubiquitination of Pcif1 targets could be assessed at different ages.

The fact that many of the Bmi1 phenotypes described in Chapters 3 and 4 of this thesis were also only seen at specific ages, some overlapping with the age at which beta cell

replication is altered in *Pcif1* heterozygous mice, raises the possibility that Pcif1 is regulating Bmi1 in an age-dependent manner, thus allowing the Bmi1-dependent phenotypes to become evident.

6.2.2 Limitations of whole body heterozygous models.

The animal studies presented in this thesis are limited by the global heterozygous nature of the mutations. Complete global deletion of *Pcif1* is lethal, making analysis of these animals impossible [119]. However, it is likely that deletion solely in the beta cell would allow the animals to survive post-natally. In the case of complete loss of Pcif1 in the beta cells, more dominant phenotypes may become evident. For example, targets of Pcif1 that are degraded upon ubiquitination should be increased with a reduction in Pcif1. This was evident in the case of Pdx1 even in a heterozygous model [119]. However, the dynamics of translation and degradation will vary for different proteins. Therefore subtle changes that may not be appreciable might be more robust with complete deletion of *Pcif1* in the beta cell.

In the case of global loss of *Bmi1*, the mice are very sick and die early in life [96,107]. It is likely that tissue-specific deletion would alleviate many of the phenotypes associated with this shortened lifespan, such as the neural and hematopoetic deficiencies. This would allow for assessment of complete loss of Bmi1 in the tissue of interest later in adulthood. Additionally, dissecting the role of Bmi1 in specific tissues would give a more clear picture of the contributions of Bmi1 in different tissues to influence whole body glucose homeostasis.

One caveat to the idea of complete deletion of Bmi1 in a tissue of interest is that it may be informative to study the effect of different levels of Bmi1, rather than simply the presence or absence of the protein. It is possible that there is a hierarchy of Bmi1 targets

that are differentially regulated depending on how much Bmi1 is present. Given the evidence that Bmi1 levels change in response to a variety of stimuli, including insulin and age, it would be interesting to modulate Bmi1 levels to mimic these conditions and assess binding to and expression of targets. It is possible that the relationship between Bmi1 and the expression of its targets is not linear, but rather that there are preferential targets that are bound under high or low levels of Bmi1 expression.

Additionally, studying the regulation of Bmi1 would be impossible in a model of complete deletion. It would be most informative to use a heterozygous, tissue-specific *Bmi1* model in order to detect both decreases and increases in Bmi1 after different manipulations. For example, given that Pcif1 has been shown to promote Bmi1 ubiquitination, deletion of *Pcif1* in the context of *Bmi1* heterozygosity may result in normalization of Bmi1 levels.

6.2.3 Bmi1 target(s) upstream of insulin signaling

One of the biggest questions that stems from the work described in Chapter 3 is what might be mediating the effect of Bmi1 on Akt phosphorylation. At this point, most of the immediately obvious candidates have been eliminated, including known regulators of Akt activity as well as known targets of Bmi1. The RNA-seq dataset described in Chapter 3 may begin to provide some direction. However, this will not necessarily identify the direct Bmi1 target responsible for the enhancement of Akt phosphorylation. A Bmi1 ChIP-seq would identify direct Bmi1 targets and could be overlaid with the RNA-seq to identify which targets are differentially expressed in *Bmi1*$^{+/+}$ and *Bmi1*$^{+/-}$ livers. One limitation of this approach is that it would not identify the factor(s) directly upstream of Akt if they are not direct Bmi1 targets. However, some targeted cell-based approaches may help to delineate the signaling in between Bmi1 and Akt.

It would be expected that Bmi1 targets would be de-repressed in *Bmi1*$^{+/-}$ livers. Therefore, a reasonable approach might be to identify genes that appear on both the list

of Bmi1-occupied genes as well as those whose expression is elevated in *Bmi1*$^{+/-}$ livers by RNA-seq. These candidate genes could then be overexpressed in a cell system where Bmi1 levels have been shown to influence Akt phosphorylation. Hepatocytes would be the obvious choice but would be harder to manipulate than an immortalized cell line. If overexpression of one or more targets led to an increase in Akt phosphorylation in response to insulin, these are likely targets worth pursuing. Knockdown of these in the context of *Bmi1* heterozygosity (or knockdown) would provide further confirmation; if the candidate gene is, in fact, mediating the effect of Bmi1 on Akt, knockdown should block the ability of *Bmi1* heterozygosity to influence Akt phosphorylation.

6.2.4 Role of insulin in regulating Bmi1 levels

Confirm or exclude role of Pcif1 in regulating hepatic Bmi1 levels

One potential explanation of acute insulin resulting in reduced Bmi1 protein is Pcif1-mediated ubiquitination and subsequent degradation. Pcif1 has been demonstrated to ubiquitinate Bmi1 [112], possibly resulting in protein degradation. It would be useful to determine whether the half-life of Bmi1 is affected by the presence or absence of Pcif1. Additionally, insulin stimulation with and without a proteasome inhibitor would help to include or exclude the possibility that Bmi1 protein is reduced via proteasomal degradation.

Activity of Pcif1 appears to be reduced under high glucose conditions in Min6 [119]. Given that high glucose levels lead to high insulin levels, it is reasonable to hypothesize that Pcif1 activity is enhanced by insulin as well as or instead of high glucose. If insulin does in fact induce Pcif1-mediated degradation of Bmi1, deletion of Pcif1 should block the ability of insulin to decrease Bmi1 protein levels.

Characterize Bmi1 phosphorylation in liver

In order to determine whether phosphorylation of Bmi1 plays a role in the effect of insulin on Bmi1 protein levels, the phosphorylation state of Bmi1 could be assessed before and after insulin stimulation. Then a non-phosphorylatable Bmi1 could be used to either block the response to insulin or enhance Akt phosphorylation in the absence of insulin, depending on whether Bmi1 phosphorylation goes up or down in response to insulin. Bmi1 has been shown to be phosphorylated by both Akt and MAPKAP kinase 3 (3pK), both of which are downstream of insulin [116,132]. It would therefore be reasonable to hypothesize that Bmi1 is phosphorylated in response to insulin. However, given the described role of Bmi1 in regulating Akt phosphorylation, it could be difficult to dissect a primary role of insulin from a secondary role of increased Akt activity.

Determine role of relative Bmi1 levels in insulin resistance

One of the most important directions to pursue from Chapter 4 is to determine how insulin is affecting Bmi1 levels and what the temporal component is to that regulation. There appears to be a different response to acute versus chronic insulin, where Bmi1 protein is reduced by acute insulin administration or hyperinsulinemia in young animals, such as the 2 month old DLKO mice, but increased in the context of chronically elevated insulin, such as in aging or LIRKO mice.

In fully characterizing the role of Bmi1 in regulating insulin sensitivity, it will be important to determine why Bmi1 levels are high in insulin resistant states. It is possible that the increase in Bmi1 in older animals is due to an upstream factor that is no longer sensitive to insulin. However, given that genetically reducing Bmi1 levels is protective from age-induced insulin resistance, this is unlikely. Alternatively, the role of Bmi1 may be in inhibiting the progression of insulin signaling. Therefore, when insulin stimulation lowers

Bmi1 levels, the repression is relieved. In the case of older animals, Bmi1 levels start higher at baseline and most likely remain higher than insulin sensitive animals in response to insulin. If this were the case, a Bmi1 mutant protein that cannot be degraded may be sufficient to induce insulin resistance by constantly repressing the insulin signaling pathway.

6.2.5 Expand on TRAP analysis

Establish optimal stressors to characterize beta cell stress response

The described pilot experiments utilized thapsigargin treatment to induce ER stress in Min6 cells. However, thapsigargin is not a physiologically relevant stressor; rather, it is a tool to visualize the results of extreme ER stress. The results from this initial screen can be expanded to investigate more globally the effect of ER stress on translation efficiencies. This analysis will give a broad picture of the effects of massive ER stress and will identify pathways and targets involved in general ER stress response. More physiologically and pathophysiologically relevant stressors should be used to follow up on specific targets and pathways. Future experiments may include introduction of stress via fatty acid treatment, high glucose treatment, or overexpression of the mutant Akita insulin, which is unable to properly fold and therefore accumulates in the ER [157], both in cell lines and mouse models.

Due to its potent and fast-acting effect on the ER, thapsigargin may be the ideal agent with which to study the temporal development of ER stress and the response of the cells. However, it will be important to also utilize more physiologically-relevant stressors in order to develop a model that more closely mimics the response of the beta cell to physiological or pathophysiological stress.

The initial experiments described here were established in a cell line. Further work will expand on Min6 results in mouse models. Use of a mouse expressing an inducible, beta cell-specific EGFP-L10a will allow for isolation of both a pure beta cell population by EGFP sorting as well as the isolation of ribosome-associated mRNA specifically from beta cells. This *in vivo* model can be utilized in concert with available models of beta cell stress, including *Pdx1* deletion, high fat diet, or the Akita mutation. It will be particularly interesting to see how well the translatome profiles align under different models of ER stress. The similarities may help to develop a general model of beta cell stress response, whereas the differences will reveal how the cell tailors its response to different stressors.

Mining for motifs in UTR

One advantage to collecting data on a global scale is the ability to look for patterns. In particular, it would be interesting to mine the data set to identify similarities in the untranslated regions (UTRs) of genes that are up-regulated in response to stress. This type of analysis has the potential to reveal characteristics of a transcript that allow translation to progress during times of stress. A similar approach was undertaken by Thoreen et al to identify a 5' terminal oligopyrimidine (TOP) motif present in transcripts whose translation was dependent on mTORC1 [158]. It is likely that these motifs are important in stress response as well, given the role of mTORC1 in regulating protein synthesis [159–161].

Ribosome profiling

One limitation of the TRAP methodology as described is that it does not account for changes in the density of ribosome binding per transcript. For example, one ribosome bound to one mRNA will theoretically result in far less translated protein than ten

ribosomes bound to the same mRNA. The methodology used in Chapter 5 does not account for those differences. However, the data obtained can still be used to identify large changes in translational efficiencies. Looking at individual ribosome footprinting would allow for a more fine-tuned picture. In this process, ribosome-associated mRNA is isolated as described above and subsequently subjected to RNase digestion. mRNA that is bound by ribosomes will be protected from digestion. Sequencing the protected mRNA will therefore provide quantification of how many ribosomes were associated with each transcript.

REFERENCES

[1] N.C. Leite, C.A. Villela-Nogueira, C.R.L. Cardoso, G.F. Salles, Non-alcoholic fatty liver disease and diabetes: From physiopathological interplay to diagnosis and treatment, World J. Gastroenterol. WJG. 20 (2014) 8377–8392. doi:10.3748/wjg.v20.i26.8377.

[2] D. Porte, S.E. Kahn, beta-cell dysfunction and failure in type 2 diabetes: potential mechanisms., Diabetes. 50 (2001) S160. doi:10.2337/diabetes.50.2007.S160.

[3] J.C. Florez, Newly identified loci highlight beta cell dysfunction as a key cause of type 2 diabetes: Where are the insulin resistance genes?, Diabetologia. 51 (2008) 1100–1110. doi:10.1007/s00125-008-1025-9.

[4] S. O'Rahilly, Science, medicine, and the future. Non-insulin dependent diabetes mellitus: the gathering storm, BMJ. 314 (1997) 955–959.

[5] C. Kelly, N.H. McClenaghan, P.R. Flatt, Role of islet structure and cellular interactions in the control of insulin secretion, Islets. 3 (2011) 41–47. doi:10.4161/isl.3.2.14805.

[6] A.R. Saltiel, C.R. Kahn, Insulin signalling and the regulation of glucose and lipid metabolism, Nature. 414 (2001) 799–806. doi:10.1038/414799a.

[7] S. Seino, T. Shibasaki, K. Minami, Dynamics of insulin secretion and the clinical implications for obesity and diabetes, J. Clin. Invest. 121 (2011) 2118–2125. doi:10.1172/JCI45680.

[8] M. Teta, S.Y. Long, L.M. Wartschow, M.M. Rankin, J.A. Kushner, Very slow turnover of beta-cells in aged adult mice, Diabetes. 54 (2005) 2557–2567.

[9] J.J. Meier, A.E. Butler, Y. Saisho, T. Monchamp, R. Galasso, A. Bhushan, et al., Beta-cell replication is the primary mechanism subserving the postnatal expansion of beta-cell mass in humans, Diabetes. 57 (2008) 1584–1594. doi:10.2337/db07-1369.

[10] A.M. Ackermann, M. Gannon, Molecular regulation of pancreatic beta-cell mass development, maintenance, and expansion, J. Mol. Endocrinol. 38 (2007) 193–206. doi:10.1677/JME-06-0053.

[11] D.T. Finegood, L. Scaglia, S. Bonner-Weir, Dynamics of beta-cell mass in the growing rat pancreas. Estimation with a simple mathematical model, Diabetes. 44 (1995) 249–256.

[12] J.A. Kushner, M.A. Ciemerych, E. Sicinska, L.M. Wartschow, M. Teta, S.Y. Long, et al., Cyclins D2 and D1 are essential for postnatal pancreatic beta-cell growth, Mol. Cell. Biol. 25 (2005) 3752–3762. doi:10.1128/MCB.25.9.3752-3762.2005.

[13] S. Georgia, A. Bhushan, Beta cell replication is the primary mechanism for maintaining postnatal beta cell mass, J. Clin. Invest. 114 (2004) 963–968. doi:10.1172/JCI22098.

[14] I. Cozar-Castellano, N. Fiaschi-Taesch, T.A. Bigatel, K.K. Takane, A. Garcia-Ocaña, R. Vasavada, et al., Molecular control of cell cycle progression in the pancreatic beta-cell, Endocr. Rev. 27 (2006) 356–370. doi:10.1210/er.2006-0004.

[15] S.G. Rane, P. Dubus, R.V. Mettus, E.J. Galbreath, G. Boden, E.P. Reddy, et al., Loss of Cdk4 expression causes insulin-deficient diabetes and Cdk4 activation results in beta-islet cell hyperplasia, Nat. Genet. 22 (1999) 44–52. doi:10.1038/8751.

[16] J. Krishnamurthy, C. Torrice, M.R. Ramsey, G.I. Kovalev, K. Al-Regaiey, L. Su, et al., Ink4a/Arf expression is a biomarker of aging, J. Clin. Invest. 114 (2004) 1299–1307. doi:10.1172/JCI22475.

[17] J. Avruch, Insulin signal transduction through protein kinase cascades, Mol. Cell. Biochem. 182 (1998) 31–48.

[18] A. Ullrich, J. Schlessinger, Signal transduction by receptors with tyrosine kinase activity, Cell. 61 (1990) 203–212. doi:10.1016/0092-8674(90)90801-K.

[19] X.J. Sun, P. Rothenberg, C.R. Kahn, J.M. Backer, E. Araki, P.A. Wilden, et al., Structure of the insulin receptor substrate IRS-1 defines a unique signal transduction protein, Nature. 352 (1991) 73–77. doi:10.1038/352073a0.

[20] X.J. Sun, L.M. Wang, Y. Zhang, L. Yenush, M.G. Myers, E. Glasheen, et al., Role of IRS-2 in insulin and cytokine signalling, Nature. 377 (1995) 173–177. doi:10.1038/377173a0.

[21] B.E. Lavan, W.S. Lane, G.E. Lienhard, The 60-kDa phosphotyrosine protein in insulin-treated adipocytes is a new member of the insulin receptor substrate family, J. Biol. Chem. 272 (1997) 11439–11443.

[22] D. Cai, S. Dhe-Paganon, P.A. Melendez, J. Lee, S.E. Shoelson, Two new substrates in insulin signaling, IRS5/DOK4 and IRS6/DOK5, J. Biol. Chem. 278 (2003) 25323–25330. doi:10.1074/jbc.M212430200.

[23] V.R. Fantin, J.D. Sparling, J.W. Slot, S.R. Keller, G.E. Lienhard, B.E. Lavan, Characterization of insulin receptor substrate 4 in human embryonic kidney 293 cells, J. Biol. Chem. 273 (1998) 10726–10732.

[24] A. Virkamäki, K. Ueki, C.R. Kahn, Protein-protein interaction in insulin signaling and the molecular mechanisms of insulin resistance, J. Clin. Invest. 103 (1999) 931–943. doi:10.1172/JCI6609.

[25] C.M. Taniguchi, B. Emanuelli, C.R. Kahn, Critical nodes in signalling pathways: insights into insulin action, Nat. Rev. Mol. Cell Biol. 7 (2006) 85–96. doi:10.1038/nrm1837.

[26] D.R. Alessi, S.R. James, C.P. Downes, A.B. Holmes, P.R. Gaffney, C.B. Reese, et al., Characterization of a 3-phosphoinositide-dependent protein kinase which phosphorylates and activates protein kinase Balpha, Curr. Biol. CB. 7 (1997) 261–269.

[27] S. Frame, P. Cohen, GSK3 takes centre stage more than 20 years after its discovery, Biochem. J. 359 (2001) 1–16.

[28] T.E. Harris, J.C. Lawrence, TOR signaling, Sci. STKE Signal Transduct. Knowl. Environ. 2003 (2003) re15. doi:10.1126/stke.2122003re15.

[29] D.M. Muoio, C.B. Newgard, Molecular and metabolic mechanisms of insulin resistance and β-cell failure in type 2 diabetes, Nat. Rev. Mol. Cell Biol. 9 (2008) 193–205. doi:10.1038/nrm2327.

[30] M. Stumvoll, B.J. Goldstein, T.W. van Haeften, Type 2 diabetes: principles of pathogenesis and therapy, The Lancet. 365 (2005) 1333–1346. doi:10.1016/S0140-6736(05)61032-X.

[31] T. Kitamura, Y. Kitamura, S. Kuroda, Y. Hino, M. Ando, K. Kotani, et al., Insulin-induced phosphorylation and activation of cyclic nucleotide phosphodiesterase 3B by the serine-threonine kinase Akt, Mol. Cell. Biol. 19 (1999) 6286–6296.

[32] M. Watanabe, H. Hayasaki, T. Tamayama, M. Shimada, Histologic distribution of insulin and glucagon receptors, Braz. J. Med. Biol. Res. Rev. Bras. Pesqui. Médicas E Biológicas Soc. Bras. Biofísica Al. 31 (1998) 243–256.

[33] M.D. Michael, R.N. Kulkarni, C. Postic, S.F. Previs, G.I. Shulman, M.A. Magnuson, et al., Loss of Insulin Signaling in Hepatocytes Leads to Severe Insulin Resistance and Progressive Hepatic Dysfunction, Mol. Cell. 6 (2000) 87–97. doi:10.1016/S1097-2765(05)00015-8.

[34] J.C. Brüning, M.D. Michael, J.N. Winnay, T. Hayashi, D. Hörsch, D. Accili, et al., A muscle-specific insulin receptor knockout exhibits features of the metabolic syndrome of NIDDM without altering glucose tolerance, Mol. Cell. 2 (1998) 559–569.

[35] M. Blüher, M.D. Michael, O.D. Peroni, K. Ueki, N. Carter, B.B. Kahn, et al., Adipose tissue selective insulin receptor knockout protects against obesity and obesity-related glucose intolerance, Dev. Cell. 3 (2002) 25–38.

[36] R.N. Kulkarni, J.C. Brüning, J.N. Winnay, C. Postic, M.A. Magnuson, C.R. Kahn, Tissue-specific knockout of the insulin receptor in pancreatic beta cells creates an insulin secretory defect similar to that in type 2 diabetes, Cell. 96 (1999) 329–339.

[37] A.M. Fernández, J.K. Kim, S. Yakar, J. Dupont, C. Hernandez-Sanchez, A.L. Castle, et al., Functional inactivation of the IGF-I and insulin receptors in skeletal muscle causes type 2 diabetes, Genes Dev. 15 (2001) 1926–1934. doi:10.1101/gad.908001.

[38] V.T. Samuel, G.I. Shulman, Integrating Mechanisms for Insulin Resistance: Common Threads and Missing Links, Cell. 148 (2012) 852–871. doi:10.1016/j.cell.2012.02.017.

[39] B.B. Kahn, J.S. Flier, Obesity and insulin resistance, J. Clin. Invest. 106 (2000) 473–481. doi:10.1172/JCI10842.

[40] G.S. Hotamisligil, Endoplasmic Reticulum Stress and the Inflammatory Basis of Metabolic Disease, Cell. 140 (2010) 900–917. doi:10.1016/j.cell.2010.02.034.

[41] T. Nakamura, M. Furuhashi, P. Li, H. Cao, G. Tuncman, N. Sonenberg, et al., Double-Stranded RNA-Dependent Protein Kinase Links Pathogen Sensing with Stress and Metabolic Homeostasis, Cell. 140 (2010) 338–348. doi:10.1016/j.cell.2010.01.001.

[42] S.B. Cullinan, J.A. Diehl, Coordination of ER and oxidative stress signaling: The PERK/Nrf2 signaling pathway, Int. J. Biochem. Cell Biol. 38 (2006) 317–332. doi:10.1016/j.biocel.2005.09.018.

[43] F. Urano, X. Wang, A. Bertolotti, Y. Zhang, P. Chung, H.P. Harding, et al., Coupling of Stress in the ER to Activation of JNK Protein Kinases by Transmembrane Protein Kinase IRE1, Science. 287 (2000) 664–666. doi:10.1126/science.287.5453.664.

[44] J. Deng, P.D. Lu, Y. Zhang, D. Scheuner, R.J. Kaufman, N. Sonenberg, et al., Translational Repression Mediates Activation of Nuclear Factor Kappa B by Phosphorylated Translation Initiation Factor 2, Mol. Cell. Biol. 24 (2004) 10161–10168. doi:10.1128/MCB.24.23.10161-10168.2004.

[45] P. Hu, Z. Han, A.D. Couvillon, R.J. Kaufman, J.H. Exton, Autocrine Tumor Necrosis Factor Alpha Links Endoplasmic Reticulum Stress to the Membrane Death Receptor Pathway through IRE1α-Mediated NF-κB Activation and Down-Regulation of TRAF2 Expression, Mol. Cell. Biol. 26 (2006) 3071–3084. doi:10.1128/MCB.26.8.3071-3084.2006.

[46] H. Yamazaki, N. Hiramatsu, K. Hayakawa, Y. Tagawa, M. Okamura, R. Ogata, et al., Activation of the Akt-NF-κB Pathway by Subtilase Cytotoxin through the ATF6 Branch of the Unfolded Protein Response, J. Immunol. 183 (2009) 1480–1487. doi:10.4049/jimmunol.0900017.

[47] C. Hetz, The unfolded protein response: controlling cell fate decisions under ER stress and beyond, Nat. Rev. Mol. Cell Biol. 13 (2012) 89–102. doi:10.1038/nrm3270.

[48] P. Walter, D. Ron, The Unfolded Protein Response: From Stress Pathway to Homeostatic Regulation, Science. 334 (2011) 1081–1086. doi:10.1126/science.1209038.

[49] D.L. Eizirik, M. Miani, A.K. Cardozo, Signalling danger: endoplasmic reticulum stress and the unfolded protein response in pancreatic islet inflammation, Diabetologia. 56 (2013) 234–241. doi:10.1007/s00125-012-2762-3.

[50] Y. Kimata, D. Oikawa, Y. Shimizu, Y. Ishiwata-Kimata, K. Kohno, A role for BiP as an adjustor for the endoplasmic reticulum stress-sensing protein Ire1, J. Cell Biol. 167 (2004) 445–456. doi:10.1083/jcb.200405153.

[51] C. Evans-Molina, M. Hatanaka, R.G. Mirmira, Lost in translation: endoplasmic reticulum stress and the decline of β-cell health in diabetes mellitus, Diabetes Obes. Metab. 15 (2013) 159–169. doi:10.1111/dom.12163.

[52] T.J. Biden, E. Boslem, K.Y. Chu, N. Sue, Lipotoxic endoplasmic reticulum stress, β cell failure, and type 2 diabetes mellitus, Trends Endocrinol. Metab. (n.d.). doi:10.1016/j.tem.2014.02.003.

[53] F.C. Schuit, P.A. In't Veld, D.G. Pipeleers, Glucose stimulates proinsulin biosynthesis by a dose-dependent recruitment of pancreatic beta cells, Proc. Natl. Acad. Sci. U. S. A. 85 (1988) 3865–3869.

[54] K.L. Lipson, S.G. Fonseca, S. Ishigaki, L.X. Nguyen, E. Foss, R. Bortell, et al., Regulation of insulin biosynthesis in pancreatic beta cells by an endoplasmic reticulum-resident protein kinase IRE1, Cell Metab. 4 (2006) 245–254. doi:10.1016/j.cmet.2006.07.007.

[55] D.A. Cunha, P. Hekerman, L. Ladrière, A. Bazarra-Castro, F. Ortis, M.C. Wakeham, et al., Initiation and execution of lipotoxic ER stress in pancreatic beta-cells, J. Cell Sci. 121 (2008) 2308–2318. doi:10.1242/jcs.026062.

[56] D.R. Laybutt, A.M. Preston, M.C. Akerfeldt, J.G. Kench, A.K. Busch, A.V. Biankin, et al., Endoplasmic reticulum stress contributes to beta cell apoptosis in type 2 diabetes, Diabetologia. 50 (2007) 752–763. doi:10.1007/s00125-006-0590-z.

[57] S. Seton-Rogers, Translation: Switching to cap-independence, Nat. Rev. Cancer. 8 (2008) 6–7. doi:10.1038/nrc2303.

[58] I. Ventoso, A. Kochetov, D. Montaner, J. Dopazo, J. Santoyo, Extensive Translatome Remodeling during ER Stress Response in Mammalian Cells, PLoS ONE. 7 (2012) e35915. doi:10.1371/journal.pone.0035915.

[59] M.F. Offield, T.L. Jetton, P.A. Labosky, M. Ray, R.W. Stein, M.A. Magnuson, et al., PDX-1 is required for pancreatic outgrowth and differentiation of the rostral duodenum, Dev. Camb. Engl. 122 (1996) 983–995.

[60] D.A. Stoffers, N.T. Zinkin, V. Stanojevic, W.L. Clarke, J.F. Habener, Pancreatic agenesis attributable to a single nucleotide deletion in the human IPF1 gene coding sequence, Nat. Genet. 15 (1997) 106–110. doi:10.1038/ng0197-106.

[61] J. Jonsson, L. Carlsson, T. Edlund, H. Edlund, Insulin-promoter-factor 1 is required for pancreas development in mice, Nature. 371 (1994) 606–609. doi:10.1038/371606a0.

[62] M. Brissova, M. Shiota, W.E. Nicholson, M. Gannon, S.M. Knobel, D.W. Piston, et al., Reduction in pancreatic transcription factor PDX-1 impairs glucose-stimulated insulin secretion, J. Biol. Chem. 277 (2002) 11225–11232. doi:10.1074/jbc.M111272200.

[63] S. Gremlich, C. Bonny, G. Waeber, B. Thorens, Fatty Acids Decrease IDX-1 Expression in Rat Pancreatic Islets and Reduce GLUT2, Glucokinase, Insulin, and Somatostatin Levels, J. Biol. Chem. 272 (1997) 30261–30269. doi:10.1074/jbc.272.48.30261.

[64] D.H. Zangen, S. Bonner-Weir, C.H. Lee, J.B. Latimer, C.P. Miller, J.F. Habener, et al., Reduced Insulin, GLUT2, and IDX-1 in β-Cells After Partial Pancreatectomy, Diabetes. 46 (1997) 258–264. doi:10.2337/diab.46.2.258.

[65] M.M. Sachdeva, K.C. Claiborn, C. Khoo, J. Yang, D.N. Groff, R.G. Mirmira, et al., Pdx1 (MODY4) regulates pancreatic beta cell susceptibility to ER stress, Proc. Natl. Acad. Sci. U. S. A. 106 (2009) 19090–19095. doi:10.1073/pnas.0904849106.

[66] Y. Wang, J. Liu, C. Liu, A. Naji, D.A. Stoffers, MicroRNA-7 regulates the mTOR pathway and proliferation in adult pancreatic β-cells, Diabetes. 62 (2013) 887–895. doi:10.2337/db12-0451.

[67] M.E. Cerf, Beta cell dynamics: beta cell replenishment, beta cell compensation and diabetes, Endocrine. 44 (2013) 303–311. doi:10.1007/s12020-013-9917-y.

[68] G. Kwon, C.A. Marshall, K.L. Pappan, M.S. Remedi, M.L. McDaniel, Signaling elements involved in the metabolic regulation of mTOR by nutrients, incretins, and growth factors in islets, Diabetes. 53 Suppl 3 (2004) S225–232.

[69] L.C. Alonso, T. Yokoe, P. Zhang, D.K. Scott, S.K. Kim, C.P. O'Donnell, et al., Glucose infusion in mice: a new model to induce beta-cell replication, Diabetes. 56 (2007) 1792–1801. doi:10.2337/db06-1513.

[70] S. Bonner-Weir, D. Deery, J.L. Leahy, G.C. Weir, Compensatory growth of pancreatic beta-cells in adult rats after short-term glucose infusion, Diabetes. 38 (1989) 49–53.

[71] M. Paris, C. Bernard-Kargar, M.-F. Berthault, L. Bouwens, A. Ktorza, Specific and combined effects of insulin and glucose on functional pancreatic beta-cell mass in vivo in adult rats, Endocrinology. 144 (2003) 2717–2727. doi:10.1210/en.2002-221112.

[72] M.E. Cerf, High fat programming of beta-cell failure, Adv. Exp. Med. Biol. 654 (2010) 77–89. doi:10.1007/978-90-481-3271-3_5.

[73] M. Prentki, C.J. Nolan, Islet beta cell failure in type 2 diabetes, J. Clin. Invest. 116 (2006) 1802–1812. doi:10.1172/JCI29103.

[74] A. Hershko, A. Ciechanover, The ubiquitin system, Annu. Rev. Biochem. 67 (1998) 425–479. doi:10.1146/annurev.biochem.67.1.425.

[75] J. Peng, D. Schwartz, J.E. Elias, C.C. Thoreen, D. Cheng, G. Marsischky, et al., A proteomics approach to understanding protein ubiquitination, Nat. Biotechnol. 21 (2003) 921–926. doi:10.1038/nbt849.

[76] X.-J. Yang, C.-M. Chiang, Sumoylation in gene regulation, human disease, and therapeutic action, F1000prime Rep. 5 (2013) 45. doi:10.12703/P5-45.

[77] Y. Kulathu, D. Komander, Atypical ubiquitylation — the unexplored world of polyubiquitin beyond Lys48 and Lys63 linkages, Nat. Rev. Mol. Cell Biol. 13 (2012) 508–523. doi:10.1038/nrm3394.

[78] J.S. Thrower, L. Hoffman, M. Rechsteiner, C.M. Pickart, Recognition of the polyubiquitin proteolytic signal, EMBO J. 19 (2000) 94–102. doi:10.1093/emboj/19.1.94.

[79] L. Song, M. Rape, Substrate-specific regulation of ubiquitination by the anaphase-promoting complex, Cell Cycle Georget. Tex. 10 (2011) 52–56.

[80] Y. David, T. Ziv, A. Admon, A. Navon, The E2 ubiquitin-conjugating enzymes direct polyubiquitination to preferred lysines, J. Biol. Chem. 285 (2010) 8595–8604. doi:10.1074/jbc.M109.089003.

[81] Z. Chen, C.M. Pickart, A 25-kilodalton ubiquitin carrier protein (E2) catalyzes multi-ubiquitin chain synthesis via lysine 48 of ubiquitin, J. Biol. Chem. 265 (1990) 21835–21842.

[82] Y. Kravtsova-Ivantsiv, A. Ciechanover, Non-canonical ubiquitin-based signals for proteasomal degradation, J. Cell Sci. 125 (2012) 539–548. doi:10.1242/jcs.093567.

[83] M. Sadowski, R. Suryadinata, A.R. Tan, S.N.A. Roesley, B. Sarcevic, Protein monoubiquitination and polyubiquitination generate structural diversity to control distinct biological processes, IUBMB Life. 64 (2012) 136–142. doi:10.1002/iub.589.

[84] J.I. Belle, A. Nijnik, H2A-DUBbing the mammalian epigenome: Expanding frontiers for histone H2A deubiquitinating enzymes in cell biology and physiology, Int. J. Biochem. Cell Biol. 50 (2014) 161–174. doi:10.1016/j.biocel.2014.03.004.

[85] Y. Nagai, T. Kojima, Y. Muro, T. Hachiya, Y. Nishizawa, T. Wakabayashi, et al., Identification of a novel nuclear speckle-type protein, SPOP, FEBS Lett. 418 (1997) 23–26. doi:10.1016/S0014-5793(97)01340-9.

[86] A. Liu, B.M. Desai, D.A. Stoffers, Identification of PCIF1, a POZ domain protein that inhibits PDX-1 (MODY4) transcriptional activity, Mol. Cell. Biol. 24 (2004) 4372–4383.

[87] J.M. Zapata, V. Martínez-García, S. Lefebvre, Phylogeny of the TRAF/MATH domain, Adv. Exp. Med. Biol. 597 (2007) 1–24. doi:10.1007/978-0-387-70630-6_1.

[88] L. Pintard, J.H. Willis, A. Willems, J.-L.F. Johnson, M. Srayko, T. Kurz, et al., The BTB protein MEL-26 is a substrate-specific adaptor of the CUL-3 ubiquitin-ligase, Nature. 425 (2003) 311–316. doi:10.1038/nature01959.

[89] L. Xu, Y. Wei, J. Reboul, P. Vaglio, T.-H. Shin, M. Vidal, et al., BTB proteins are substrate-specific adaptors in an SCF-like modular ubiquitin ligase containing CUL-3, Nature. 425 (2003) 316–321. doi:10.1038/nature01985.

[90] D. Kent, E.W. Bush, J.E. Hooper, Roadkill attenuates Hedgehog responses through degradation of Cubitus interruptus, Development. 133 (2006) 2001–2010. doi:10.1242/dev.02370.

[91] J. Liu, M. Ghanim, L. Xue, C.D. Brown, I. Iossifov, C. Angeletti, et al., Analysis of Drosophila Segmentation Network Identifies a JNK Pathway Factor Overexpressed in Kidney Cancer, Science. 323 (2009) 1218–1222. doi:10.1126/science.1157669.

[92] Q. Zhang, L. Zhang, B. Wang, C.-Y. Ou, C.-T. Chien, J. Jiang, A Hedgehog-Induced BTB Protein Modulates Hedgehog Signaling by Degrading Ci/Gli Transcription Factor, Dev. Cell. 10 (2006) 719–729. doi:10.1016/j.devcel.2006.05.004.

[93] Kathryn C Claiborn, Mira M Sachdeva, Corey E Cannon, David N Groff, Jeffrey D Singer, Doris A Stoffers, Pdx1 regulation of pancreatic beta cell function and survival is modified by the ubiquitin ligase substrate adaptor Pcif1, Unpubl. Manuscr. (2010).

[94] J.E. Kwon, M. La, K.H. Oh, Y.M. Oh, G.R. Kim, J.H. Seol, et al., BTB domain-containing speckle-type POZ protein (SPOP) serves as an adaptor of Daxx for ubiquitination by Cul3-based ubiquitin ligase, J. Biol. Chem. 281 (2006) 12664–12672. doi:10.1074/jbc.M600204200.

[95] M. La, K. Kim, J. Park, J. Won, J.-H. Lee, Y.-M. Fu, et al., Daxx-mediated transcriptional repression of MMP1 gene is reversed by SPOP, Biochem. Biophys. Res. Commun. 320 (2004) 760–765. doi:10.1016/j.bbrc.2004.06.022.

[96] S. Dhawan, S.-I. Tschen, A. Bhushan, Bmi-1 regulates the Ink4a/Arf locus to control pancreatic beta-cell proliferation, Genes Dev. 23 (2009) 906–911. doi:10.1101/gad.1742609.

[97] A.H. Lund, M. van Lohuizen, Polycomb complexes and silencing mechanisms, Curr. Opin. Cell Biol. 16 (2004) 239–246. doi:10.1016/j.ceb.2004.03.010.

[98] R. Cao, Y.-I. Tsukada, Y. Zhang, Role of Bmi-1 and Ring1A in H2A ubiquitylation and Hox gene silencing, Mol. Cell. 20 (2005) 845–854. doi:10.1016/j.molcel.2005.12.002.

[99] X. Shen, Y. Liu, Y.-J. Hsu, Y. Fujiwara, J. Kim, X. Mao, et al., EZH1 mediates methylation on histone H3 lysine 27 and complements EZH2 in maintaining stem cell identity and executing pluripotency, Mol. Cell. 32 (2008) 491–502. doi:10.1016/j.molcel.2008.10.016.

[100] Y.B. Schwartz, V. Pirrotta, A new world of Polycombs: unexpected partnerships and emerging functions, Nat. Rev. Genet. 14 (2013) 853–864. doi:10.1038/nrg3603.

[101] H. Wang, L. Wang, H. Erdjument-Bromage, M. Vidal, P. Tempst, R.S. Jones, et al., Role of histone H2A ubiquitination in Polycomb silencing, Nature. 431 (2004) 873–878. doi:10.1038/nature02985.

[102] L. Di Croce, K. Helin, Transcriptional regulation by Polycomb group proteins, Nat. Struct. Mol. Biol. 20 (2013) 1147–1155. doi:10.1038/nsmb.2669.

[103] J.J. Jacobs, K. Kieboom, S. Marino, R.A. DePinho, M. van Lohuizen, The oncogene and Polycomb-group gene bmi-1 regulates cell proliferation and senescence through the ink4a locus, Nature. 397 (1999) 164–168. doi:10.1038/16476.

[104] M. van Lohuizen, S. Verbeek, B. Scheijen, E. Wientjens, H. van der Gulden, A. Berns, Identification of cooperating oncogenes in E mu-myc transgenic mice by provirus tagging, Cell. 65 (1991) 737–752.

[105] J.J.L. Jacobs, B. Scheijen, J.-W. Voncken, K. Kieboom, A. Berns, M. van Lohuizen, Bmi-1 collaborates with c-Myc in tumorigenesis by inhibiting c-Myc-induced apoptosis via INK4a/ARF, Genes Dev. 13 (1999) 2678–2690.

[106] J. Lessard, G. Sauvageau, Bmi-1 determines the proliferative capacity of normal and leukaemic stem cells, Nature. 423 (2003) 255–260. doi:10.1038/nature01572.

[107] N.M. van der Lugt, J. Domen, K. Linders, M. van Roon, E. Robanus-Maandag, H. te Riele, et al., Posterior transformation, neurological abnormalities, and severe hematopoietic defects in mice with a targeted deletion of the bmi-1 proto-oncogene, Genes Dev. 8 (1994) 757–769.

[108] A.V. Molofsky, S. He, M. Bydon, S.J. Morrison, R. Pardal, Bmi-1 promotes neural stem cell self-renewal and neural development but not mouse growth and survival by repressing the p16Ink4a and p19Arf senescence pathways, Genes Dev. 19 (2005) 1432–1437. doi:10.1101/gad.1299505.

[109] S.W.M. Bruggeman, M.E. Valk-Lingbeek, P.P.M. van der Stoop, J.J.L. Jacobs, K. Kieboom, E. Tanger, et al., Ink4a and Arf differentially affect cell proliferation and neural stem cell self-renewal in Bmi1-deficient mice, Genes Dev. 19 (2005) 1438–1443. doi:10.1101/gad.1299305.

[110] L. Fan, C. Xu, C. Wang, J. Tao, C. Ho, L. Jiang, et al., Bmi1 is required for hepatic progenitor cell expansion and liver tumor development, PloS One. 7 (2012) e46472. doi:10.1371/journal.pone.0046472.

[111] S.-I. Tschen, S. Dhawan, T. Gurlo, A. Bhushan, Age-dependent decline in beta-cell proliferation restricts the capacity of beta-cell regeneration in mice, Diabetes. 58 (2009) 1312–1320. doi:10.2337/db08-1651.

[112] I. Hernández-Muñoz, A.H. Lund, P. van der Stoop, E. Boutsma, I. Muijrers, E. Verhoeven, et al., Stable X chromosome inactivation involves the PRC1 Polycomb complex and requires histone MACROH2A1 and the CULLIN3/SPOP ubiquitin E3 ligase, Proc. Natl. Acad. Sci. U. S. A. 102 (2005) 7635–7640. doi:10.1073/pnas.0408918102.

[113] G.N. Maertens, S. El Messaoudi-Aubert, S. Elderkin, K. Hiom, G. Peters, Ubiquitin-specific proteases 7 and 11 modulate Polycomb regulation of the INK4a tumour suppressor, EMBO J. 29 (2010) 2553–2565. doi:10.1038/emboj.2010.129.

[114] K. Nacerddine, J.-B. Beaudry, V. Ginjala, B. Westerman, F. Mattiroli, J.-Y. Song, et al., Akt-mediated phosphorylation of Bmi1 modulates its oncogenic potential, E3

ligase activity, and DNA damage repair activity in mouse prostate cancer, J. Clin. Invest. 122 (2012) 1920–1932. doi:10.1172/JCI57477.

[115] J.W. Voncken, D. Schweizer, L. Aagaard, L. Sattler, M.F. Jantsch, M. van Lohuizen, Chromatin-association of the Polycomb group protein BMI1 is cell cycle-regulated and correlates with its phosphorylation status, J. Cell Sci. 112 (Pt 24) (1999) 4627–4639.

[116] J.W. Voncken, H. Niessen, B. Neufeld, U. Rennefahrt, V. Dahlmans, N. Kubben, et al., MAPKAP kinase 3pK phosphorylates and regulates chromatin association of the polycomb group protein Bmi1, J. Biol. Chem. 280 (2005) 5178–5187. doi:10.1074/jbc.M407155200.

[117] M. Furukawa, Y.J. He, C. Borchers, Y. Xiong, Targeting of protein ubiquitination by BTB-Cullin 3-Roc1 ubiquitin ligases, Nat. Cell Biol. 5 (2003) 1001–1007. doi:10.1038/ncb1056.

[118] G. Li, W. Ci, S. Karmakar, K. Chen, R. Dhar, Z. Fan, et al., SPOP Promotes Tumorigenesis by Acting as a Key Regulatory Hub in Kidney Cancer, Cancer Cell. 25 (2014) 455–468. doi:10.1016/j.ccr.2014.02.007.

[119] K.C. Claiborn, M.M. Sachdeva, C.E. Cannon, D.N. Groff, J.D. Singer, D.A. Stoffers, Pcif1 modulates Pdx1 protein stability and pancreatic β cell function and survival in mice, J. Clin. Invest. 120 (2010) 3713–3721. doi:10.1172/JCI40440.

[120] G.L. Szot, P. Koudria, J.A. Bluestone, Murine Pancreatic Islet Isolation, J. Vis. Exp. (2007). doi:10.3791/255.

[121] J.A. Kassis, J.L. Brown, Polycomb group response elements in Drosophila and vertebrates, Adv. Genet. 81 (2013) 83–118. doi:10.1016/B978-0-12-407677-8.00003-8.

[122] J. Sharif, T.A. Endo, S. Ito, O. Ohara, H. Koseki, Embracing change to remain the same: conservation of polycomb functions despite divergence of binding motifs among species, Curr. Opin. Cell Biol. 25 (2013) 305–313. doi:10.1016/j.ceb.2013.02.009.

[123] R.M. Carr, R.T. Patel, V. Rao, R. Dhir, M.J. Graham, R.M. Crooke, et al., Reduction of TIP47 improves hepatic steatosis and glucose homeostasis in mice, Am. J. Physiol. Regul. Integr. Comp. Physiol. 302 (2012) R996–1003. doi:10.1152/ajpregu.00177.2011.

[124] D.W. Lamming, L. Ye, P. Katajisto, M.D. Goncalves, M. Saitoh, D.M. Stevens, et al., Rapamycin-induced insulin resistance is mediated by mTORC2 loss and uncoupled from longevity, Science. 335 (2012) 1638–1643. doi:10.1126/science.1215135.

[125] Z. Sun, R.A. Miller, R.T. Patel, J. Chen, R. Dhir, H. Wang, et al., Hepatic Hdac3 promotes gluconeogenesis by repressing lipid synthesis and sequestration, Nat. Med. 18 (2012) 934–942. doi:10.1038/nm.2744.

[126] R.A. Miller, Q. Chu, J. Le Lay, P.E. Scherer, R.S. Ahima, K.H. Kaestner, et al., Adiponectin suppresses gluconeogenic gene expression in mouse hepatocytes independent of LKB1-AMPK signaling, J. Clin. Invest. 121 (2011) 2518–2528. doi:10.1172/JCI45942.

[127] M. Kitazawa, Circadian rhythms, metabolism, and insulin sensitivity: transcriptional networks in animal models, Curr. Diab. Rep. 13 (2013) 223–228. doi:10.1007/s11892-012-0354-8.

[128] G. Gargiulo, M. Cesaroni, M. Serresi, N. de Vries, D. Hulsman, S.W. Bruggeman, et al., In Vivo RNAi Screen for BMI1 Targets Identifies TGF-β/BMP-ER

Stress Pathways as Key Regulators of Neural- and Malignant Glioma-Stem Cell Homeostasis, Cancer Cell. 23 (2013) 660–676. doi:10.1016/j.ccr.2013.03.030.

[129] M. Lu, M. Wan, K.F. Leavens, Q. Chu, B.R. Monks, S. Fernandez, et al., Insulin regulates liver metabolism in vivo in the absence of hepatic Akt and Foxo1, Nat. Med. 18 (2012) 388–395. doi:10.1038/nm.2686.

[130] K. Nowak, K. Kerl, D. Fehr, C. Kramps, C. Gessner, K. Killmer, et al., BMI1 is a target gene of E2F-1 and is strongly expressed in primary neuroblastomas, Nucleic Acids Res. 34 (2006) 1745–1754. doi:10.1093/nar/gkl119.

[131] J.-H. Cho, M. Dimri, G.P. Dimri, A Positive Feedback Loop Regulates the Expression of Polycomb Group Protein BMI1 via WNT Signaling Pathway, J. Biol. Chem. 288 (2013) 3406–3418. doi:10.1074/jbc.M112.422931.

[132] J. Kim, J. Hwangbo, P.K.Y. Wong, p38 MAPK-Mediated Bmi-1 Down-Regulation and Defective Proliferation in ATM-Deficient Neural Stem Cells Can Be Restored by Akt Activation, PLoS ONE. 6 (2011) e16615. doi:10.1371/journal.pone.0016615.

[133] Y. Liu, F. Liu, H. Yu, X. Zhao, G. Sashida, A. Deblasio, et al., Akt phosphorylates the transcriptional repressor bmi1 to block its effects on the tumor-suppressing ink4a-arf locus, Sci. Signal. 5 (2012) ra77. doi:10.1126/scisignal.2003199.

[134] R. Somwar, M. Perreault, S. Kapur, C. Taha, G. Sweeney, T. Ramlal, et al., Activation of p38 mitogen-activated protein kinase alpha and beta by insulin and contraction in rat skeletal muscle: potential role in the stimulation of glucose transport., Diabetes. 49 (2000) 1794–1800. doi:10.2337/diabetes.49.11.1794.

[135] M. Scharf, S. Neef, R. Freund, C. Geers-Knörr, M. Franz-Wachtel, A. Brandis, et al., Mitogen-activated protein kinase-activated protein kinases 2 and 3 regulate

SERCA2a expression and fiber type composition to modulate skeletal muscle and cardiomyocyte function, Mol. Cell. Biol. 33 (2013) 2586–2602. doi:10.1128/MCB.01692-12.

[136] M.D. Michael, R.N. Kulkarni, C. Postic, S.F. Previs, G.I. Shulman, M.A. Magnuson, et al., Loss of insulin signaling in hepatocytes leads to severe insulin resistance and progressive hepatic dysfunction, Mol. Cell. 6 (2000) 87–97.

[137] P. Muzzin, R.C. Eisensmith, K.C. Copeland, S.L.C. Woo, Correction of obesity and diabetes in genetically obese mice by leptin gene therapy, Proc. Natl. Acad. Sci. 93 (1996) 14804–14808.

[138] C.M. Oslowski, F. Urano, The binary switch that controls the life and death decisions of ER stressed β cells, Curr. Opin. Cell Biol. 23 (2011) 207–215. doi:10.1016/j.ceb.2010.11.005.

[139] M. Delépine, M. Nicolino, T. Barrett, M. Golamaully, G.M. Lathrop, C. Julier, EIF2AK3, encoding translation initiation factor 2-alpha kinase 3, is mutated in patients with Wolcott-Rallison syndrome, Nat. Genet. 25 (2000) 406–409. doi:10.1038/78085.

[140] H. Inoue, Y. Tanizawa, J. Wasson, P. Behn, K. Kalidas, E. Bernal-Mizrachi, et al., A gene encoding a transmembrane protein is mutated in patients with diabetes mellitus and optic atrophy (Wolfram syndrome), Nat. Genet. 20 (1998) 143–148. doi:10.1038/2441.

[141] H. Elouil, M. Bensellam, Y. Guiot, D. Vander Mierde, S.M.A. Pascal, F.C. Schuit, et al., Acute nutrient regulation of the unfolded protein response and integrated stress response in cultured rat pancreatic islets, Diabetologia. 50 (2007) 1442–1452. doi:10.1007/s00125-007-0674-4.

[142] A.K. Cardozo, F. Ortis, J. Storling, Y.-M. Feng, J. Rasschaert, M. Tonnesen, et al., Cytokines Downregulate the Sarcoendoplasmic Reticulum Pump Ca2+ ATPase 2b and Deplete Endoplasmic Reticulum Ca2+, Leading to Induction of Endoplasmic Reticulum Stress in Pancreatic β-Cells, Diabetes. 54 (2005) 452–461. doi:10.2337/diabetes.54.2.452.

[143] T. Kono, G. Ahn, D.R. Moss, L. Gann, A. Zarain-Herzberg, Y. Nishiki, et al., PPAR-? Activation Restores Pancreatic Islet SERCA2 Levels and Prevents ?-Cell Dysfunction under Conditions of Hyperglycemic and Cytokine Stress, Mol. Endocrinol. 26 (2012) 257–271. doi:10.1210/me.2011-1181.

[144] T. Hara, J. Mahadevan, K. Kanekura, M. Hara, S. Lu, F. Urano, Calcium efflux from the endoplasmic reticulum leads to β-cell death, Endocrinology. 155 (2014) 758–768. doi:10.1210/en.2013-1519.

[145] F. Michelangeli, J.M. East, A diversity of SERCA Ca2+ pump inhibitors, Biochem. Soc. Trans. 39 (2011) 789–797. doi:10.1042/BST0390789.

[146] G.E. Kass, S. Orrenius, Calcium signaling and cytotoxicity., Environ. Health Perspect. 107 (1999) 25–35.

[147] A. Verkhratsky, Physiology and Pathophysiology of the Calcium Store in the Endoplasmic Reticulum of Neurons, Physiol. Rev. 85 (2005) 201–279. doi:10.1152/physrev.00004.2004.

[148] J. Doutheil, C. Gissel, U. Oschlies, K.-A. Hossmann, W. Paschen, Relation of neuronal endoplasmic reticulum calcium homeostasis to ribosomal aggregation and protein synthesis: implications for stress-induced suppression of protein synthesis, Brain Res. 775 (1997) 43–51. doi:10.1016/S0006-8993(97)00899-8.

[149] M. T, A. S, O. I, P. W, Response of neurons to an irreversible inhibition of endoplasmic reticulum Ca2+-ATPase: relationship between global protein synthesis and expression and translation of individual genes, (2001). http://www.biochemj.org/bj/356/0805/bj3560805.htm (accessed August 9, 2014).

[150] Q. Zong, M. Schummer, L. Hood, D.R. Morris, Messenger RNA translation state: The second dimension of high-throughput expression screening, Proc. Natl. Acad. Sci. 96 (1999) 10632–10636. doi:10.1073/pnas.96.19.10632.

[151] K. Kapeli, G.W. Yeo, Genome-wide approaches to dissect the roles of RNA binding proteins in translational control: implications for neurological diseases, Front. Neurosci. 6 (2012) 144. doi:10.3389/fnins.2012.00144.

[152] E. Sanz, L. Yang, T. Su, D.R. Morris, G.S. McKnight, P.S. Amieux, Cell-type-specific isolation of ribosome-associated mRNA from complex tissues, Proc. Natl. Acad. Sci. U. S. A. 106 (2009) 13939–13944. doi:10.1073/pnas.0907143106.

[153] M. Heiman, A. Schaefer, S. Gong, J.D. Peterson, M. Day, K.E. Ramsey, et al., A translational profiling approach for the molecular characterization of CNS cell types, Cell. 135 (2008) 738–748. doi:10.1016/j.cell.2008.10.028.

[154] J.P. Doyle, J.D. Dougherty, M. Heiman, E.F. Schmidt, T.R. Stevens, G. Ma, et al., Application of a Translational Profiling Approach for the Comparative Analysis of CNS Cell Types, Cell. 135 (2008) 749–762. doi:10.1016/j.cell.2008.10.029.

[155] N.C. Bramswig, L.J. Everett, J. Schug, C. Dorrell, C. Liu, Y. Luo, et al., Epigenomic plasticity enables human pancreatic α to β cell reprogramming, J. Clin. Invest. 123 (2013) 1275–1284. doi:10.1172/JCI66514.

[156] C.-J. Huang, H.-Y. Chen, W.-Y. Lin, K.B. Choo, Differential expression of speckled POZ protein, SPOP: putative regulation by miR-145, J. Biosci. 39 (2014) 401–413.

[157] M.A. Weiss, Diabetes mellitus due to the toxic misfolding of proinsulin variants, FEBS Lett. 587 (2013) 1942–1950. doi:10.1016/j.febslet.2013.04.044.

[158] C.C. Thoreen, L. Chantranupong, H.R. Keys, T. Wang, N.S. Gray, D.M. Sabatini, A unifying model for mTORC1-mediated regulation of mRNA translation, Nature. 485 (2012) 109–113. doi:10.1038/nature11083.

[159] C.C. Dibble, B.D. Manning, Signal integration by mTORC1 coordinates nutrient input with biosynthetic output, Nat. Cell Biol. 15 (2013) 555–564. doi:10.1038/ncb2763.

[160] N. Hay, N. Sonenberg, Upstream and downstream of mTOR, Genes Dev. 18 (2004) 1926–1945. doi:10.1101/gad.1212704.

[161] Y. Zhang, J. Nicholatos, J.R. Dreier, S.J.H. Ricoult, S.B. Widenmaier, G.S. Hotamisligil, et al., Coordinated regulation of protein synthesis and degradation by mTORC1, Nature. advance online publication (2014). doi:10.1038/nature13492.